U.S.NRC

United States Nuclear Regulatory Commission

Protecting People and the Environment

Uncertainties in Predicted Isotopic Compositions for High Burnup PWR Spent Nuclear Fuel

Office of Nuclear Regulatory Research

AVAILABILITY OF REFERENCE MATERIALS
IN NRC PUBLICATIONS

Uncertainties in Predicted Isotopic Compositions for High Burnup PWR Spent Nuclear Fuel

Prepared by
I.C. Gauld, G. Ilas, and G. Radulescu

Oak Ridge National Laboratory
Managed by UT-Battelle, LLC
Oak Ridge, TN 37831-6170

M. Aissa, NRC Project Manager

NRC Job Code N6540

Office of Nuclear Regulatory Research

ABSTRACT

Experimental isotopic assay data for 51 spent fuel samples acquired from domestic and international programs have been compiled to provide a database to validate computational predictions of spent fuel isotopic compositions important to criticality safety (burnup credit), reactor physics, spent fuel storage and transportation, and waste management applications. The data were selected on the basis that they include extensive actinide and fission product isotopic assay measurements. The experimental data were acquired for fuels irradiated in six different pressurized water reactors: the Three Mile Island 1 and Calvert Cliffs 1 reactors operated in the United States, the Takahama-3 reactor in Japan, the Gösgen reactor in Switzerland, the GKN II reactor in Germany, and the Vandellós II reactor in Spain. The fuel samples cover enrichments from 2.6 to 4.7 wt % ^{235}U, and a wide burnup range, from 9 to 78 GWd/MTU. In this report, spent fuel isotopic compositions calculated using two-dimensional isotope depletion models and ENDF/B-V–based cross section libraries in the SCALE 5 code system are benchmarked against the experimental isotopic data to validate the code and nuclear data libraries and provide estimates of isotopic bias and uncertainty for nuclides of highest importance to safety and licensing applications. The procedures used to evaluate the experimental data and assess the results are described.

TABLE OF CONTENTS

LIST OF FIGURES

LIST OF FIGURES (continued)

LIST OF FIGURES (continued)

LIST OF TABLES

ACKNOWLEDGMENTS

ACRONYMS AND ABBREVIATIONS

ANL	Argonne National Laboratory
ARIANE	Actinides Research In A Nuclear Element
ATM	approved testing material
BPR	burnable poison rods
CE	Combustion Engineering
CEA	Commissariat à l'Énergie Atomique
C/E	calculated-to-experimental
CSN	Consejo de Seguridad Nuclear
DOE	U.S. Department of Energy
ENRESA	Empresa Nacional de Residuo Radioactivo
ENUSA	Empresa Nacional del Uranio, S. A.
EPRI	Electric Power Research Institute
GE-VNC	General Electric Vallecitos Nuclear Center
GKN II	Gemeinschaftskernkraftwerk Neckar Unit II
ICPMS	inductively coupled plasma mass spectrometry
ID	isotope dilution
IDMS	isotope dilution mass spectrometry
ITU	Institute for Transuranium Elements
JAERI	Japan Atomic Energy Research Institute
KRI	Khlopin Radium Institute
LA	luminescent analysis
LWR	light water reactor
MALIBU	MOX and UOX LWR Fuels Irradiated to High Burnup
MOX	mixed oxide
MS	mass spectrometry
NEA	Nuclear Energy Agency
NRC	U.S. Nuclear Regulatory Commission
OCRWM	Office of Civilian Radioactive Waste Management
OECD	Organisation for Economic Co-operation and Development
ORNL	Oak Ridge National Laboratory
PNNL	Pacific Northwest National Laboratory
PSI	Paul Scherrer Institute
PWR	pressurized water reactor
REBUS	Reactivity Tests for a Direct Evaluation of the Burnup Credit on Selected irradiated LWR fuel bundles
RSD	relative standard deviation
SCALE	Standardized Computer Analyses for Licensing Evaluation
SCK•CEN	Studiecentrum voor Kernenergie - Centre d'Étude de l'Énergie Nucléaire
SFCOMPO	Spent Fuel Isotopic Composition Database
TIMS	thermal ionization mass spectrometry
TMI-1	Three Mile Island Unit 1
UOX	uranium oxide
YMP	Yucca Mountain Project

1 INTRODUCTION

Analysis and evaluation of the bias and uncertainties in the predicted isotopic composition of spent nuclear fuel are essential for evaluating the performance and validating the accuracy of computer codes and nuclear data used for light water reactor (LWR) safety and licensing calculations. Bias and uncertainty in predicted spent fuel isotopic compositions are important in developing safety margins for uncertainty, required in criticality calculations that utilize burnup credit (reduction of reactivity associated with fuel irradiation). Isotopic uncertainties are also an important source of uncertainty in calculated radionuclide activities that define the radiation sources used in postulated severe accident analysis, and dose rates and decay heat generation rates for spent fuel handling, transportation, and storage facilities. The trend in the nuclear industry towards the use of higher fuel enrichments, advanced fuel designs, optimized fuel management strategies, and increasing capacity factors has resulted in progressively higher burnup fuel being discharged from commercial LWR plants in the United States. Assemblies now attain average burnups of 60 GWd/MTU, with local fuel rod burnup values achieving even higher values. The majority of measured isotopic assay data that are currently publicly available to validate code accuracy involve fuel with burnups less than 40 GWd/MTU and enrichments below 4 wt % ^{235}U, severely limiting the ability to validate computer code predictions for high burnup fuel. Thus, fuel currently being discharged from nuclear reactors has characteristics that extend well beyond regimes where experimental validation data are readily available.

Under a project sponsored by the U.S. Nuclear Regulatory Commission (NRC) Office of Nuclear Regulatory Research, experimental isotopic assay data representative of modern fuel designs and burnup characteristics have been acquired and documented in a series of reports for the purpose of code validation, and the spent fuel measurements have been applied to validate isotopic calculations performed using the Standardized Computer Analyses for Licensing Evaluation (SCALE) code system:[1]

- NUREG/CR-6968 – Analysis of Experimental Data for High Burnup PWR Spent Fuel Isotopic Validation—Calvert Cliffs, Takahama, and Three Mile Island Reactors;[2]

- NUREG/CR-6969 – Analysis of Experimental Data for High Burnup PWR Spent Fuel Isotopic Validation—ARIANE and REBUS Programs (UO$_2$ Fuel);[3]

- NUREG/CR-7013 – Analysis of Experimental Data for High Burnup PWR Spent Fuel Isotopic Validation—Vandellós II Reactor;[4]

- Analysis of Experimental Data for High Burnup PWR Spent Fuel Isotopic Validation–MALIBU Program (UO$_2$ Fuel). The MALIBU program data are currently commercially protected, and details of the experiments are not yet available to the public.[5]

The experimental data analyzed in the present study were limited to include only pressurized water reactor (PWR) fuels. The fuel samples were selected on the basis that they cover a relatively wide burnup range and include both extensive actinide and fission product measurements. Isotopic data for 51 UO$_2$ fuel samples from commercial assemblies were acquired from domestic and international programs, and measurements for more than 60 isotopes are evaluated. The selected samples were obtained from fuel rods with initial fuel enrichments from 2.6 to 4.7 wt % ^{235}U and cover a large burnup range from 8 to 79 GWd/MTU. A summary of the experimental programs and spent fuel samples evaluated in this report is listed in Table 1.1.

This report was prepared to compile and evaluate isotopic assay measurements from different experiments into a single document as part of a comprehensive computational validation exercise. The present data established an experimental database that can be used to develop guidance on isotopic bias and uncertainties, particularly as they apply to applications involving high burnup spent fuel. The isotopic uncertainties are selectively evaluated for nuclides of high importance to burnup credit, nuclear criticality safety, radiation source terms (neutron and gamma ray sources), and decay heat applications.

The report is organized into the following sections:

- Section 2 gives an overview of the analyzed fuel samples considered and the experimental programs from which the measurement data were acquired.

- Section 3 reviews the measurement techniques and uncertainties.

- Section 4 describes the computational analysis methods and models.

- Section 5 compares the measured and calculated isotopic results, describes the criteria used to evaluate the different data sets, and discusses the results of the evaluation.

- Section 6 presents conclusions.

Sections 2–4 present an overview of the experimental programs and the analysis results. A more detailed description of the experiments and the fuel design and reactor operating information required to perform benchmark code calculations can be found in the separate reports for each program.

Table 1.1. Summary of evaluated spent fuel measurements

Reactor (country)	Measurement laboratory[a]	Experimental program[a]	Assembly design	Enrichment (wt % ^{235}U)	No. of samples	Measurement methods[b]	Burnup(s) (GWd/MTU)
TMI-1 (USA)	ANL (USA)	OCRWM (YMP)	15 × 15	4.013	11	ICPMS, α-spec, γ-spec	44.8–55.7
TMI-1 (USA)	GE-VNC (USA)	OCRWM (YMP)	15 × 15	4.657	8	TIMS, α-spec, γ-spec	22.8–29.9
Calvert Cliffs 1 (USA)	PNNL, KRI (USA, Russia)	ATM	14 × 14	3.038	3	IDMS, LA, α-spec, γ-spec	27.4, 37.1, 44.3
Takahama 3 (Japan)	JAERI (Japan)	JAERI	17 × 17	2.63, 4.11	16	IDMS, α-spec, γ-spec	7.8–47.3
Gösgen (Switzerland)	SCK•CEN, ITU (Belgium, Germany)	ARIANE	15 × 15	3.5, 4.1	3	TIMS, ICPMS, α-spec, β-spec, γ-spec	31.1, 52.5, 60.7
GKN II (Germany)	SCK•CEN (Belgium)	REBUS	18 × 18	3.8	1	TIMS, ICPMS α-spec, γ-spec	54.1
Vandellós II (Spain)	Studsvik Nuclear AB (Sweden)	CSN/ENUSA/ ENRESA	17 × 17	4.498	6	ICPMS, γ-spec	42.9–78.3
Gösgen (Switzerland)	SCK•CEN, CEA, PSI (Belgium, France, Switzerland)	MALIBU	15 × 15	4.3	3	TIMS, ICPMS, α-spec, γ-spec	46.0, 50.8, 70.3

[a]Key to laboratory and experimental program abbreviations:
ATM = Approved Testing Material Program
JAERI = Japan Atomic Energy Research Institute
YMP = U.S. Department of Energy Yucca Mountain Project
REBUS, ARIANE, and MALIBU are international programs coordinated by Belgonucleaire, Belgium
CSN = Spanish Regulatory Authority, Consejo de Seguridad Nuclear
ENUSA = Spanish fuel vendor, Empresa Nacional del Uranio, S.A.
PNNL = Pacific Northwest National Laboratory
KRI = Khlopin Radium Institute
GE-VNC = General Electric Vallecitos Nuclear Center
ANL = Argonne National Laboratory
SCK•CEN = Studiecentrum voor Kernenergie - Centre d'Étude de l'Énergie Nucléaire
PSI = Paul Scherrer Institute
CEA = Commissariat à l'Énergie Atomique
ITU = Institute for Transuranium Elements

[b]Key to measurement method abbreviations:
ICPMS = inductively coupled plasma mass spectrometry
TIMS = thermal ionization mass spectrometry
LA = luminescence analysis
IDMS = isotopic dilution mass spectrometry
α-spec = alpha spectrometry
β-spec = beta spectrometry
γ-spec = gamma-ray spectrometry

2 OVERVIEW OF EXPERIMENTAL PROGRAMS AND FUEL CHARACTERISTICS

This section of the report provides a brief description of the experimental programs and the fuel samples analyzed. All of the data evaluated in this report were obtained from PWR spent fuel samples. Because the NRC research project under which this work was performed focused on analyses for high burnup fuels, most of the data are acquired from relatively recent experimental programs that include measurements for modern fuel designs and operating characteristics. In addition, the newer programs generally include measurements for isotopes of importance to a broader range of spent fuel applications. However, several samples from older programs are also included to provide additional data for low and moderate burnup fuels such that sufficient data are available to assess trends in the bias and uncertainty.

Data were acquired from domestic and international programs and include isotopic measurements for 51 UO_2 fuel samples from assemblies irradiated in six different PWRs:

1. Calvert Cliffs Unit 1 reactor, United States;

2. Gemeinschaftskernkraftwerk Neckar (GKN) Unit II reactor, Germany;

3. Gösgen reactor, Switzerland;

4. Takahama Unit 3 reactor, Japan;

5. Three Mile Island Unit 1 (TMI-1) reactor, United States; and

6. Vandellós II reactor, Spain.

The matrix of spent fuel samples analyzed in this work is listed Table 2.1. Information on the specific nuclides measured in each sample and the measurement accuracies can be found in Section 5 of this report.

2.1 Calvert Cliffs 1

Isotopic measurements for spent fuel samples from the Calvert Cliffs Unit 1 reactor were performed in 1987 and 1992 at the Material Characterization Center at Pacific Northwest National Laboratory (PNNL) for the Approved Testing Material (ATM) Program.[6,7] The measurements were designed to characterize mid-burnup spent fuel representative of reactors operating in the United States. Three samples, designated ATM-104, were measured from fuel rod MKP109 of a Combustion Engineering (CE) 14 × 14 assembly identified as D047. Assembly D047 was present in the reactor core for four consecutive cycles, from cycle 2 to cycle 5. The assembly had 176 fuel rods and 5 large guide tubes. There were no burnable poison rods or gadolinium-bearing rods in the assembly during any of the irradiation cycles. The assembly configuration and location of measured rod MKP109 in the assembly are shown in Figure 2.1.

The samples, identified as 104-MKP109-LL, 104-MKP109-CC, and 104-MKP109-P, had burnup values of approximately 27.4, 37.1, and 44.3 GWd/MTU, respectively. The burnup of the samples was determined by the laboratory from the ^{148}Nd measurements using the ASTM Standard Test Method E321 (Neodymium-148 method).[8] The initial enrichment of the MKP109 fuel rod was 3.038 wt % ^{235}U. The Calvert Cliffs ATM-104 samples were selected for the present study because extensive data for fission products important to burnup credit were measured in these samples.

Table 2.1. Summary of evaluated spent fuel samples

Reactor and Assembly type	Program	Measurement laboratory	Assembly ID	Fuel type	Fuel rod ID	Sample ID	Enrichment (wt % ^{235}U)	Sample burnup (GWd/MTU)
Calvert Cliffs 1 14 × 14	ATM-104	PNNL, KRI	D047	UO2	MKP109	MKP109-LL	3.038	27.4
			D047	UO2	MKP109	MKP109-CC	3.038	37.1
			D047	UO2	MKP109	MKP109-P	3.038	44.3
Takahama 3 17 × 17	JAERI	JAERI	NT3G23	UO2	A17	SF95-1	4.11	8.6
			NT3G23	UO2	A17	SF95-2	4.11	14.3
			NT3G23	UO2	A17	SF95-3	4.11	17.4
			NT3G23	UO2	A17	SF95-4	4.11	17.7
			NT3G23	UO2	A17	SF95-5	4.11	25.4
			NT3G23	UO2-Gd2O3	C13	SF96-1	2.63	24.4
			NT3G23	UO2-Gd2O3	C13	SF96-2	2.63	29.6
			NT3G23	UO2-Gd2O3	C13	SF96-3	2.63	30.4
			NT3G23	UO2-Gd2O3	C13	SF96-4	2.63	30.4
			NT3G24	UO2-Gd2O3	C13	SF96-5	2.63	30.7
			NT3G24	UO2	J17	SF97-1	4.11	35.4
			NT3G24	UO2	J17	SF97-2	4.11	36.7
			NT3G24	UO2	J17	SF97-3	4.11	40.8
			NT3G24	UO2	J17	SF97-4	4.11	42.2
			NT3G24	UO2	J17	SF97-5	4.11	47.0
			NT3G24	UO2	J17	SF97-6	4.11	47.3
TMI 1 15 × 15	YMP	GE-VNC	NJ070G	UO2	O1	O1-S1	4.657	25.8
			NJ070G	UO2	O1	O1-S2	4.657	29.9
			NJ070G	UO2	O1	O1-S3	4.657	26.7
			NJ070G	UO2	O12	O12-S4	4.657	23.7
			NJ070G	UO2	O12	O12-S5	4.657	26.5
			NJ070G	UO2	O12	O12-S6	4.657	24.0
			NJ070G	UO2	O13	O13-S7	4.657	22.8
			NJ070G	UO2	O13	O13-S8	4.657	26.3
		ANL	NY05YU	UO2	H6	A1B	4.013	44.8
			NY05YU	UO2	H6	D2	4.013	44.8
			NY05YU	UO2	H6	B2	4.013	50.1
			NY05YU	UO2	H6	C1	4.013	50.2
			NY05YU	UO2	H6	D1A4	4.013	50.4
			NY05YU	UO2	H6	A2	4.013	50.6
			NY05YU	UO2	H6	C3	4.013	51.3
			NY05YU	UO2	H6	C2B	4.013	52.6
			NY05YU	UO2	H6	B3J	4.013	53.0
			NY05YU	UO2	H6	B1B	4.013	54.5
			NY05YU	UO2	H6	D1A2	4.013	55.7
GKN II 18 × 18	REBUS	SCK•CEN	416	UO2	M11	MA11	3.8	54.1
Gösgen 15 × 15	ARIANE	ITU	1601/1701	UO2	P7/R11	GU4	4.1	31.1
		SCK•CEN, ITU	1601/1701	UO2	P7/R11	GU3	4.1	52.5
		SCK•CEN	12-40	UO2	M13	GU1	3.5	60.7
	MALIBU	SCK•CEN	19-64	UO2	F12	GGU2/2	4.3	46.0
		PSI	19-64	UO2	F12	GGU2/1	4.3	50.8
		CEA, PSI	19-64	UO2	F12	GGU1	4.3	70.3
Vandellos II 17 × 17	ENUSA/ CSN	Studsvik	EC45/EF05	UO2	WZR0058	E58-88	4.498	42.5
			EC45/EF05	UO2	WZR0058	E58-148	4.498	54.8
			EC45/EF05	UO2	WZR0058	E58-260	4.498	64.6
			EC45/EF05	UO2	WZR0058	E58-700	4.498	77.0
			EC45/EF05	UO2	WZtR165	165-2a	4.498	78.3
			EC46/EF05	UO2	WZtR160	160-800	4.498	70.9

The ATM-104 data served as the basis for the Organisation for Economic Co-operation and Development (OECD)/Nuclear Energy Agency (NEA) burnup credit criticality safety calculation benchmark Phase I-B.[9] The assembly design, operating data, and isotopic results are available publicly through the NEA Spent Fuel Isotopic Composition Database (SFCOMPO).[10]
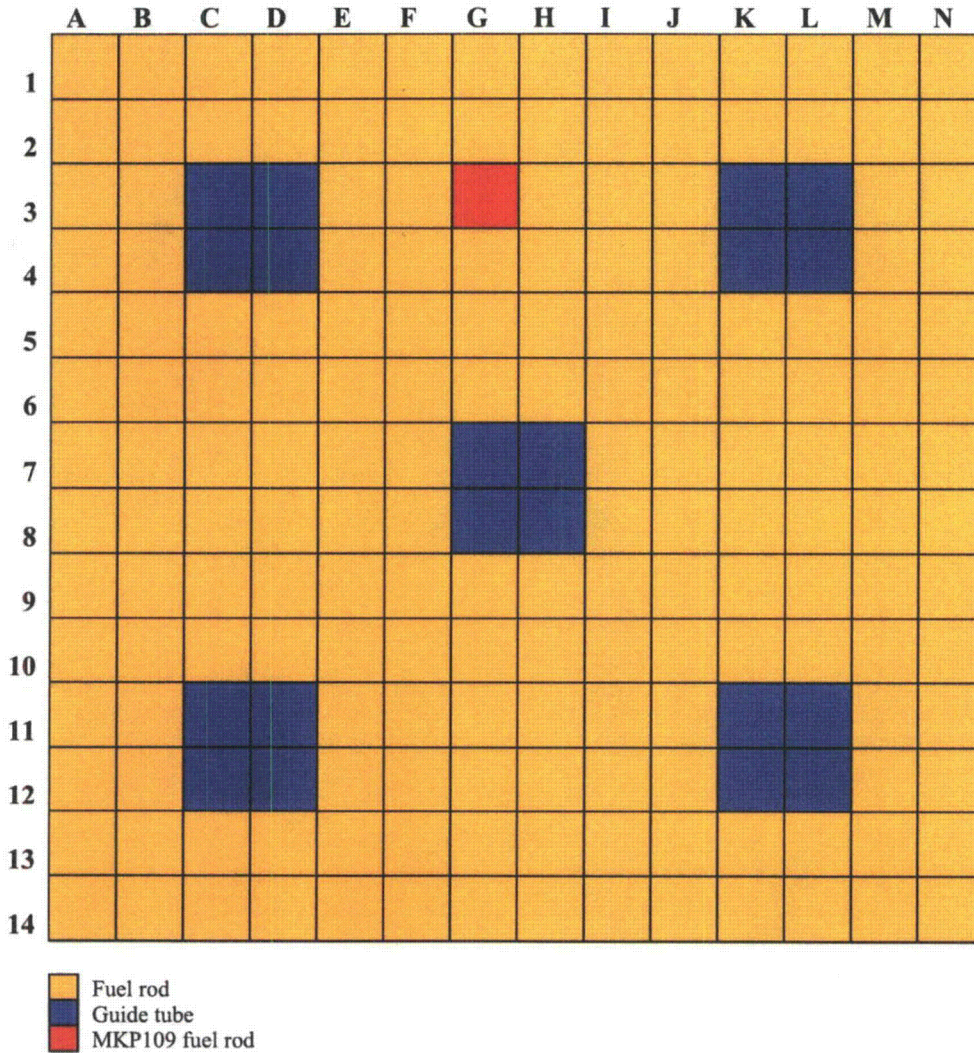
Figure 2.1. Layout for Calvert Cliffs 1 assembly D047.

2.2   Takahama 3

The Japan Atomic Energy Research Institute (JAERI) carried out a series of projects from 1990 to 1999 to obtain high-quality experimental isotopic assay data to support the development of burnup credit for storage and transport of spent fuel. The measurements included destructive radiochemical analyses of 16 spent fuel samples from 3 fuel rods identified as SF95, SF96, and SF97.[11,12] Rods SF95 and SF97 were standard UO_2 fuel rods with 4.11 wt % ^{235}U initial enrichment; SF96 was a UO_2-Gd_2O_3 poison rod with an initial fuel enrichment of 2.63 wt % ^{235}U and a Gd_2O_3 content of 6%. Rods SF95 and SF96 were

from assembly NT3G23, and rod SF97 was from assembly NT3G24. These two assemblies were standard 17×17 design, with 264 fuel rods and 25 water-filled guide tubes. Fourteen of the fuel rods in each of these assemblies contained Gd_2O_3 poison.

Assembly NT3G23 was irradiated in the reactor for two consecutive cycles, cycle 5 and cycle 6. Assembly NT3G24 was irradiated for three consecutive cycles, starting from cycle 5. The configuration of the assembly, including the location of the measured rods, is illustrated in Figure 2.2. The design and operating data and isotopic results are available publicly through the Spent Fuel Isotopic Composition Database (SFCOMPO) database.[15]
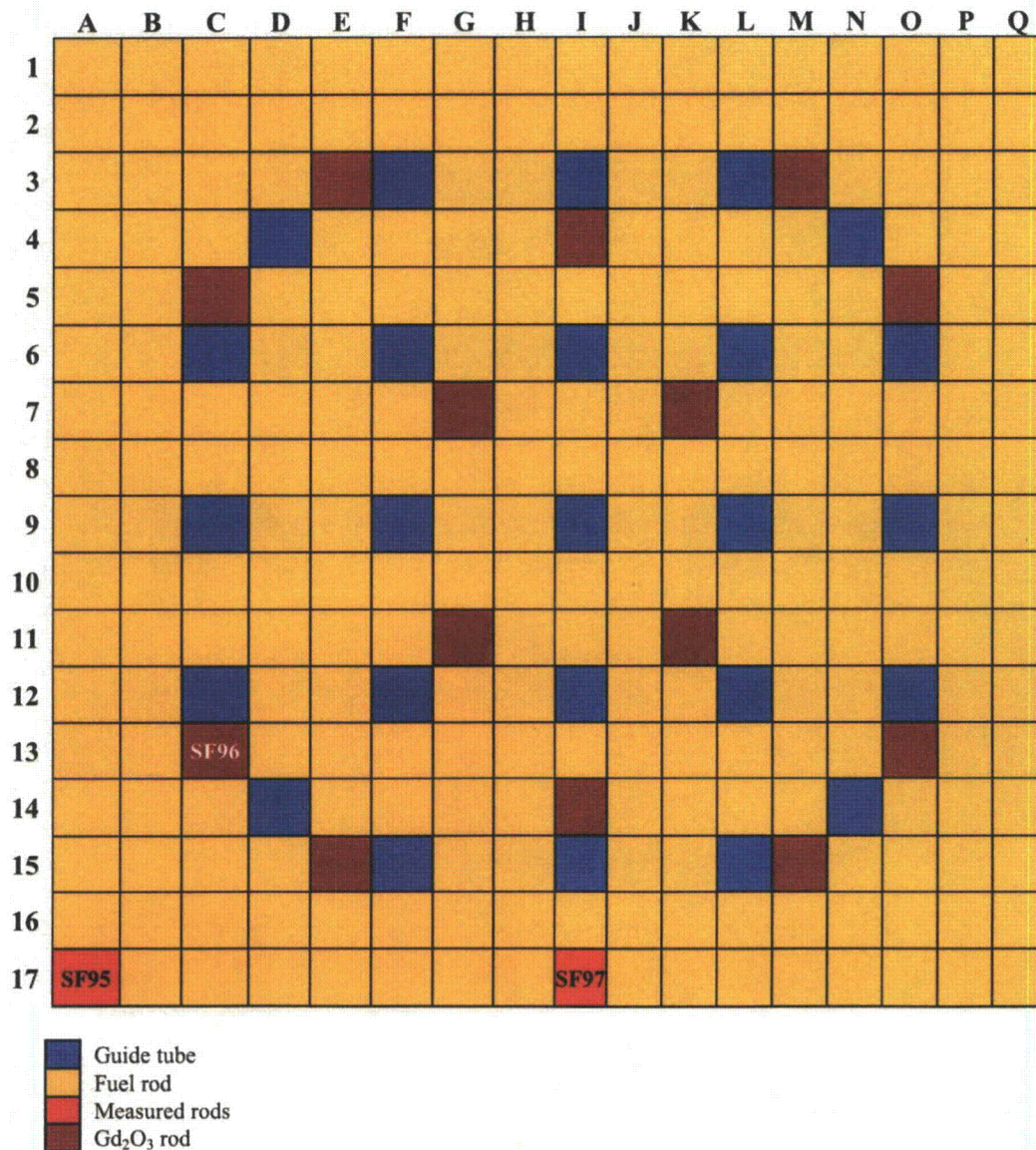
Figure 2.2. Layout for Takahama-3 assemblies NT3G23 and NT3G24 and sample locations.

The sample burnup was determined by JAERI from measurements using the ASTM Standard Test Method E 321 (Neodymium-148 method). The burnup of samples from the two UO_2 fuel rods, SF95 and SF97, were between 14 and 47 GWd/MTU. The burnup of samples from the UO_2-Gd_2O_3 poison rod SF96, estimated by JAERI, were between 7.8 and 28.9 GWd/MTU. It was found in a previous study[2] that the use of sample burnup values reported by JAERI for the SF96 samples resulted in predicted ^{148}Nd concentrations that were 5 to 9% less than the measured concentrations. The differences are likely due to a limitation of the ASTM ^{148}Nd method to estimate burnup for fuels containing burnable poisons, since the standard method does not account for the energy produced by neutron capture in the gadolinium poison. This energy contribution is typically included in most physics codes. Therefore, in this study the calculations were performed to a burnup that matched the measured ^{148}Nd content of the fuel.

2.3 Three Mile Island 1

Measurements on 19 spent fuel samples from the TMI-1 reactor were performed under the auspices of the U.S. Department of Energy (DOE) Office of Civilian Radioactive Waste Management (OCRWM) Yucca Mountain Project in 1998–2000.[13] Fuel rods were obtained from two assemblies, identified as NJ05YU and NJ070G. Both assemblies are B&W 15 × 15 Mark II design, with 208 fuel rods, 16 guide tubes, and 1 instrument tube. Radiochemical analyses were performed at two independent analytical laboratories—Argonne National Laboratory (ANL) and the General Electric Vallecitos Nuclear Center (GE-VNC).

Measurements for 11 samples from rod H6 of assembly NJ05YU were performed in 1998 and 2000 at ANL.[14,15] Fuel rod H6 was irradiated for two cycles (cycles 9 and 10), achieving sample burnups from 45 to 56 GWd/MTU. Assembly NJ05YU contained 16 burnable poison rods (BPRs) with Al_2O_3–B_4C absorber, which were present during cycle 9. All the fuel rods in this assembly had an initial fuel enrichment of 4.013 wt % ^{235}U.

Another eight measured samples were from three rods—O1, O12, and O13—of assembly NJ070G and were analyzed in 1999 at GE-VNC.[16] Assembly NJ070G was present in the reactor during cycle 10 only, and it also contained 16 BPRs during this cycle. Four fuel rods in assembly NJ070G had 2.0 wt % Gd_2O_3 poison with an initial enrichment of 4.19 wt % ^{235}U. The other 204 regular fuel rods had an initial enrichment of 4.657 wt % ^{235}U. The measured samples from rods O1, O12, and O13 achieved burnups between 23 and 30 GWd/MTU. The location of the measured rods in both assemblies is shown in Figure 2.3.

Both assemblies were standard commercial designs. However, during cycle 10 the reactor experienced anomalies that resulted in significant deposits (crud and/or oxide layers) on fuel rods and fuel failures.[17] The rods used in the present study were selected for postirradiation examinations to investigate the cause of the anomalies. Rods O2, O4 through O8, and O11, not included in this study, were known to have failed. Consequently, the TMI-1 fuel may have experienced nontypical operating conditions and possible geometry perturbations (e.g., rod bowing) and/or temperature variances caused by deviation from normal design parameters. The uncertainties in the actual operating conditions need to be considered when evaluating calculated TMI-1 results.
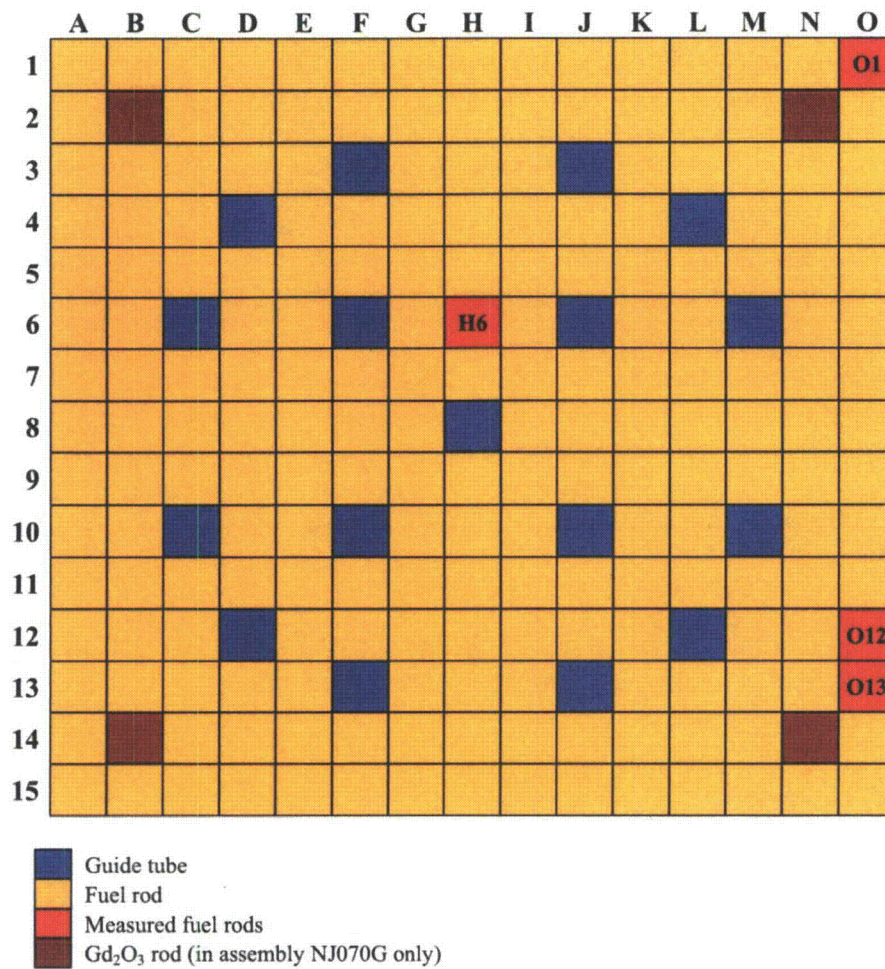
Figure 2.3. Layout for TMI-1 assembly NJ05YU (rod H6) and NJ070G (rods O1, O12, O13).

2.4 Gösgen

A total of six UO_2 samples were measured from fuel rods irradiated in the Gösgen PWR reactor operated in Switzerland. The Gösgen reactor operates with a 15 × 15 fuel assembly design with 205 fuel rods and 20 guide tubes. Three samples were measured as part of the ARIANE (Actinides Research In A Nuclear Element) international program[18,19,20] managed by Belgonucleaire. Three additional high burnup samples were analyzed in the MALIBU (Radiochemical Analysis of MOX and UOX LWR Fuels Irradiated to High Burnup) program,[21] now managed by Studiecentrum voor Kernenergie–Centre d'Étude de l'Énergie Nucléaire (SCK•CEN) in Belgium. Measurements have been carried out on both low enriched uranium oxide (UOX) and mixed oxide (MOX) fuels under these programs; however, only the UO_2 samples are evaluated in this report.

These internationally sponsored programs are designed to provide very high-quality evaluated isotopic measurement data for computer code validation. An important element of these programs is the use of independent laboratories to cross-check radiochemical assay measurements to reduce the measurement uncertainties and improve confidence in the data. The laboratories participating in the ARIANE program were SCK•CEN in Belgium, Paul Scherrer Institute (PSI) in Switzerland, and the Institute for Transuranium Elements (ITU) in Germany. The MALIBU program laboratories included SCK•CEN, PSI, and Commissariat à l'Énergie Atomique (CEA) in France.

ARIANE samples evaluated in this study are designated as GU1, GU3, and GU4. Sample GU1 had an initial enrichment of 3.5 wt % ^{235}U and was from assembly 12-40, irradiated for four consecutive cycles, starting in cycle 12. The GU1 fuel rod resided next to a control rod guide tube. Several of the fuel rods adjacent to the GU1 rod were replaced in the last two irradiation cycles (14 and 15). The other two samples, GU3 and GU4, were obtained from a rod of assembly 1601 with an initial enrichment of 4.1 wt % ^{235}U and irradiated for three consecutive cycles, starting in cycle 16. The GU3/4 rod was irradiated in assembly 1601 during cycle 16 and cycle 17 and in assembly 1701 during cycle 18. Assembly 1701 had an initial enrichment of 4.3 wt % ^{235}U and was previously irradiated during cycle 17. The GU1, GU3, and GU4 samples had burnups of 60.7, 52.5, and 31.1 GWd/MTU, respectively.

The MALIBU samples, designated GGU1, GGU2/1, and GGU2/2, were obtained from the same fuel rod of assembly 19-64. The initial enrichment of the fuel in this assembly was 4.3 wt % ^{235}U. Sample GGU1 was taken from the location of peak axial burnup of 70.3 GWd/MTU, and samples GGU2/1 and GGU2/2 were obtained from the lower end of the rod and had a burnup of 50.8 and 46.0 GWd/MTU, respectively. Assembly 19-64 was irradiated four consecutive cycles, from cycle 19 to cycle 22. The layout of the Gösgen assemblies showing the location of the measured rods is illustrated in Figure 2.4.

The Gösgen reactor started operating with MOX fuel assemblies in 1997. Therefore, the UO_2 fuels measured under the ARIANE program (discharged in 1994) were not exposed to MOX fuel. However, the UO_2 fuel measured under the MALIBU program was exposed to MOX fuel. Typically, MOX cores operate with about 1/3 MOX fuel assemblies, while the other assemblies are standard UO_2 assemblies. The impact of MOX fuel residing adjacent to the measured assemblies was investigated and found to be minor. Moreover, the GGU2 fuel rod was located away from the periphery of the assembly and was not subject to spectral and flux gradient effects due to the presence of the MOX fuel.

The relocation of the measured fuel rods in the ARIANE program adds considerable complexity and some additional uncertainty to the analysis. For the GU1 rod, the replacement rods in assembly 12-40 were indicated to have a burnup very similar to that of the original rods. Therefore, explicit modeling of the rod replacement was not considered to be necessary. However, for the GU3/4 rod, the second assembly (1701) had a burnup considerably lower than the original assembly (1601). To prevent

potentially biasing the calculated results due to the possible spectral changes caused my moving the fuel rod to another assembly during the last cycle, the calculations explicitly modeled the burnup of fuel rods in assemblies 1601 and 1701, and included the reconstitution of fuel rods in assembly 1701 in cycle 18.
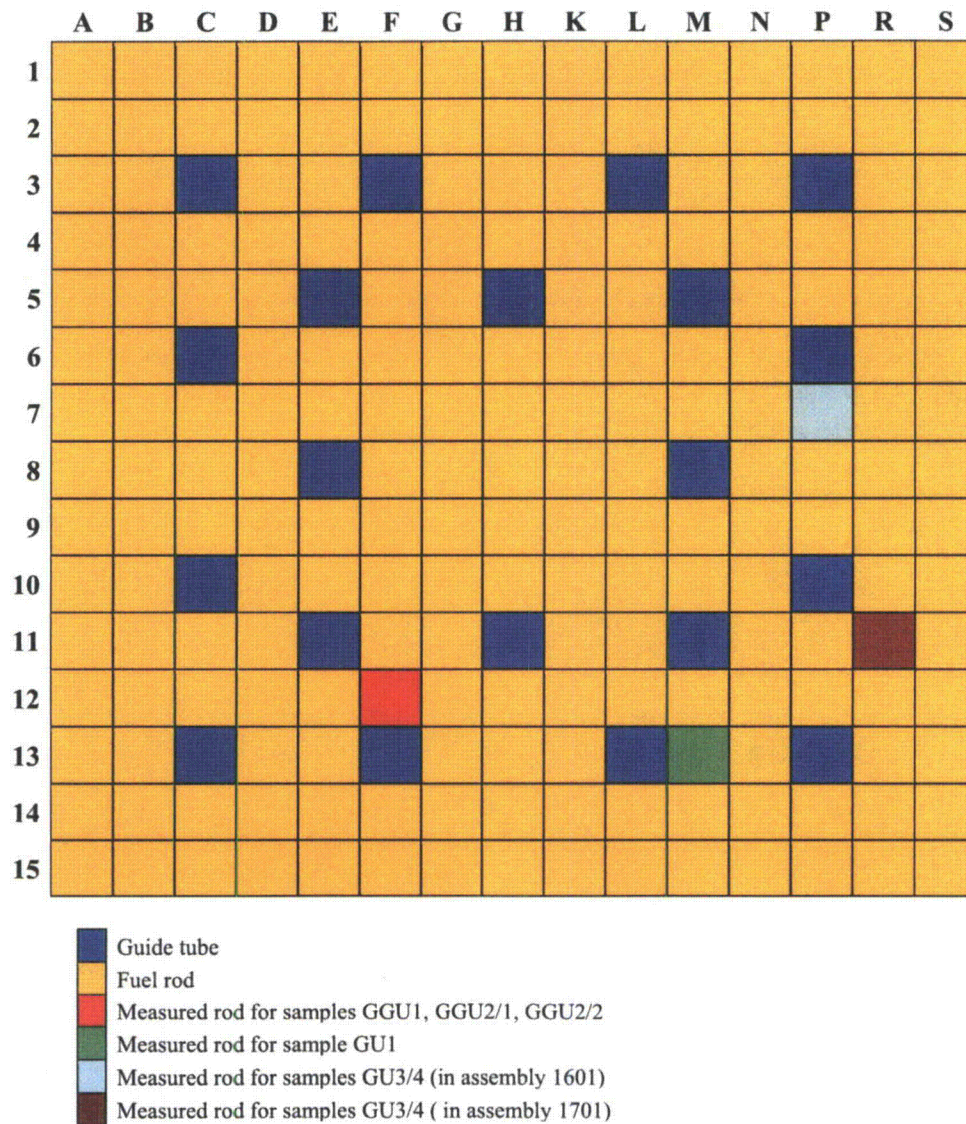
Figure 2.4. Assembly layout and positions of Gösgen ARIANE and MALIBU samples.

2.5 GKN II

Isotopic measurements were reported in the REBUS[22] (Reactivity Tests for a Direct Evaluation of the Burnup Credit on Selected irradiated LWR fuel bundles) International Program for one UO_2 fuel sample from 18 × 18 PWR assembly 416 operated in the GKN II reactor located in Neckarwestheim, Germany. The assembly had 300 fuel rods and 24 guide tubes. Twelve of the fuel rods contained Gd_2O_3 at 7.0 wt % and had an initial enrichment of 2.6 wt % ^{235}U; the regular fuel rods had an initial enrichment of 3.8 wt % ^{235}U. The assembly was irradiated for four consecutive cycles, from cycle 5 to 8, and was discharged in 1997. The measured sample was obtained from a section of UO_2 fuel rod M11 that included approximately three fuel pellets. The sample achieved a burnup of 54.0 GWd/MTU.

The REBUS Program, managed by Belgonucleaire, was dedicated to the validation of computer codes for criticality calculations that take into account the reduction of reactivity of spent fuel due to burnup (burnup credit). REBUS involved critical measurements in the VENUS facility using spent fuel rod segments. These segments were later destructively assayed to measure the isotopic content of the fuel. The isotopic results were measured by the SCK•CEN laboratory.

Although the GKN II reactor currently operates with a MOX core, assembly 416 was irradiated in the reactor during a period when it operated only with UO_2 fuel and, therefore, was not subject to possible effects from adjacent MOX assemblies. Rod M11 was located towards the interior of assembly 416, away from the guide tubes and, therefore, is expected to have resided in an asymptotic region of uniform flux (Figure 2.5).

2.6 Vandellós II

Six spent fuel samples were measured from three fuel rods, identified as WZR0058, WZtR165, and WZtR160, from two 17 × 17 fuel assemblies irradiated in the Vandellós II PWR reactor operated in Spain. The measurements were performed as part of a high burnup fuel program coordinated by the Spanish safety council Consejo de Seguridad Nuclear (CSN), fuel vendor Empresa Nacional del Uranio, S.A. (ENUSA), and research organization Empresa Nacional de Residuo Radioactivo (ENRESA).[23,24] The Vandellós fuel samples from the Spanish program represent the highest burnup samples evaluated in this report. The samples had a 4.498 wt % ^{235}U initial enrichment and achieved burnup values from 43 to 78 GWd/MTU. The isotopic measurements were performed at Studsvik Nuclear Laboratory in Sweden.

The rods were irradiated for five consecutive cycles, from cycle 7 to cycle 11. From cycle 7 to 10, rods WZR0058 and WZtR165 resided in assembly EC45 and rod WZtR160 resided in assembly EC46. The initial enrichment of assemblies EC45 and EC46 was 4.498 wt % ^{235}U. After cycle 10, the rods were removed from their original assemblies and inserted into rebuilt assembly EF05 and irradiated during cycle 11. Assembly EF05, with 4.240 wt % ^{235}U initial enrichment, had a burnup of 26.5 GWd/MTU at end-of-cycle (EOC) 10.

The 17 × 17 assemblies have 264 fuel rods, 24 guide tubes, and 1 instrument tube; no burnable poison rods or gadolinium-bearing rods were present in the assembly during any of the irradiation cycles. The layout of the assemblies showing the locations of the measured rods in the original and rebuilt assemblies is illustrated in Figure 2.6. During cycles 7 to 10, all three rods are located at the periphery of the fuel assembly. Assemblies EC45 and EC46 were located at the edge of the core during cycle 10.
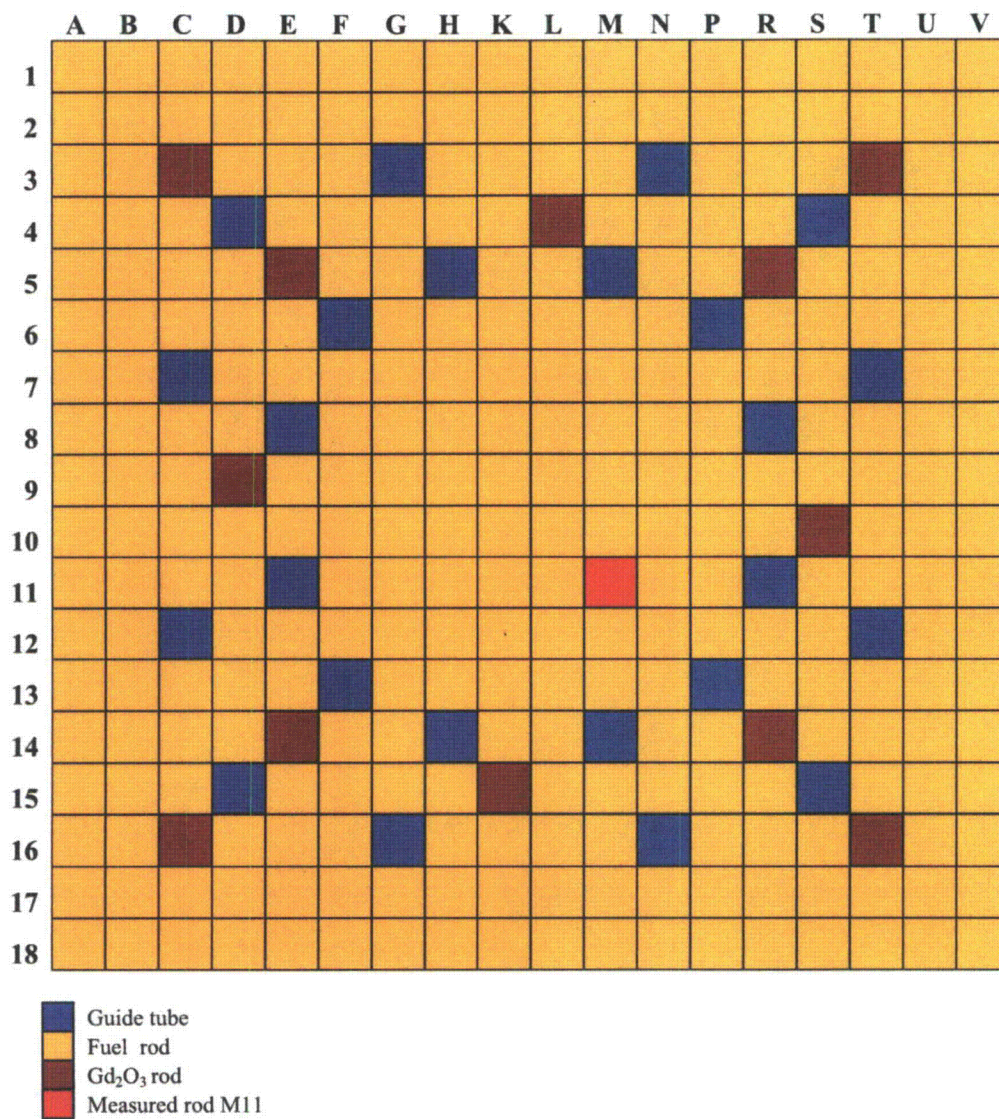
Figure 2.5. Assembly layout for GKN II (REBUS) sample rod M11.

Similar to the analysis of the ARIANE GU3/4 samples, modeling the relocation of the Vandellós fuel rods in cycle 11 adds considerable complexity to the calculations, but was considered necessary due to the significant nature of the reconfiguration. In addition, the location of the assemblies at the core edge in cycle 10 resulted in some measured rods being aligned at the core periphery, and subjected to additional moderation. To minimize any bias in the calculated results due to approximations in the actual configuration, assembly boundary regions were explicitly modeled. The added complexity also adds uncertainty in the models and this should be considered when analyzing the validation results.

Standard fuel rod
Measured rod WZR0058 in cycles 7-10 (A12 of assembly EC45)
Measured rod WZR0058 in cycle 11 (O5 of assembly EF05)
Measured rod WZtR165 in cycles 7-10 (Q10 of assembly EC45)
Measured rod WZtR165 in cycle 11 (M3 of assembly EF05)
Measured rod WZtR160 in cycles 7-10 (A10 of assembly EC46)
Measured rod WZtR160 in cycle 11 (E15 of assembly EF05)
Guide tube
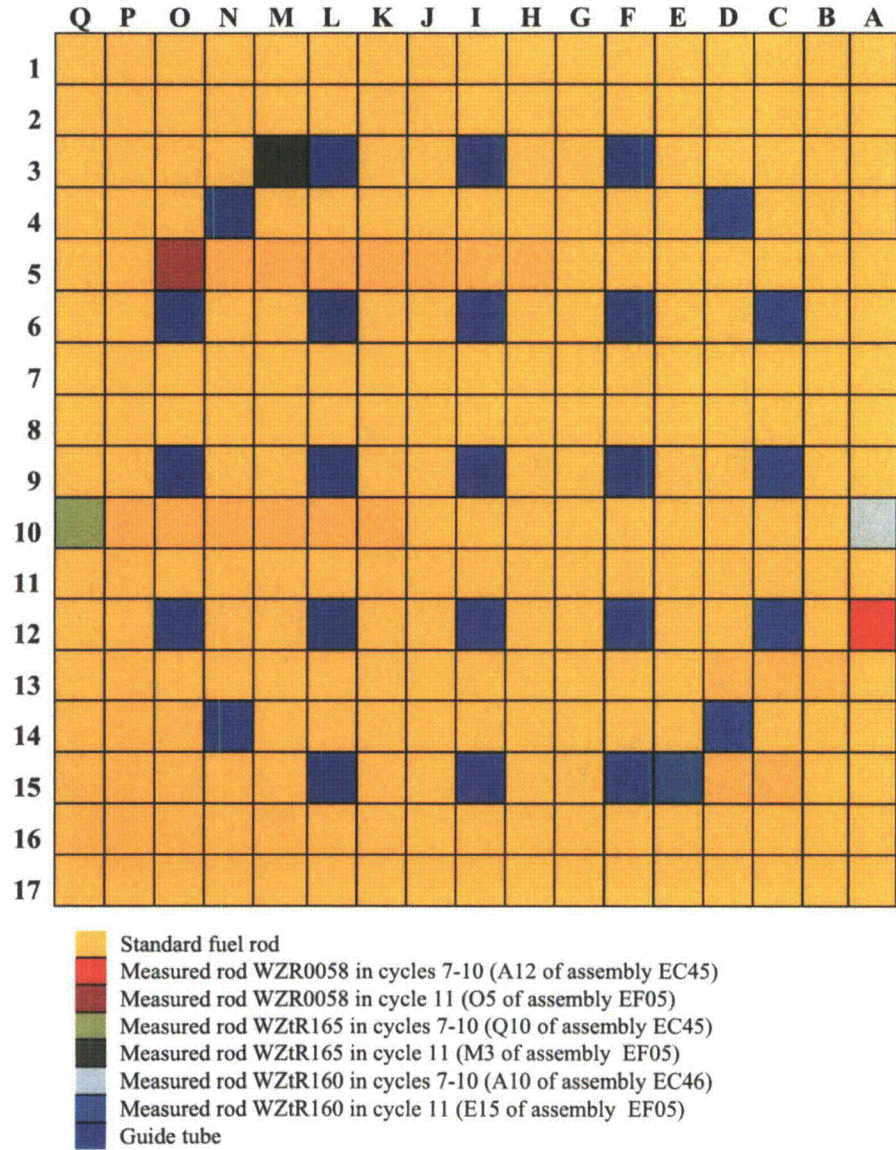
Figure 2.6. Assembly layout for Vandellós II samples.

3 MEASUREMENT METHODS AND UNCERTAINTIES

The accuracy and precision of the measurements are considerations in the evaluation of experimental data and in establishing estimates of bias and uncertainty in computational models. The precision is dependent on many factors including the fuel dissolution procedures, isotopic concentration in the sample, chemical separations techniques, mass spectrometry analysis methods and instruments, calibration methods, and standards.

Thermal Ionization Mass Spectrometry (TIMS) is generally used for high precision measurements of uranium, plutonium, and neodymium isotopes. However, several laboratories use Inductively Coupled Plasma Mass Spectrometry (ICPMS), which has lower precision but offers more rapid and cost-effective routine analysis of nuclides. These measurements provide the isotopic distribution of mass for each element. The measurement of absolute nuclide content requires the use of standard spike solutions (isotopic dilution), calibration with external sources, or other techniques such as α or γ counting to determine the absolute content for one of the isotopes. Therefore, the accuracy of the measurements is highly dependent on both the mass spectrometry methods and the method of calibration.

This section summarizes the measurement methods and the accuracies as estimated by each laboratory. The main experimental methods and the experimental uncertainties, expressed in terms of relative standard deviation (RSD), for each isotope measured at each of the laboratories are listed in Table 3.1 and Table 3.2. The reported accuracies are, in some cases, estimated based on different measures of uncertainty. Some laboratories report the error based only on repeat measurements of standard solutions (instrument precision). Other laboratories report errors based on benchmark exercises and past experience in analyzing fuel samples that include uncertainties and bias due to sample preparations, chemical techniques, instrument precision, and drift. Some cross-check measurements performed by independent laboratories provide the most reliable method of confirming the estimated measurement uncertainties. Measurement errors were not reported for the PNNL measurements of ^{133}Cs.

3.1 PNNL Measurements

The isotopic measurements performed by PNNL under the ATM-104 program at the Materials Characterization Center (MCC) were made using the following main analytical methods:

- γ-spectrometry for ^{137}Cs;
- α-spectrometry for ^{241}Am and ^{237}Np;
- β-spectrometry for ^{99}Tc and ^{90}Sr;
- Isotope dilution mass spectrometry (IDMS) for Nd, U, and Pu nuclides using a calibrated triple spike of ^{150}Nd, ^{233}U, and ^{242}Pu;
- Mass spectrometry (MS) after elemental separation of Cs, for ^{133}Cs and ^{135}Cs; and
- ICPMS measurements relative to ^{143}Nd and ^{145}Nd for lanthanide elements Sm, Eu, and Gd.

The lanthanide measurements performed by PNNL were carried out by ICPMS without previous chemical separation into individual elements. Therefore, there was isotopic interference for the elements corresponding to nuclides with mass numbers 147 (Pm, Sm), 150 (Nd, Sm), 151 (Sm, Eu), and 155 (Eu, Gd). The reported data corresponding to these four mass numbers were adjusted by PNNL based on calculations in order to infer information for individual isotopes. The PNNL lanthanide data are not considered for validation purposes in this report to avoid introducing uncertainties related to the calculated adjustments.[7]

Table 3.1. Summary of actinide measurement methods and estimated uncertainties

Nuclide ID	PNNL Method[a]	PNNL RSD[b] (%)	KRI Method	KRI RSD (%)	JAERI Method	JAERI RSD (%)	GE-VNC Method	GE-VNC RSD (%)	ANL Method	ANL RSD (%)	Studsvik Method	Studsvik RSD (%)	SCK•CEN Method	SCK•CEN RSD (%)	ITU Method	ITU RSD (%)	CEA Method	CEA RSD (%)	PSI Method	PSI RSD (%)
^{234}U	IDMS	1.6			IDMS	1.0	TIMS	0.5	ICPMS	4.4	ICPMS	22.0	TIMS	2.5	TIMS	0.0	TIMS	3.2	ICPMS	1.5
^{235}U	IDMS	1.6			IDMS	0.1	TIMS	0.5	ICPMS	3.7	ICPMS	8.7	TIMS	1.0	TIMS	1.2	TIMS	3.0	ICPMS	1.9
^{236}U	IDMS	1.6			IDMS	2.0	TIMS	0.5	ICPMS	5.8	ICPMS	6.9	TIMS	0.4	TIMS	0.8	TIMS	3.0	ICPMS	0.6
^{238}U	IDMS	1.6			IDMS	0.1	TIMS	0.5	ICPMS	4.2	ICPMS	na	TIMS	0.3	TIMS	0.0	TIMS	3.1	ICPMS	0.6
^{238}Pu	IDMS	1.6			IDMS	0.5	α-sp	2.5	α-sp	7.9	ICPMS	7.0	TIMS, α-sp	1.6	TIMS	1.1	TIMS	3.1	ICPMS	9.8
^{239}Pu	IDMS	1.6			IDMS	0.3	TIMS	0.6	ICPMS	5.7	ICPMS	5.8	TIMS	0.3	TIMS	0.3	TIMS	3.1	ICPMS	4.5
^{240}Pu	IDMS	1.6			IDMS	0.3	TIMS	0.6	ICPMS	6.2	ICPMS	6.6	TIMS	0.3	TIMS	0.3	TIMS	3.1	ICPMS	4.5
^{241}Pu	IDMS	1.6			IDMS	0.3	TIMS	0.6	ICPMS	4.6	ICPMS	6.9	TIMS	0.3	TIMS	1.7	TIMS	3.1	ICPMS	4.5
^{242}Pu	IDMS	1.6			IDMS	0.3	TIMS	0.6	ICPMS	6.7	ICPMS	6.9	TIMS	0.3	TIMS	0.3	TIMS	3.1	ICPMS	4.5
^{237}Np	α-sp	1.9			α-sp	10.0	α-sp	2.9	ICPMS	5.6	ICPMS	8.5	ICPMS	10.0	ICPMS	4.8	ICPMS	4.6	ICPMS	4.5
^{241}Am	α-sp	4.9			MS, α-sp	2.0	TIMS, α-sp	3.5	γ-sp	7.1	ICPMS	4.9	TIMS	1.8	ICPMS	5.9	TIMS	3.3	ICPMS	1.2
^{242m}Am					MS, α-sp	10.0	TIMS, α-sp	3.5	ICPMS	3.1			TIMS	5.5			TIMS	3.1	ICPMS	16.5
^{243}Am					MS, α-sp	5.0	TIMS, α-sp	3.5	ICPMS	5.9	ICPMS	8.4	TIMS	1.8	ICPMS	6.7	TIMS	3.1	ICPMS	1.2
^{242}Cm					MS, α-sp	10.0	TIMS, α-sp	10.0					α-sp	16.0			TIMS	10.5		
^{243}Cm					MS, α-sp	2.0	TIMS, α-sp	2.75					γ-sp	36.8			TIMS	3.1		
^{244}Cm					MS, α-sp	2.0	TIMS, α-sp	2.75			ICPMS	10.0	α-sp	1.8	ICPMS	6.4	TIMS	3.1	ICPMS	1.5
^{245}Cm					MS, α-sp	2.0	TIMS, α-sp	2.75					TIMS	2.9	ICPMS	10.2	TIMS	3.1	ICPMS	1.5
^{246}Cm					MS, α-sp	5.0					ICPMS	22.0	TIMS	10.1			TIMS	3.1	ICPMS	1.5
^{247}Cm					MS, α-sp	10.0														

[a] Main analytical technique is listed; some nuclides required multiple techniques to eliminate interferences.

[b] Laboratory relative standard deviation (RSD) values shown are the maximum of the measurement errors reported for the samples evaluated in this report.

Table 3.2. Summary of fission product measurement methods and uncertainties

Nuclide ID	PNNL Method[a]	PNNL RSD[b] (%)	KRI Method	KRI RSD (%)	JAERI Method	JAERI RSD (%)	GE-VNC Method	GE-VNC RSD (%)	ANL Method	ANL RSD (%)	Studsvik Method	Studsvik RSD (%)	SCK•CEN Method	SCK•CEN RSD (%)	ITU Method	ITU RSD (%)	CEA Method	CEA RSD (%)	PSI Method	PSI RSD (%)
^{133}Cs	IDMS	N/A									ICPMS	8.0	TIMS	2.5	ICPMS	1.6	TIMS	3.2	ICPMS	1.9
^{134}Cs					γ-sp	3.0	γ-sp	1.75			γ-sp	14.7	TIMS	2.5	ICPMS	4.1	TIMS	3.2	ICPMS	1.9
^{135}Cs	IDMS	14.0									ICPMS	8.5	TIMS	2.5	ICPMS	1.7	TIMS	3.1	ICPMS	1.9
^{137}Cs	γ-sp	3.5			γ-sp	3.0	γ-sp	1.75	γ-sp	4.8	γ-sp	6.4	γ-sp	2.5	ICPMS	1.5	TIMS	3.2	ICPMS	1.9
^{140}Ce											ICPMS	2.4								
^{142}Ce											ICPMS	2.6								
^{144}Ce					γ-sp	10.0					γ-sp	14.1	γ-sp	5.0			γ-sp	22.7	γ-sp	21.1
^{142}Nd					IDMS	0.1					ICPMS	7.9	TIMS	5.0	ICPMS	5.1	TIMS	3.3	ICPMS	5.0
^{143}Nd	IDMS	1.0			IDMS	0.1	TIMS	0.75	ICPMS	5.5	ICPMS	4.3	TIMS	0.3	ICPMS	6.2	TIMS	3.1	ICPMS	4.9
^{144}Nd	IDMS	N/A			IDMS	0.1					ICPMS	4.8	TIMS	0.3	ICPMS	5.9	TIMS	3.1	ICPMS	4.9
^{145}Nd	IDMS	1.0			IDMS	0.1	TIMS	0.75	ICPMS	6.2	ICPMS	4.4	TIMS	0.3	ICPMS	5.9	TIMS	3.1	ICPMS	4.9
^{146}Nd	IDMS	N/A			IDMS	0.1	TIMS	0.75			ICPMS	4.3	TIMS	0.3	ICPMS	7.4	TIMS	3.1	ICPMS	4.9
^{148}Nd	IDMS	N/A			IDMS	0.1	TIMS	0.75	ICPMS	7.1	ICPMS	4.5	TIMS	0.3	ICPMS	6.7	TIMS	3.0	ICPMS	5.0
^{150}Nd	IDMS	N/A			IDMS	0.1	TIMS	0.75			ICPMS	5.2	TIMS	0.3	ICPMS	6.8	TIMS	3.1	ICPMS	5.3
^{147}Pm													β-sp	9.0	ICPMS	6.8	ICPMS	12.9	ICPMS	16.7
^{147}Sm			MS, LA	3.8	IDMS	0.1	TIMS	0.85	ICPMS	10.1	ICPMS	4.7	TIMS	5.0	ICPMS	10.6	ICPMS	3.2	ICPMS	1.6
^{148}Sm			MS, LA	3.8	IDMS	0.1					ICPMS	4.6	TIMS	0.4	ICPMS	4.0	ICPMS	3.1	ICPMS	1.5
^{149}Sm			MS, LA	20.1	IDMS	0.1	TIMS	0.9	ICPMS	8.1	ICPMS	8.3	TIMS	1.1	ICPMS	21.4	ICPMS	6.3	ICPMS	10.8
^{150}Sm			MS, LA	4.6	IDMS	0.1	TIMS	0.85	ICPMS	5.0	ICPMS	4.5	TIMS	0.4	ICPMS	3.4	ICPMS	3.1	ICPMS	1.5
^{151}Sm			MS, LA	38.5	IDMS	0.1	TIMS	0.85	ICPMS	7.1	ICPMS	5.4	TIMS	0.4	ICPMS	33.8	ICPMS	3.1	ICPMS	1.5
^{152}Sm			MS, LA	4.3	IDMS	0.1	TIMS	0.85	ICPMS	4.5	ICPMS	4.5	TIMS	0.4	ICPMS	3.2	ICPMS	3.1	ICPMS	1.5
^{154}Sm			MS, LA	6.0	IDMS	0.1					ICPMS	4.7	TIMS	0.4	ICPMS	10.6	ICPMS	3.1	ICPMS	1.6
^{151}Eu			MS, LA	9.9			TIMS	0.9	ICPMS	12.5	ICPMS	8.7	TIMS	1.0			ICPMS	8.7		
^{153}Eu			MS, LA	100.0			TIMS	0.9	ICPMS	5.2			TIMS	1.7	ICPMS	5.5	ICPMS	3.1	ICPMS	2.3
^{154}Eu			MS, LA, γ-sp	3.4	γ-sp	3.0					ICPMS	6.7	γ-sp	3.0	ICPMS	11.9	ICPMS	3.1	ICPMS	2.4
^{155}Eu			MS, LA, γ-sp	8.8					γ-sp	7.2		6.1	γ-sp	4.9	ICPMS	16.1	ICPMS	3.2	ICPMS	4.3
^{154}Gd			IDMS	3.9							ICPMS	5.9								
^{155}Gd			IDMS	4.2					TIMS	1.4	ICPMS	8.0	ICPMS	8.3	TIMS	2.5	ICPMS	6.9				
^{156}Gd			IDMS	3.9							ICPMS	4.6								
^{158}Gd			IDMS	3.9							ICPMS	4.8								
^{160}Gd			IDMS	12.1							ICPMS	19.4					ICPMS	3.4	ICPMS	4.4
^{90}Sr	β-sp	5.7											β-sp	8.0	ICPMS	0.4	TIMS	3.1	ICPMS	3.1
^{95}Mo									ICPMS	4.2			ICPMS	5.0	ICPMS	1.1	ICPMS	3.2	ICPMS	3.3
^{99}Tc	β-sp	3.5							ICPMS	8.0			ICPMS	8.8	ICPMS	0.9	ICPMS	3.1	ICPMS	3.8
^{101}Ru									ICPMS	5.8			ICPMS	12.2	ICPMS	0.9	ICPMS	3.9	ICPMS	3.6
^{106}Ru					γ-sp	5.0					γ-sp	15.0	γ-sp	14.2	ICPMS	4.1	γ-sp	20.1	γ-sp	14.3
^{103}Rh									ICPMS	3.8			ICPMS	4.9	ICPMS	3.3	ICPMS	4.5	ICPMS	1.9
^{109}Ag									ICPMS	5.9			ICPMS	9.1			ICPMS	7.0	ICPMS	31.8
^{125}Sb					γ-sp	10.0							ICPMS	9.4			γ-sp	13.7	γ-sp	17.0

[a] Main analytical technique is listed; some nuclides required multiple techniques to eliminate interferences.

[b] Laboratory relative standard deviation (RSD) values shown are the maximum of the measurement errors reported for the samples evaluated in this report. Values not reported are listed as N/A.

The metallic fission product ^{99}Tc was not evaluated in undissolved residues. Technetium and other metallic elements, most notably Rh, Ru, Pd, and Mo, segregate in irradiated fuels into a metallic, particulate phase that is virtually insoluble in nitric acid.[25] Significant discrepancies between ^{99}Tc measurements and predictions for the ATM-103 program[26] fuel were attributed to residual material that had not completely dissolved. However, significant discrepancies or indication of potentially undissolved material were not noted in the ATM-104 reports and the ^{99}Tc results were therefore used in this study.

3.2 KRI Measurements

More extensive lanthanide fission product measurements that used chemical separations were later performed at the Khlopin Radium Institute (KRI) in Russia[27] in 1995, at the request of PNNL, using archived ATM-104 fuel samples from rod MKP109. The KRI samples are referenced in other reports, and in this report, as 87-81, 87-72, and 87-63, respectively. In addition to measurements of specific nuclides [143]Nd, [145]Nd, [155]Eu, [155]Gd, [147]Sm, [149]Sm [151]Sm, and [152]Sm, KRI provided results for most isotopes of Nd, Eu, Sm, and Gd that could be measured by mass spectrometry.

The measurement methods included:

- Chemical separation of rare earth elements and transuranics followed by chemical separation of lanthanides elements,
- IDMS for neodymium and gadolinium isotopes using a spike of [142]Nd and [160]Gd,
- Luminescent analysis (LA)—laser induced fluorometry for absolute measurement of europium and samarium content in the sample,
- MS for europium and samarium nuclides to determine relative isotope ratios, and
- γ-spectrometry for [154]Eu and [155]Eu.

The experimental results were reported by KRI as the ratio of nuclide mass to [145]Nd mass and as the nuclide mass percentage relative to the corresponding element total mass. As absolute concentrations were not reported by KRI, the [145]Nd values measured by PNNL were used as the basis to renormalize the KRI data in units of g/g U in order to provide a consistent comparison with PNNL measurement data. A study of the KRI and PNNL relative atomic percent results, relative to [145]Nd concentration, showed that the neodymium isotopic data measured in all three samples at both laboratories agreed to within one standard deviation experimental uncertainty.[2]

The experimental error varies with the method and the nuclide under consideration. The uncertainties listed for KRI (Sm, Eu, Gd) include the error propagation due to the [145]Nd renormalization.

3.3 JAERI Measurements

The JAERI radiochemical analysis laboratory performed measurements for the Takahama-3 fuel samples. After sample cutting and dissolution, the elements were separated using an ion exchange separation column. The following main experimental techniques were used to determine the nuclide concentrations:[11]

- IDMS
  - major actinides: U, Pu
  - lanthanides: Nd, Sm
- α-spectrometry plus MS
  - Am, Cm
- γ-spectrometry
  - ^{106}Ru, ^{134}Cs, ^{137}Cs, ^{144}Ce, ^{154}Eu, ^{125}Sb
- α-spectrometry
  - ^{237}Np

The reported experimental uncertainties were not specific to each sample but were typical values based on previous experience. The reported uncertainties are less than 0.5% for all measured isotopes of Pu, Sm, Nd, ^{235}U, and ^{238}U. For minor actinides measured by MS and α-spectrometry, the experimental errors are larger, in the 2 to 10% range. The measurement errors for nuclides determined by γ-spectrometry are 3 to 10%. Based on experience with international programs that have used interlaboratory cross-check measurements, the reported uncertainties of <1% for U, Pu, Nd, and Sm appear to be unrealistically small. It is likely that these values represent the ability of the MS analytical instrument to reproduce results based on repeat measurements of solutions and may not account for all potential sources of bias and uncertainty.

3.4 GE-VNC Measurements

The GE-VNC laboratory performed isotopic measurements[16] for the samples selected from three fuel rods (O1, O12, O13) from TMI-1 assembly NJ070G. Most of the 32 nuclides measured at GE-VNC were determined by high precision TIMS and some through γ- or α-spectrometry. The GE-VNC measurements included most actinides and fission products but did not include the group of metallic fission products (e.g., Rh, Ru, Tc, Mo, and Ag) or ^{133}Cs.

The nuclide concentrations in the samples measured by TIMS were determined from measurements of spiked and unspiked samples. The experimental errors were reported as relative uncertainty at a 95% confidence level. The percent RSD uncertainty, shown in the table, was estimated as half (1/1.96) of the reported uncertainty at a 95% confidence level. The percent RSD uncertainty is 0.6% for all plutonium nuclides except ^{238}Pu, 0.5% for ^{235}U, and 0.8% for neodymium isotopes.

The nuclide concentrations were reported as g/g ^{238}U, where the ^{238}U value is the measured concentration in the sample after irradiation. To provide a consistent basis for the experimental data, the results were adjusted to a common basis of g/g U, where U is the mass of initial uranium (unirradiated).

3.5 ANL Measurements

ANL performed radiochemical isotopic analyses[14] for 11 samples cut from fuel rod H6 of TMI-1 assembly NJ05YU. The fuel segments were cut at GE-VNC but were measured only by ANL. The analysis samples were prepared by dissolution of small quantities (approximately 0.1–0.2 g aliquots) of crushed fuel powder, homogenized to provide a uniformity of <1.5% RSD, as determined by multiple measurements of uranium and plutonium isotopes. Analyses were carried out using a quadrupole ICPMS, γ-spectrometry, and α-spectrometry to determine the isotopic concentrations of 31 nuclides.

The measurements at ANL included all of the important actinides and most fission products considered important to burnup credit and other spent nuclear fuel safety applications, with the exception of the ^{133}Cs and ^{134}Cs isotopes. Measurements included metallic fission products in the main solution; however,

21

undissolved residues were not measured. The results were reported relative to the measured ^{238}U content in the sample, as g/g ^{238}U, and converted for this study to units of g/g U using the measurement data.

Two measures of experimental uncertainty were reported by ANL—a within-sample precision and a bias uncertainty. The within-sample precision was estimated by ANL as one standard deviation obtained through repeated measurements of a fuel sample. The bias uncertainty was estimated from deviations observed in two separate measurement campaigns involving duplicate fuel samples (obtained from fuel cut from adjacent segments of the rod) performed at different times. Phase I measurements were performed in September 1998, and Phase II measurements were performed in May 2000. Therefore, the precision and bias uncertainty estimated from these measurements is expected to provide a reliable estimate of the experimental error.

The total uncertainty is observed to be relatively large: 3.7% for ^{235}U, 4.2% for ^{238}U, and 5–8% for plutonium isotopes. A large 7.1% measurement error for ^{148}Nd is potentially problematic for isotopic validation purposes because ^{148}Nd is used to experimentally determine the burnup of the fuel sample. Any error in the burnup estimate will propagate as error in calculated values for all isotopes. This potential error must be considered in any evaluation of the data, as described in Section 5 of this report.

3.6 Studsvik Nuclear AB Measurements

Studsvik Nuclear AB performed isotopic analysis of spent fuel samples from the Vandellós II reactor. Measurements were carried out in two experimental campaigns: Phase I measurements,[28, 29, 30] performed in 2002–2003, and Phase 2 measurements,[31] performed in 2007. As part of the second experimental campaign at Studsvik, new measurements were performed to increase the number of available samples and improve the accuracy of the previous measurements. A reanalysis of samples E58-88 and E58-793 was carried out in the second campaign using solutions available from the initial campaign. Two new samples were measured in Phase 2: one sample identified as E58-257, cut from rod WZR0058, and one sample identified as 160-800, cut from rod WZtR160.

The measurements were performed using elemental separation and ICPMS for isotopic analysis. The measurements were carried out using three main methods:

- γ-scanning analysis
- ICPMS with external calibration
- ICPMS with isotopic dilution

The measurement data were reported as weight percentages relative to measured ^{238}U in the sample and converted in this study to units relative to initial uranium using measured data.

The magnitude of the errors for the measured nuclide concentrations varies with the experimental method and the concentration. For nuclides analyzed by γ-scanning, the reported errors are in the 12–15% range except for ^{137}Cs, which is about 6%. For the isotopes determined by ICPMS and external one-point calibration, the measurement errors are in the 8–10% range with the exception of ^{246}Cm, reported with an uncertainty of 15–22%. In the case of the actinides and fission products measured using isotope dilution, the experimental errors range between 2 and 22%, depending on the nuclide. The errors for ^{235}U are in the range 3 to 9%; ^{236}U, between 4 and 7%; and ^{234}U, between 7 and 22%. The plutonium nuclides were measured with an uncertainty of 3 to 8%. For the fission products analyzed by isotopic dilution, including Ce, Nd, Sm, Eu, and Gd (except ^{160}Gd), the experimental errors were, on average, between 2 and 5%.

3.7 SCK•CEN Measurements

SCK•CEN has performed isotopic measurements for fuel samples from the international experimental programs managed by Belgonucleaire.[21] The following main experimental techniques[20] have been applied for measurements performed at SCK•CEN:

- TIMS
  - major (U, Pu) and minor (Am and ^{245,246}Cm) actinides
  - lanthanides: Nd, Sm, ^{144}Ce, ^{155}Gd, ^{151}Eu, ^{153}Eu
  - Cs vector nuclides: $^{133-135}$Cs
- ICPMS with external calibration
  - metallics: ^{95}Mo, ^{99}Tc, ^{101}Ru, ^{103}Rh, ^{109}Ag, ^{125}Sb
  - ^{237}Np
- γ-spectrometry
  - ^{106}Ru, ^{137}Cs, ^{144}Ce, ^{154}Eu, ^{155}Eu, ^{243}Cm
- α-spectrometry
  - ^{242}Cm, ^{244}Cm
- β-spectrometry
  - ^{90}Sr

The metallic species (^{95}Mo, ^{99}Tc, ^{101}Ru, ^{103}Rh, ^{105}Pd, ^{108}Pd, and ^{109}Ag) frequently do not dissolve completely in nitric acid. Undissolved residues were analyzed separately by SCK•CEN and the results added to the concentrations measured in the main solutions. Based on experience in the ARIANE program, the fraction of undissolved material varies significantly for different samples and laboratories, from several percent to more than 50%, and the fraction was not observed to be highly dependent on the burnup of the fuel.

3.8 ITU Measurements

The fuel isotopic measurement methods used at ITU were similar to those used at SCK•CEN. The following two main experimental techniques[20] were used for measurements performed at ITU:

- TIMS
  - major actinides (U, Pu)
- ICPMS with ID (isotope dilution) analysis
  - all other measured nuclides

The measurements made exclusive use of ICPMS methods for the fission product nuclides. The reported ITU uncertainties are considerably larger than those reported by SCK•CEN. A cross-check analysis of the ITU measurements for sample GU3 with SCK•CEN results for the same sample indicated a systematic bias for some of the ITU results relative to the higher precision TIMS methods used by SCK•CEN. In particular, discrepancies likely associated with the ITU measurements were noted for Am, Nd, and ^{106}Ru in the ARIANE report. The isotopic data for sample GU3 were the recommended data of the ARIANE report, generally obtained as a weighted average of the results reported by ITU and SCK•CEN. The results for sample GU4, measured only by ITU, were in accordance with the ARIANE program evaluation criteria.

3.9 PSI Measurements

The measurements performed at PSI in Switzerland employed the following experimental techniques:

- Multi-collector ICPMS with ID
  - o actinides: U, Pu, Am, Cm
  - o lanthanides: Nd, Sm, Eu, Gd
  - o Cs vector nuclides
  - o ^{90}Sr
- Mono-collector (quadrupole) ICPMS with external calibration
  - o ^{237}Np
  - o metallics: ^{95}Mo, ^{99}Tc, ^{101}Ru, ^{103}Rh, ^{109}Ag
- γ-spectrometry
  - o ^{106}Ru, ^{125}Sb, ^{144}Ce

3.10 CEA Measurements

The following main experimental techniques have been applied for measurements performed at CEA in France:

- TIMS
  - o actinides: U, Pu, Am, Cm
  - o lanthanides: Nd
  - o Cs vector nuclides
  - o ^{90}Sr
- Multi-collector ICPMS with ID
  - o lanthanides: Sm, Eu, Gd
- Mono-collector (quadrupole) ICPMS with external calibration
  - o metallics: ^{95}Mo, ^{99}Tc, ^{101}Ru, ^{103}Rh, ^{109}Ag
  - o ^{237}Np
- γ-spectrometry
  - o ^{106}Ru, ^{125}Sb, ^{144}Ce

4 COMPUTATIONAL ANALYSIS METHODS

Computational analysis of the spent fuel isotopic composition was carried out using the two-dimensional (2-D) TRITON/NEWT depletion sequence in version 5.1 of the SCALE computer code system,[1] released publicly in 2006. Details of the measurements, operating history data, and the computational models and have been reported separately in Refs. 2–4. A brief description of the codes and methods employed in the computational analysis is provided in this section.

4.1 TRITON/NEWT

The TRITON/NEWT depletion sequence[32] couples the 2-D arbitrary polygonal mesh transport code NEWT with the point depletion and decay code ORIGEN to perform burnup simulations. At each depletion step, the neutron transport flux solution from NEWT is used to generate cross sections for the ORIGEN calculation; the isotopic composition data resulting from each isotopic depletion step is employed in the subsequent transport calculation to obtain updated cross sections for the next depletion step in an iterative manner throughout the irradiation history.

NEWT is a 2-D discrete ordinates (S_N) multigroup transport code that uses an Extended Step Characteristics method solver. This method allows cells to be defined in the form of arbitrary polygons and has an automatic fine grid generation feature. The S_N method in NEWT allows arbitrary-order angular scattering (P_N approximation) and arbitrary quadrature order. NEWT has a coarse-mesh finite-difference (CMFD) accelerator that uses a low-order solution for homogenized cells in a coarse spatial grid to substantially reduce the number of iterations needed for flux and eigenvalue convergence.

TRITON can simulate the depletion of multiple mixtures and regions in a fuel assembly model. This is a powerful feature for nuclide inventory analysis of measured fuel rods, as it allows an accurate representation of the local flux distribution and environmental effects on a specific fuel rod in the assembly.

4.1.1 Computational Models

Calculations were performed using assembly models that included as many details as were available. The following subsections discuss the modeling approach and provide examples of the assembly models used in this study. The Calvert Cliffs assembly model provides an example of the models used for many standard commercial assemblies. Some samples, including several Gösgen samples, were obtained from fuel rods that experienced movement, or reconfiguration, in the assembly during irradiation. Other assemblies, such as from the Vandellós reactor, were located at the edge of the core during one of the cycles and required more detailed modeling of the assembly surroundings. Including these details in the models results in a more accurate representation of the neutronic environment in the fuel that influences the calculated isotopic compositions. Therefore, to increase the accuracy of the assembly models, all available information was used in the simulations. The following sections describe these models as examples of the modeling methods and level of detail. A complete description of the models used for each assembly can be found in the primary reference reports.

4.1.1.1 Calvert Cliffs

An example of the NEWT assembly model is illustrated in Figure 4.1 for Calvert Cliffs CE 14 × 14 assembly D047. Only half of the assembly was modeled using symmetry in the assembly. The measured rod MKP109, shown in the lattice and labeled, was depleted separately with the four nearest neighbor rods. All other rods in the assembly were depleted as a single material. This was found adequate to

calculate the local neutronic environment of measured rod MKP109. A similar modeling approach was used for all other samples.

standard fuel rods
measured fuel rod
nearest neighbors of measured fuel rod
guide tube
moderator
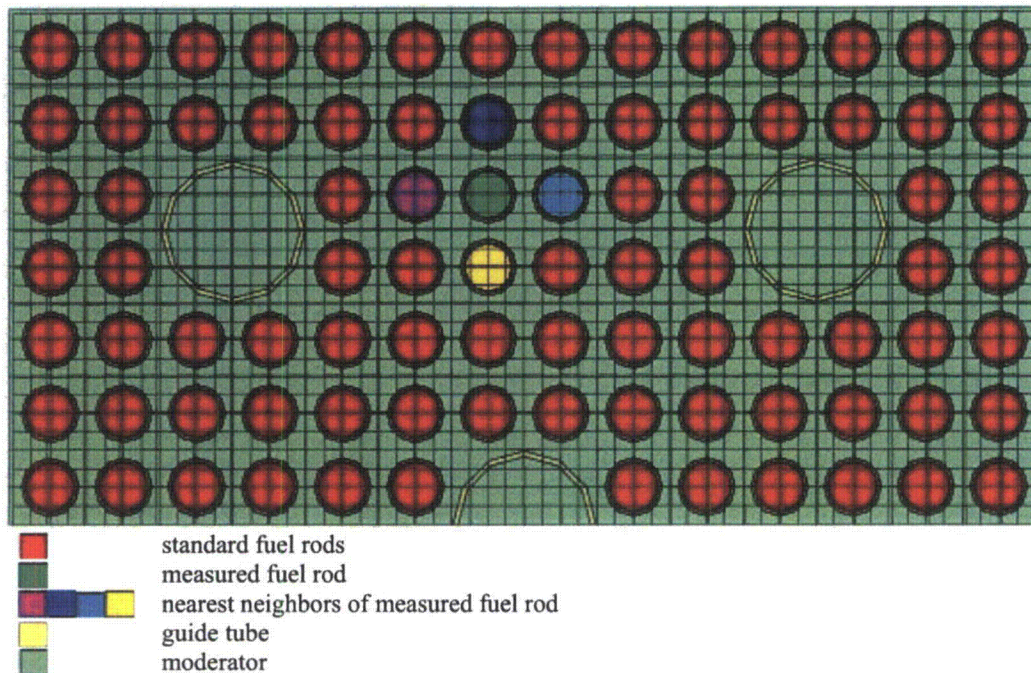
Figure 4.1. Illustration of the NEWT model used for Calvert Cliffs assembly D047.

4.1.1.2 Gösgen

Gösgen assembly 12-40, from which sample GU1 was acquired, was reconfigured after the first two cycles (cycles 12 and 13). Several fuel rods adjacent to the GU1 rod were replaced with fuel rods from another assembly. A detailed irradiation history for the replacement rods was not available; however, the burnup of the replacement rods was very similar to that of the original rods, and the effect of the rod reconstitution was considered to be minor and was therefore not simulated.

A reconfiguration of Gösgen assembly 1601, from which sample rod GU3/4 was acquired, was more significant. The GU3/4 rod was removed from assembly 1601 after two cycles and placed in a low burnup assembly 1701 and irradiated for one additional cycle. Because of potential flux perturbations caused by the fuel rod reconfiguration, the rod movement was explicitly simulated in the calculation models. This was accomplished using two separate models—one for assembly 1601 and the second for assembly 1701 with the GU3/4 fuel rod isotopic compositions determined from the assembly 1601 model.

4.1.1.3 Vandellós

Measured rods WZR0058, WZtR165, and WZtR160 were irradiated for four consecutive cycles (cycles 7 to 10) in assemblies EC45, EC45, and EC46, respectively, and one cycle (cycle 11) in the rebuilt assembly EF05. At the time of the reconfiguration, assembly EF05 had been previously irradiated for only one cycle and therefore had a significantly lower burnup than the original EC45 or EC46 assemblies. The fuel rod movement was modeled explicitly.[4] Information was available on the adjacent assemblies and was used in the simulation models because the measured fuel rods were located at the assembly

periphery and subjected to the potential influence of surrounding neighbors. The assembly models used to perform calculations for the spent fuel samples in fuel rod WZR0058 are illustrated as follows: (1) assembly EC45 during the first three cycles (Figure 4.2), (2) assembly EC45 at the outer edge of the core during the fourth cycle (Figure 4.3), and (3) assembly EF05 containing rod WZR0058 during the final cycle (Figure 4.4).

■ (green)	rod WZR0058
■ (yellow)	assembly EC45 rods
■ (red)	neighbor rod
■ (dark blue)	neighbor rod
■ (magenta)	neighbor rod
■ (olive green)	neighbor rod
■ (light blue)	E10 assembly rods adjacent to EC45
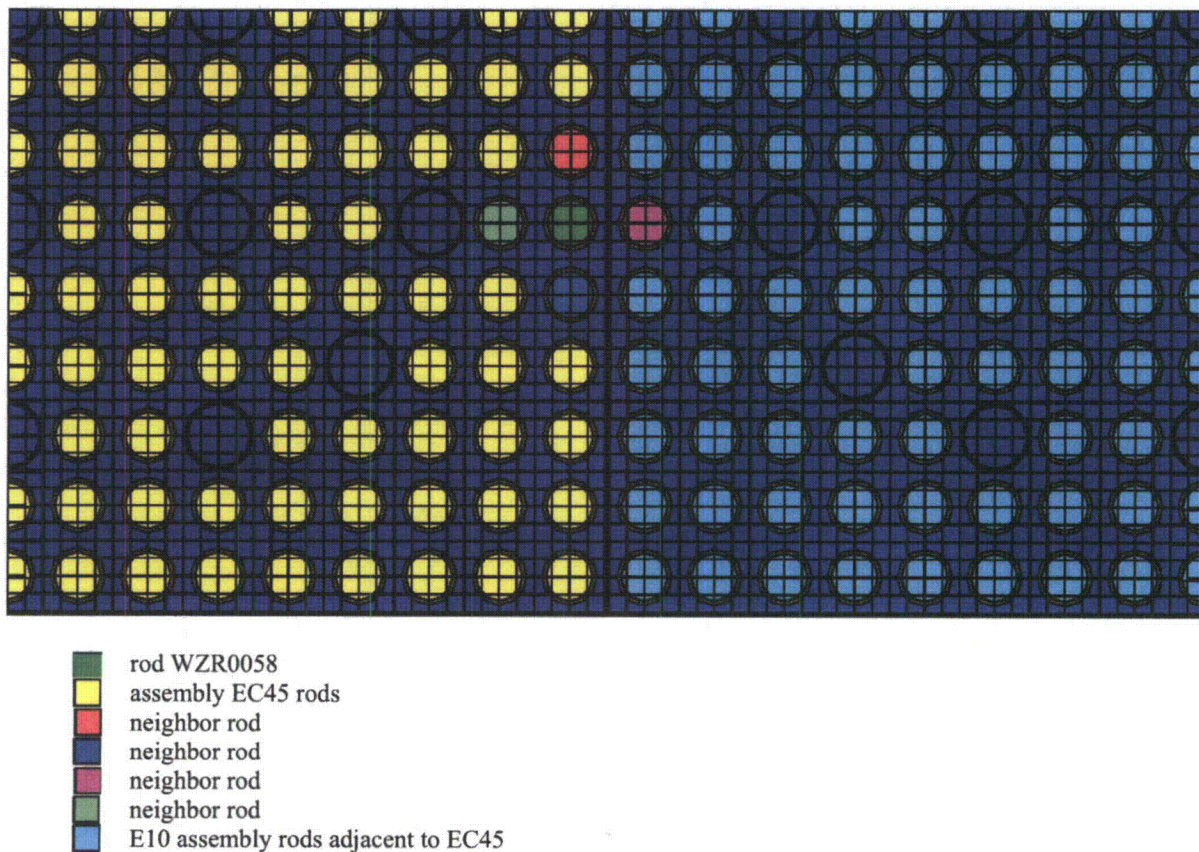
Figure 4.2. TRITON assembly model for Vandellós II samples from rod WZR0058 (cycles 7–9).
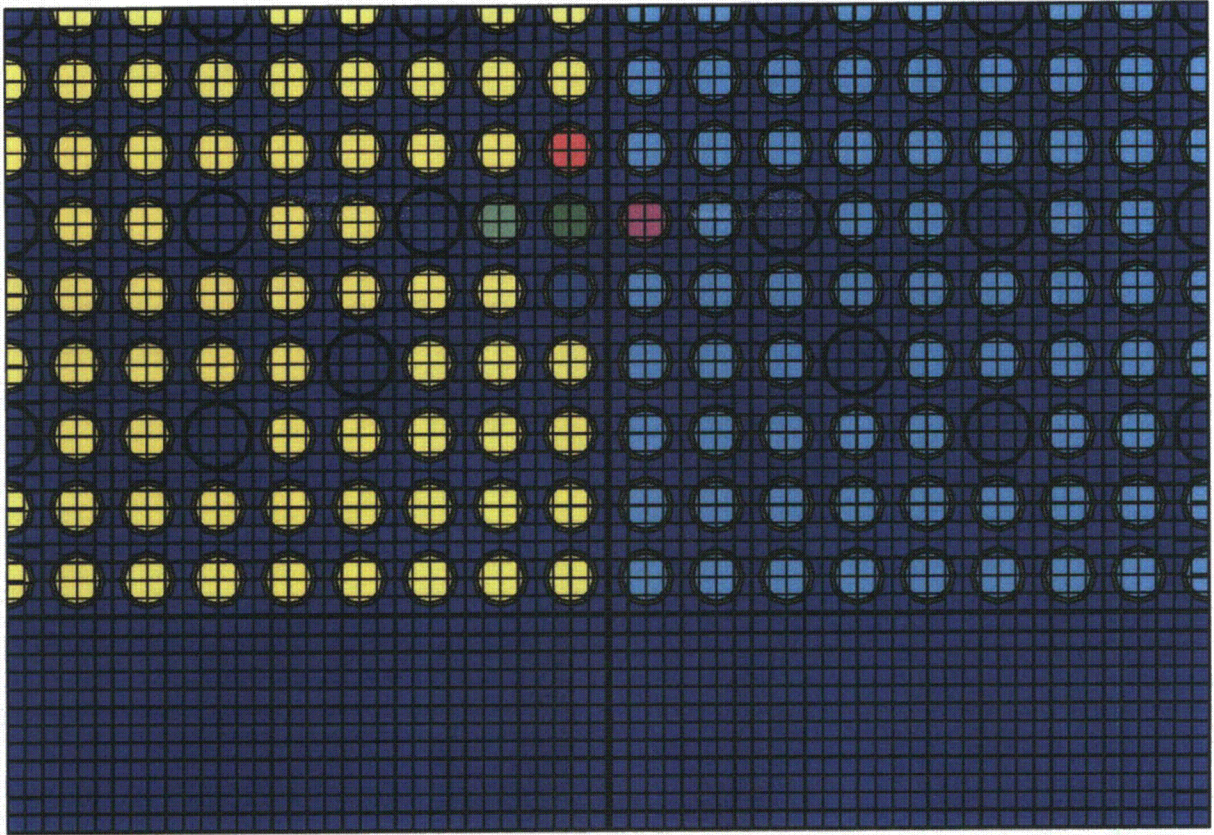
rod WZR0058
assembly EC45 rods
neighbor rod
neighbor rod
neighbor rod
neighbor rod
G15 assembly rods adjacent to EC45

Figure 4.3. TRITON assembly model for Vandellós II samples from rod WZR0058 (cycle 10).
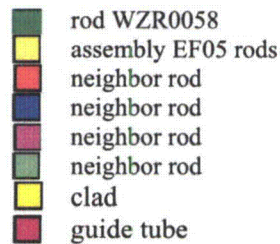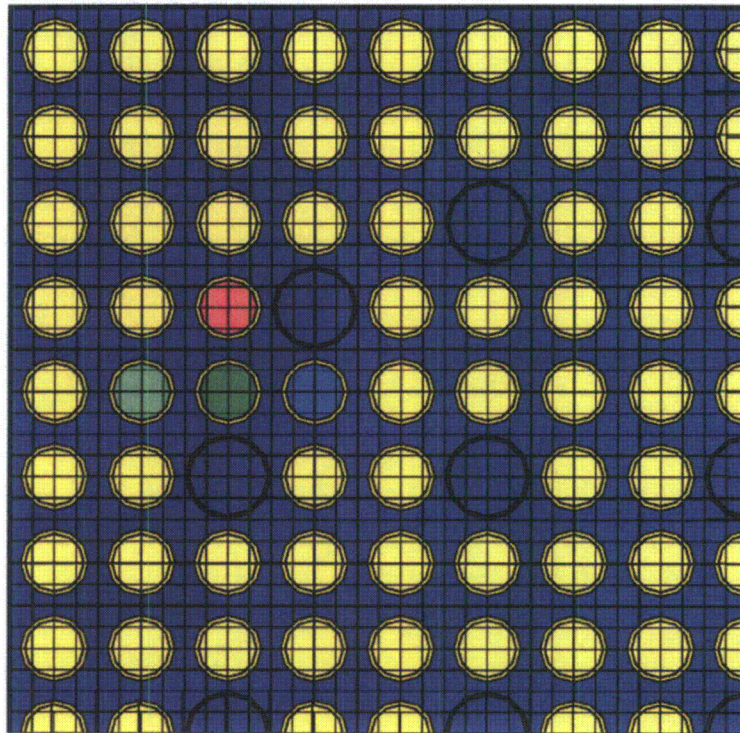
Figure 4.4. TRITON assembly model for Vandellós II samples from rod WZR0058 (cycle 11).

4.2 Cross-Section Libraries

Neutron transport calculations were performed using the SCALE 44-group cross-section library that contains 22 thermal-upscatter groups. The 44-group library is collapsed from the ENDF/B-V SCALE 238-group library using an LWR fuel flux spectrum.

4.3 Resonance Processing

The NITAWL module in SCALE, which is based on the Nordheim Integral Treatment, was used in this study for self-shielding of the resolved resonance cross sections. The NITAWL module was used in this study based on its demonstrated performance for LWR fuel analyses. NITAWL, however, cannot be used with the ENDF/B–VI and –VII cross-section libraries, and it does not allow fuel rod subdivision (i.e., fuel rods must be treated as a single region with one radial zone).

4.4 Isotopic Depletion Calculations

Isotope transmutation and decay calculations were performed with the ORIGEN code. Cross sections used in the ORIGEN calculations are generated automatically during the TRITON depletion analysis using region- and time-dependent cross sections calculated by NEWT. Burnup-dependent cross sections for 232 isotopes defined in the 44-group library are generated based on the transport calculation solution (addnux = 3 input option). This procedure ensures that cross sections are updated for many of the key isotopes of interest to spent fuel safety applications and their capture and/or decay precursors.

5 ANALYSIS RESULTS AND DISCUSSION

The experimental isotopic data considered in this study include measurements of more than 60 isotopes obtained from 51 spent fuel samples. The analysis is based on the collection of the isotopic validation results reported separately.[2-4] The data for Gösgen samples measured under the MALIBU experimental program are currently commercial proprietary and can not be made publicly available at this time.

This section describes the isotopes that are important to several spent fuel safety applications, presents the results of the comparisons of isotopic calculations with experiment, and reviews the results. Evaluation of the results by measurement laboratory provides information on the accuracy and consistency of the analytical techniques. Comparison of results from different laboratories can be used to identify potential problems related to experimental methods, specific isotopes, or fuel samples. The results are also evaluated as a function of sample burnup to identify trends in the bias, particularly as these trends relate to high burnup fuel. Recommendations related to the quality and application of the experimental data sets are presented.

5.1 Important Isotopes in Spent Nuclear Fuel Safety Analyses

Uncertainty in the predicted isotopic composition in spent fuel represents one of the largest sources of uncertainty in criticality calculations that take credit for the irradiated fuel composition (burnup credit), spent fuel decay heat, neutron and gamma radiation source terms, and nuclide concentrations and activities used in radiological safety calculations. The isotopes identified as being of highest importance to several safety-related applications are described here.

Measurements for individual isotopes have direct application to the evaluation of uncertainties in safety applications involving irradiated nuclear fuel, particularly in areas where direct integral measurements are not practical (e.g., spent fuel reactivity measurement for burnup credit) or in application regimes beyond the range for which integral measurements are available or feasible (e.g., decay heat at long cooling times of importance to repository applications). These measured data may be used to assess uncertainties in integral quantities and also identify the sources of bias in integral calculations. Because the isotopic measurements are generally performed on fuel that has cooled for several years, many of the short-lived nuclides are decayed below the detection limit. Therefore, the nuclides of radiological interest having available measurements are generally those important at times greater than about one year after discharge.

Previous studies have investigated the relative importance of individual nuclides in spent fuel applications,[33] as well as the changes in the importance of these nuclides for those applications involving high burnup fuel.[34] Table 5.1 lists 40 nuclides considered important to burnup credit, decay heat and radiological source term calculations, and high-level waste management. Measurement data are available for all isotopes in this list.

The actinides and fission products of highest importance to the neutron multiplication factor in spent fuel are well documented elsewhere.[35] Actinides widely considered for burnup credit for spent fuel storage and transport cask criticality safety analyses are ^{234}U, ^{235}U, ^{238}U, ^{238}Pu, ^{239}Pu, ^{240}Pu, ^{241}Pu, ^{242}Pu, and ^{241}Am. These nine actinides represent about 95% of the reactivity worth of the actinides and about 70% of the total reactivity worth of all nuclides in typical spent fuel. Six major fission products, ^{143}Nd, ^{149}Sm, ^{103}Rh, ^{151}Sm, ^{133}Cs, and ^{155}Gd, account for about 75% of the fission product reactivity worth, and about 20% of the total reactivity worth. The relative worth of these nuclides will vary to some degree, depending on the enrichment, burnup, assembly design, and cooling time, but the list of important nuclides will remain the same.

Table 5.1. Important nuclides in spent fuel safety applications

Isotope	Half life	Burnup credit	Radiological safety	Waste management
Se-79	2.95×10^5 years			■
Mo-95	Stable	■		
Sr-90/Y-90	28.9 years		■	■
Tc-99	2.111×10^5	■		■
Ru-101	Stable	■		
Ru-106	371.6 days		■	
Rh-103	Stable	■		
Ag-109	Stable	■		
Sb-125	2.7586 years		■	
I-129	1.6×10^7 years			■
Cs-133	Stable	■		
Cs-134	2.065 years		■	
Cs-135	2.3×10^6 years			■
Cs-137/Ba-137[a]	30.0 years		■	■
Nd-143	Stable	■		
Nd-145	Stable	■		
Nd-148 [a]	Stable			
Ce-144/Pr-144	284.9 days		■	
Gd-155	Stable	■		
Sm-147	1.06×10^{11} years	■		
Sm-149	Stable	■		
Sm-150	Stable	■		
Sm-151	90 years	■		
Sm-152	Stable	■		
Eu-151	Stable	■		
Eu-153	Stable	■		
Eu-154	8.59 years		■	
U-234	2.455×10^5 years	■		■
U-235	7.037×10^8 years	■		■
U-236	2.342×10^7 years	■		■
U-238	4.468×10^9 years	■		■
Np-237	2.14×10^6 years	■		■
Pu-238	87.71 years	■	■	■
Pu-239	2.41×10^4 years	■	■	■
Pu-240	6.56×10^3 years	■	■	■
Pu-241	14.29 years	■		■
Pu-242	3.75×10^5 years	■		■
Am-241	433 years	■	■	■
Am-243	7370 years	■		■
Cm-242	162.8 days		■	
Cm-244	18.1 years		■	

[a] Isotopes commonly used for experimental burnup determination.

The relative contribution to reactivity of actinides and fission products for typical spent fuel in a high-capacity storage cask after 5 years of cooling is illustrated in Figure 5.1.[36] The measure of nuclide importance was determined from the relative sensitivity of the neutron multiplication factor to the concentration of each individual nuclide in the fuel. The fission product ^{131}Xe is shown in the figure, but it is not generally considered in burnup credit because of its volatility.
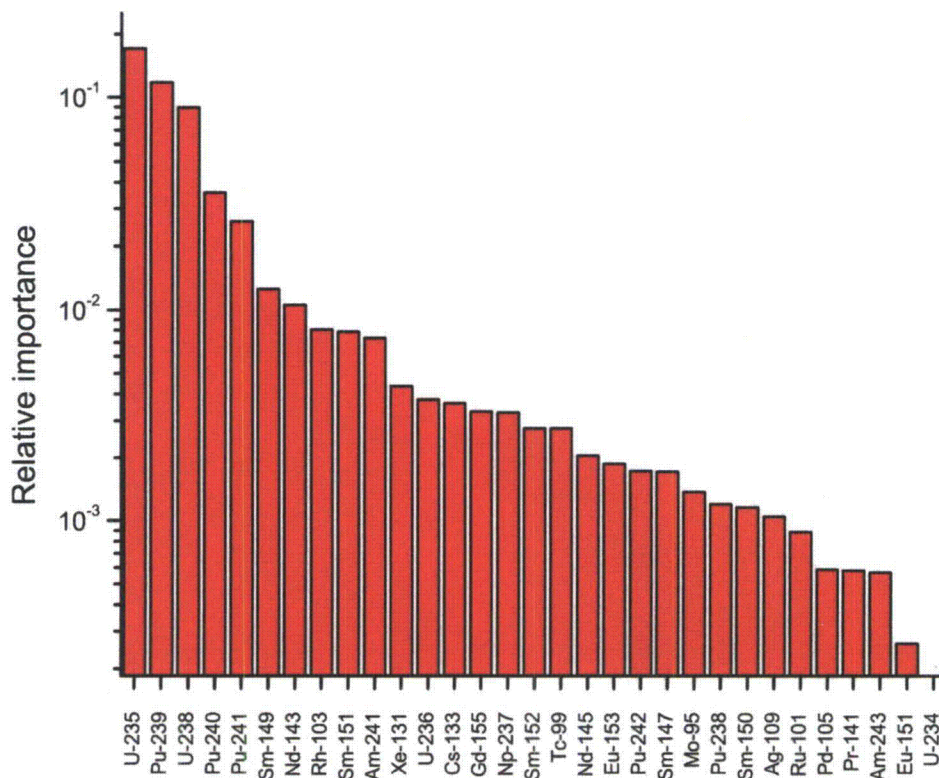
Figure 5.1. Relative isotopic importance in burnup credit criticality calculations.

Figure 5.2 shows the relative percent contribution of the most important isotopes to decay heat for cooling times up to 1000 years for typical high burnup fuel. These isotopes contribute about 95% to the total decay heat after 1 year, and more than 99% to the total decay heat beyond 2 years. Measurements of full-length assembly decay heat have been reported for cooling times from about 3 to 30 years cooling, and these measurements have been used to validate code calculations over this timeframe.[37] However, measurements for cooling times beyond 30 years have not been made.

After 30 years, fission product decay heat is dominated by ^{137}Cs and ^{90}Sr, and their decay progeny, ^{137m}Ba and ^{90}Y, respectively. Actinide decay heat becomes increasingly important at longer cooling times, with ^{241}Am, ^{238}Pu, and ^{244}Cm being the largest contributors. Isotopic measurements of the dominant nuclides have been made and can be applied to establish the accuracy of code calculations beyond the regime where integral measurements are available. Although measurements for ^{137m}Ba and ^{90}Y are not available, these nuclides are in secular equilibrium with the parent nuclides, ^{137}Cs and ^{90}Sr, and can therefore be accurately derived from the concentration of the parents.
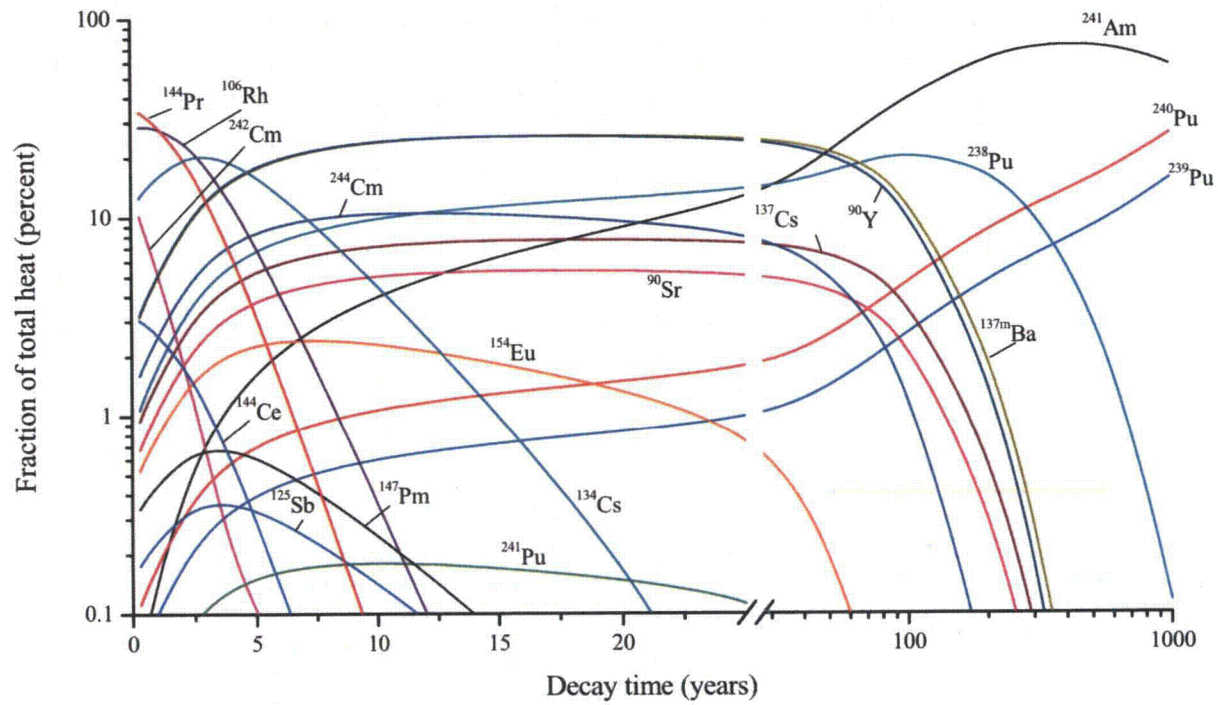
Figure 5.2. Relative isotopic contribution to the total decay heat for typical high burnup fuel.

The isotopes important in radiation shielding applications are similar to those important in decay heat calculation. The dose rates from activated fuel components (e.g., ^{60}Co) are an exception. After 10 years, the contribution from ^{137m}Ba (E_γ = 662 keV), the decay progeny of ^{137}Cs, is by far the largest component of the shielded dose rate. Other important nuclides include ^{244}Cm (spontaneous fission), ^{154}Eu, and ^{90}Y (E_γ = 2.186 MeV), the decay progeny of ^{90}Sr. For cooling times less than 10 years, the relative contributions from ^{134}Cs, ^{106}Ru, and ^{144}Pr (the decay progeny of ^{144}Ce) are dominant. Measurements for these nuclides are available and have been analyzed in this report. The relative isotopic contributions to the dose rates have been calculated for several cask designs and reported previously.[34]

Measurement data on the concentration of isotopes in spent fuel are required to support the waste management and safety assessments of spent fuel repositories. However, the isotopes of interest for waste disposal are different from those important to other applications (e.g., criticality safety). In the field of safety assessment of spent fuel and vitrified high-level waste repositories, long-lived fission products are very important radionuclides in addition to long-lived actinides. For fission product nuclides, there is broad international interest in the spent fuel and high-level vitrified waste management community in ^{14}C, ^{36}Cl, ^{79}Se, ^{99}Tc, ^{126}Sn, ^{129}I and ^{135}Cs. Measurements available for the long-lived fission products important to waste management safety assessments are much more limited, and additional experimental data are needed to fully support this application.

5.2 *Comparison of Calculated and Experimental Results*

Tables 5.2–5.7 list the relative percent error between the calculated and experimental nuclide concentrations for each analyzed sample. The methods used to measure each isotope and the experimental error reported by each laboratory can be found in Section 3. Plots showing the comparisons of calculated and measured results are provided in Appendix A (Figures A.1–A.58). For completeness, all isotopes with measured data are included in these plots. The results are plotted as a function of sample burnup and by the measurement laboratory. The results, grouped by laboratory, can aid in identifying correlated bias associated with measurement methods. The error bars shown in the plots were calculated by propagating the reported standard error of the measured nuclide concentrations to the plotted values of percent difference between calculation and experiment.

The error bars shown in the figures do not account for the additional uncertainty in the sample burnup as determined on the basis of measured ^{148}Nd concentration. In general, the measurements of ^{148}Nd were made using high-precision methods involving isotopic dilution and thermal ionization mass spectrometry. However, some laboratories reported difficulties measuring ^{148}Nd or used lower-precision methods that resulted in much larger uncertainties. Error in the sample burnup caused by measurement uncertainty will be manifested as code bias. While the burnup error is evident through the calculations, it derives from experimental quantities. Error in the sample burnup will affect the calculated concentrations of each isotope to a different extent. Including the influence of the burnup uncertainty, if available, in the error bars of C/E comparisons would provide a more realistic measure of how experimental uncertainty impacts the accuracy of the calculations.

Table 5.2. C/E-1 (%) for Calvert Cliffs samples

Sample ID	87-81 (104-MKP109-LL)	87-72 (104-MKP109-CC)	87-63 (104-MKP109-P)
Burnup (GWd/MTU)	27.35	37.12	44.34
U-234	-1.4	-2.7	2.2
U-235	-1.5	-2.4	-1.1
U-236	2.1	2.4	1.8
U-238	-0.7	-0.5	-0.2
Pu-238	-9.6	-7.3	-6.6
Pu-239	2.5	3.5	6.2
Pu-240	0.0	0.1	0.7
Pu-241	-2.5	-2.2	-0.2
Pu-242	-0.9	-0.3	-2.1
Np-237	6.4	15.5	6.9
Am-241	-4.6	-9.8	-8.1
Cs-133	0.7	1.9	3.1
Cs-134	-4.8	-14.8	-20.8
Cs-135	6.2	5.0	4.6
Cs-137	-0.8	-0.4	-1.0
Nd-143	0.5	0.9	2.2
Nd-144	-0.8	-1.0	-1.2
Nd-145	-0.6	-0.9	-0.9
Nd-146	0.7	0.8	0.9
Nd-148	0.0	0.0	0.0
Nd-150	2.2	3.2	4.1
Sm-147	3.8	0.3	-8.6
Sm-148	-1.1	-1.3	-8.3
Sm-149	-26.3	28.8	-42.4
Sm-150	6.4	8.2	4.8
Sm-151	42.7	30.9	30.3
Sm-152	23.61	30.8	24.3
Sm-154	-11.4	8.3	-6.3
Eu-151	-43.4	23.5	-57.4
Eu-152	-69.0	-48.4	-93.8
Eu-153	3.2	3.0	3.4
Eu-154	-4.2	2.5	9.3
Eu-155	-31.7	-29.9	-30.1
Gd-154	-20.7	32.3	32.7
Gd-155	-48.7	-26.4	-28.8
Gd-156	-24.9	37.2	64.6
Gd-158	-19.1	-99.4	-99.4
Gd-160	-48.6		
Tc-99	5.2	6.8	14.1
Sr-90	3.2	1.1	2.4

Table 5.3. C/E-1 (%) for Takahama-3 samples

Sample ID	SF95-1	SF95-2	SF95-3	SF95-4	SF95-5	SF97-1	SF97-2	SF97-3	SF97-4	SF97-5	SF97-6	SF96-1	SF96-2	SF96-3	SF96-4	SF96-5
Burnup (GWd/MTU	14.3	24.4	35.4	36.7	30.4	17.7	30.7	42.2	47.0	47.3	40.8	8.6	17.4	29.6	30.4	25.4
U-234	9.4	-1.4	26.4	25.1	-8.2	6.4	9.6	6.8	6.6	7.2	8.4	-7.6	-5.9	-7.6	-7.9	-6.9
U-235	0.9	2.7	3.1	3.9	2.1	3.3	0.7	1.4	1.9	0.6	2.0	1.9	1.9	3.3	1.5	1.9
U-236	0.6	-1.7	-0.1	-0.3	-1.0	1.2	-0.2	-0.3	-0.4	-0.3	-0.7	-2.0	-1.6	-0.4	-0.8	-0.4
Pu-238	8.9	-3.7	4.9	4.4	2.0	31.7	-5.5	-7.6	-10.4	-12.6	-7.0	20.4	-1.4	-1.2	-6.8	1.1
Pu-239	12.8	8.0	8.7	7.9	8.3	31.7	4.0	4.1	3.3	0.8	4.9	22.0	3.8	1.7	0.5	2.2
Pu-240	7.0	3.4	5.9	6.2	6.2	14.9	7.0	7.6	6.3	5.8	7.3	13.2	7.4	7.3	5.5	9.0
Pu-241	11.4	0.6	1.0	1.6	2.3	30.4	-2.6	-2.5	-3.0	-5.4	-1.4	26.4	1.9	1.2	-2.5	2.3
Pu-242	13.6	0.0	-0.8	-0.1	3.1	23.3	1.0	-1.1	-2.4	-2.9	-0.8	21.9	5.6	3.9	0.7	7.9
Np-237						24.5	1.8	3.8	1.2	-1.9	-0.6	36.5	45.1	65.9	58.5	52.6
Am-241	-6.5	23.4	23.9	70.3	18.7	74.5	29.2	27.9	15.4	10.4	31.9	67.6	45.0	29.1	9.7	47.2
Am-242m	22.5	17.5	17.3	19.7	22.5	111.4	25.8	18.0	6.7	1.7	18.9	31.0	9.0	23.5	2.6	10.8
Am-243	35.8	22.2	21.7	23.8	23.8	77.0	15.3	13.6	10.9	9.0	15.4	65.4	25.8	24.2	16.5	29.5
Cm-242	-16.0	-30.5	-37.5	-45.5	-18.1	19.6	-4.4	1.9	6.9	12.6	2.2	0.3	-18.6	-17.8	-22.8	-14.4
Cm-243	-6.3	-19.2	-10.5	-13.5	-20.9	29.9	-18.5	-17.4	-17.9	-20.6	-17.8					
Cm-244	30.3	-0.3	8.1	5.8	13.0	86.6	-2.3	-4.0	-6.8	-9.3	-1.1	51.8	7.3	6.7	-0.9	13.1
Cm-245	13.9	-21.5	-13.9	-19.7	-14.1	79.9	-28.4	-30.2	-33.1	-36.3	-26.2					
Cm-246	-45.1	-66.1	-21.2	-23.8	25.0	48.2	-93.2	-34.0	-38.2	-40.7	-33.5					
Cm-247							-31.5	-32.1	-35.9	-38.4	-36.0					
Nd-142	-19.0	-7.3	-15.3	-13.1	-5.4											
Nd-143	-2.0	-2.0	-1.9	-1.0	-1.4	0.4	0.2	0.2	0.7	-0.2	0.3	-4.2	-2.6	-1.9	-1.8	-3.0
Nd-144	0.0	-1.6	-1.0	-4.7	-1.2	3.3	1.4	-2.1	-3.9	-4.3	-2.3	-6.8	-6.0	-10.3	-8.0	-7.1
Nd-145	0.3	-0.3	-0.5	-0.1	0.2	0.4	1.3	0.9	1.1	1.1	0.8	-1.2	0.3	0.4	1.0	0.0
Nd-146	2.8	1.8	1.7	1.6	2.3	2.4	1.5	0.8	0.7	0.6	1.0	-1.0	0.1	0.3	0.5	0.1
Nd-148	1.0	-0.3	-0.5	-0.7	-0.1	1.7	0.9	0.2	0.0	0.0	0.4	-0.2	0.0	-0.1	-0.1	0.0
Nd-150	-0.2	0.4	-0.4	-0.3	1.1	4.3	1.9	1.6	1.3	1.4	2.1	0.7	0.7	1.3	1.0	1.7

Table 5.3 (continued)

Sample ID	SF95-1	SF95-2	SF95-3	SF95-4	SF95-5	SF97-1	SF97-2	SF97-3	SF97-4	SF97-5	SF97-6	SF96-1	SF96-2	SF96-3	SF96-4	SF96-5
Burnup (GWd/MTU)	14.3	24.4	35.4	36.7	30.4	17.7	30.7	42.2	47.0	47.3	40.8	8.6	17.4	29.6	30.4	25.4
Cs-134	-8.6	-13.9	-12.5	-12.7	-12.8	-5.4	-19.7	-17.6	-14.9	-15.4	-16.2	1.1	0.9	1.0	0.9	1.0
Cs-137	-1.6	-3.0	-2.3	-2.7	-1.6	-2.1	-2.3	-2.6	-1.8	-2.0	-2.6	5.2	-8.0	-4.8	-6.0	-3.9
Ce-144	-2.1	-2.0	-5.0	4.2	-1.7	-17.7	-10.2	-2.7	6.0	6.7	-4.8	-0.3	5.1	15.5	15.4	7.9
Eu-154	7.3	0.8	5.1	1.8	3.2	21.4	-2.7	1.3	1.9	0.3	2.4	5.0	-2.3	7.9	5.3	7.6
Ru-106	2.8	20.5	29.2	30.4	12.5	-6.5	-4.7	-2.2	8.3	80.4	-15.0	27.5	53.0	36.3	50.5	12.7
Sb-125	94.9	86.3	126.3	175.9	112.8	31.4	22.5	84.4	70.6	38.6	91.3	30.5	52.8	118.7	75.2	79.6
Sm-147						-2.3	0.6	-1.7	-2.9	-2.3	-0.9					
Sm-148						17.8	-4.2	-9.6	-12.7	-13.6	-8.1					
Sm-149						3.2	-8.5	-2.5	6.1	6.3	-3.0					
Sm-150						5.4	4.9	5.1	5.0	4.4	6.4					
Sm-151						51.4	30.0	34.3	33.3	28.0	33.9					
Sm-152						7.2	23.1	29.1	30.8	30.3	26.3					
Sm-154						3.5	0.2	0.3	-0.2	-1.1	1.0					

Table 5.4. C/E-1 (%) for TMI-1 samples measured at GE-VNC

Sample ID	O13S7	O12S4	O12S6	O1S1	O13S8	O12S5	O1S3	O1S2
Burnup (GWd/MTU)	22.8	23.7	24.0	25.8	26.3	26.5	26.7	29.9
U-234	-2.4	-0.1	0.5	-0.4	0.6	2.3	0.9	0.5
U-235	3.8	3.6	1.3	3.7	4.0	3.9	2.4	5.3
U-236	-3.0	-3.9	-4.0	-3.5	-3.0	-3.4	-2.9	-2.6
Pu-238	-15.2	-15.5	-22.9	-12.7	-18.6	-18.5	-18.9	-11.7
Pu-239	2.2	2.3	-4.1	3.0	2.0	0.0	0.4	9.8
Pu-240	-0.9	-0.8	-4.1	-0.8	-2.4	-3.6	-4.8	-1.3
Pu-241	-6.8	-6.1	-11.8	-5.4	-8.3	-9.6	-9.6	-2.9
Pu-242	-10.7	-9.8	-11.8	-8.5	-11.8	-12.2	-13.3	-11.8
Np-237	-2.7	-7.6	-7.8	1.7	-3.8	-3.4	-4.7	0.5
Am-241	-4.6	-9.0	9.7	33.2	-6.3	-8.3	0.7	12.2
Am-242m	4.4	-4.9	2.2	35.2	-10.2	-13.1	3.7	15.7
Am-243	1.1	0.9	20.9	50.1	-1.7	-3.6	13.0	19.1
Cm-242	-24.2	-28.9	-21.4	-10.7	-37.5	-34.2	-30.3	-40.0
Cm-243	-29.1	-29.2	-22.5	6.8	-31.4	-34.2	-25.3	-13.5
Cm-244	-15.9	-16.7	-6.2	30.1	-19.4	-21.6	-7.0	2.2
Cm-245	-42.2	-42.7	-42.1	-8.1	-46.4	-47.9	-37.9	-23.3
Nd-143	2.2	2.0	2.1	2.7	2.6	2.5	2.8	3.4
Nd-145	1.4	1.2	2.1	1.6	1.7	1.8	2.2	1.6
Nd-146	0.4	0.4	0.3	0.7	0.3	0.3	0.9	0.9
Nd-148	0.0	0.0	0.0	-0.1	0.0	0.0	0.0	0.0
Nd-150	-0.1	0.6	-0.2	0.0	0.2	0.1	-0.3	0.3
Cs-134	-23.1	-22.4	-23.6	-20.1	-23.4	-22.5	-21.1	-18.2
Cs-137	-5.9	-4.5	-3.6	-3.4	-6.4	-4.9	-4.1	-7.2
Sm-147	-1.8	-4.9	-3.7	-5.1	-2.4	-3.0	-5.2	-4.7
Sm-149	13.4	11.6	8.5	14.6	19.0	18.6	13.6	28.2
Sm-150	1.7	1.0	1.4	2.0	1.6	1.0	1.4	2.4
Sm-151	28.8	27.1	18.0	30.1	24.8	24.9	24.8	32.8
Sm-152	13.8	13.4	17.9	14.7	16.9	16.6	15.4	14.2
Eu-151	33.3	19.8	11.6	24.3	29.1	28.4	20.5	39.8
Eu-153	-7.7	-8.8	-8.4	-6.1	-8.5	-8.1	-6.5	-5.1
Gd-155	-38.7	-42.4	-47.1	-46.2	-41.9	-40.9	-48.2	-36.7

Table 5.5. C/E-1 (%) for TMI-1 samples from assembly NJ05YU measured at ANL

Sample ID	A1B	D2	B2	C1	D1A4	A2	C3	C2B	B3J	B1B	D1A2
Burnup (GWd/MTU)	44.8	44.8	50.1	50.2	50.5	50.6	51.3	52.6	53.0	54.5	55.7
U-234	5.6	10.0	5.6	-0.8	1.0	2.4	4.8	7.6	5.7	1.2	-3.4
U-235	0.9	24.7	14.5	11.0	-2.5	9.0	9.2	5.2	1.7	-6.5	-16.1
U-236	4.9	0.5	2.5	1.2	3.3	1.0	4.5	8.0	2.8	4.5	3.6
Pu-238	-34.6	-12.3	7.4	5.8	-6.1	-3.5	41.9	-18.8	-7.8	-8.8	9.7
Pu-239	14.6	17.2	12.3	14.7	16.5	9.9	9.1	22.3	15.1	17.7	14.0
Pu-240	19.0	7.0	11.1	11.4	18.1	9.2	8.5	23.9	18.0	22.1	21.1
Pu-241	2.0	5.3	5.5	6.6	-0.6	7.3	6.9	7.0	1.1	5.0	1.2
Pu-242	8.6	-7.8	0.6	1.9	-1.8	1.7	4.0	7.8	-7.4	12.4	15.0
Np-237	2.5	-4.3	1.7	2.0	6.2	1.8	6.1	9.0	4.8	9.6	12.5
Am-241	8.2	-14.8	-13.6	-18.7	-18.3	-3.0	-0.5	-15.9	-18.4	48.4	32.4
Am-242m					75.8			-17.1	4.7	31.0	133.0
Am-243	46.6	-1.7	-1.8	3.7	40.7	1.0	8.6	46.6	37.1	53.2	61.4
Nd-143	4.6	14.9	8.8	12.0	2.2	14.3	15.6	7.9	4.2	3.5	2.7
Nd-145	3.4	5.8	5.3	6.2	-0.4	9.5	8.1	4.8	1.6	2.8	2.2
Nd-148	0.8	0.9	0.4	0.5	0.5	0.3	0.3	0.3	0.2	0.3	-0.1
Cs-137	-13.7	-6.7	-3.7	-6.9	-1.3	-3.8	1.3	-3.6	-1.3	0.1	17.0
Sm-147	11.0	17.8	19.2	17.7	7.2	12.8	21.7	11.4	3.5	0.6	1.2
Sm-149	16.9	27.0	18.5	25.8	12.3	0.9	36.3	20.6	23.2	18.9	9.5
Sm-150	8.8	12.1	17.1	15.1	7.6	18.7	24.6	10.7	3.0	3.0	8.7
Sm-151	35.8	54.4	41.7	59.4	41.5	50.1	55.0	48.5	28.6	31.6	33.0
Sm-152	34.5	33.8	37.9	40.2	32.7	36.3	44.3	41.8	31.4	32.5	34.7
Eu-151	1.5	-30.8	-40.8	-28.2	13.7	-47.3	-43.3	6.3	-4.0	31.0	17.9
Eu-153	7.6	1.7	8.2	8.6	4.8	7.1	15.8	11.1	5.3	7.5	8.0
Eu-155	-61.5	-59.2	-55.5	-58.8	-63.2	-53.9	-52.5	-50.7	-52.2	-66.7	-45.9
Gd-155	-52.0	-47.9	-48.4	-46.3	-65.9	-34.5	-47.5	-46.8	-51.8	-47.7	-46.9
Mo-95	-3.9	8.2	-3.2	-0.8	0.5	-1.6	10.4	3.3	1.5	1.4	6.3
Tc-99	-26.0	7.4	5.3	6.3	-3.2	7.1	13.1	-12.1	-3.5	-6.7	9.2
Ru-101	-6.5	9.9	-3.6	-0.4	6.1	1.2	15.6	3.5	4.3	5.7	13.0
Rh-103	2.6	19.5	5.5	7.8	11.1	7.7	23.2	11.8	10.8	12.1	15.6
Ag-109	100.7	123.4	127.2	125.3	44.0	103.2	34.2	96.5	65.6	205.4	200.1

Table 5.6. C/E-1 (%) for Gösgen and GKN II samples

Sample ID	GU1	GU3	GU4	GGU1	GGU2/1	GGU2/2	M11
Laboratory	SCK•CEN	SCK•CEN, ITU	ITU	CEA, PSI	PSI	SCK•CEN	SCK•CEN
Program	ARIANE	ARIANE	ARIANE	MALIBU	MALIBU	MALIBU	REBUS
Burnup (GWd/MTU)	60.7	52.5	31.1	70.3	50.8	46.0	54.0
U-234	15.6	37.4	41.4	-0.7	0.4	3.3	19.7
U-235	4.4	-1.4	-0.3	-2.5	-6.6	0.2	4.3
U-236	0.4	-0.4	0.1	-2.1	0.4	1.1	-0.6
U-238	-0.3	-0.9	-0.5	-1.4	-0.1	1.0	0.0
Pu-238	-2.4	-5.4	-2.7	-4.4	-10.1	-10.4	-7.6
Pu-239	5.6	1.3	4.7	5.1	-4.2	-0.3	8.5
Pu-240	2.9	4.0	3.6	3.0	1.7	3.4	3.3
Pu-241	-0.6	-4.4	-2.6	-2.2	-6.7	-6.4	0.8
Pu-242	-3.1	-1.0	0.7	-4.7	0.7	-1.8	-2.1
Np-237		-9.6	-27.1	3.0	7.4	10.0	27.0
Am-241	8.0	11.7	-3.2	-8.4	-10.7	13.4	28.9
Am-242m	49.4	18.2		29.3	-17.2	29.5	27.3
Am-243	17.5	20.6	22.8	2.8	7.5	30.7	37.5
Cm-242	-15.5	-22.0		-10.7		-21.2	26.6
Cm-243	202.3	22.3		-16.0		-6.3	-7.9
Cm-244	2.1	-7.8	-12.5	-6.4	-1.5	-9.1	-6.1
Cm-245	-19.9	-41.6	-35.4	-27.5	-29.4	-33.7	-31.6
Cm-246	-36.7	-38.2		-37.2	-29.0	-34.0	
Nd-142	4.7	5.0	18.1	2.2	4.7	-12.0	-8.1
Nd-143	6.9	2.1	-2.1	0.9	-2.5	3.4	4.1
Nd-144	0.3	0.0	-3.3	-4.4	-2.7	1.2	-1.3
Nd-145	2.3	0.6	-0.8	-3.0	-2.5	2.5	0.9
Nd-146	3.1	0.2	-0.2	-2.6	-2.1	2.0	1.1
Nd-148	0.0	-0.4	-0.1	-4.1	-2.9	1.1	0.3
Nd-150	0.9	-0.2	2.4	-2.1	-0.8	2.0	2.2

Table 5.6 (continued)

Sample ID	GU1	GU3	GU4	GGU1	GGU2/1	GGU2/2	M11
Laboratory	SCK•CEN	SCK•CEN, ITU	ITU	CEA, PSI	PSI	SCK•CEN	SCK•CEN
Program	ARIANE	ARIANE	ARIANE	MALIBU	MALIBU	MALIBU	REBUS
Burnup (GWd/MTU)	60.7	52.5	31.1	70.3	50.8	46.0	54.0
Cs-133	7.8	3.8	3.0	3.9	3.9	4.2	8.0
Cs-134	-6.7	-10.4	-9.9	-11.5	-14.3	-15.2	
Cs-135	1.6	1.1	9.1	-1.6	-2.8	-0.4	4.4
Cs-137	1.1	3.6	9.1	-0.4	0.1	-0.3	-1.3
Ce-144	-0.1	4.4	4.4	-6.3	-8.1	-8.0	-3.7
Pm-147	39.0	124.8	-61.4	2.0	8.4	-13.2	
Sm-147	-5.7	1.7	6.8	-11.7	-5.9	-2.6	-4.8
Sm-148	-11.6	-13.1	-3.0	-20.5	-12.4	-8.0	-13.7
Sm-149	1.6	24.4	7.2	14.8	8.7	11.1	5.1
Sm-150	5.4	8.3	10.2	-3.9	0.0	4.5	2.2
Sm-151	34.0	37.2	35.7	31.4	20.4	25.5	36.9
Sm-152	26.2	38.8	27.9	25.5	24.5	28.6	30.2
Sm-154	-2.3	6.1	10.8	-4.8	-2.9	-6.8	-1.5
Eu-151	-42.7	-18.5		43.8		11.8	
Eu-153	11.5	5.4	3.4	9.1	4.1	3.6	6.8
Eu-154	18.1	-0.6	5.2	11.4	-1.1	-1.8	10.5
Eu-155	-29.3	-36.5	-32.9	-24.6	-29.4	-38.7	-42.2
Gd-155	-22.1	-20.9	-51.3	-22.8	-26.2	-38.0	-30.2
Sr-90	-20.6	3.9	2.1	-1.6	-1.1	-11.7	
Mo-95	-5.4	-2.4	-10.5	0.1	-8.7	-0.8	11.4
Tc-99	6.4	8.1	30.6	18.6	17.0	-2.6	-2.2
Ru-101	8.8	0.5	-1.4	12.8	-9.7	11.9	30.5
Ru-106	9.7	-13.1	-14.9	7.8	-3.2	2.9	
Rh-103	11.3	26.0	-5.7	6.7	-3.8	0.4	23.3
Pd-105							58.5
Pd-108							60.1
Ag-109	118.6	5.7		169.7	137.9	0.3	32.0
Sb-125	47.1	62.5		63.4	15.7	38.6	

Table 5.7. C/E-1 (%) for Vandellós II samples

Sample ID	E58-88	E58-148	E58-260	E58-700	165-2a	160-800
Burnup (GWd/MTU)	42.5	54.8	64.6	77.0	78.3	70.9
U-234	3.9	-6.1	18.9	14.3	16.9	
U-235	-4.2	-14.6	-1.9	-4.8	-1.9	
U-236	8.7	-1.3	3.0	5.6	3.3	
U-238	-0.2	-0.1	-0.4	-0.2	0.4	
Pu-238	0.3	20.4	-3.4	-2.2	-7.6	-9.1
Pu-239	0.9	4.4	2.3	2.9	-6.0	2.9
Pu-240	8.3	12.1	6.6	6.6	0.2	0.0
Pu-241	-0.9	5.6	-0.6	0.9	-7.2	-4.3
Pu-242	8.8	17.8	6.2	5.7	-1.7	-4.2
Np-237	-1.8	-11.5	-5.4	0.7	-12.8	-0.2
Am-241	23.8	29.9	19.0	23.5	10.8	19.7
Am-243	50.8	25.4	27.4	28.6	-2.8	20.6
Cm-244	106.9	103.0	79.1	99.6	68.3	62.7
Cm-246	-10.0	49.7	11.4	34.0	17.3	-14.5
Nd-142	25.3	34.0	21.9	17.2		16.5
Nd-143	-0.9	1.8	0.4	1.1	8.0	3.2
Nd-145	1.2	2.5	0.0	-1.0	4.5	2.6
Nd-146	2.4	3.9	1.9	1.4	6.0	2.7
Nd-148	0.4	-0.5	1.3	-2.3	-6.8	1.7
Nd-150	-0.4	8.0	-0.5	6.7	-6.2	0.9
Cs-133	3.1	6.1	-3.6	10.6	15.8	
Cs-134	-25.1	-14.3	-15.8	-11.2	-11.8	-12.6
Cs-135	-10.8	-15.1	-20.5	-2.2	-7.5	
Cs-137	-5.2	0.2	-1.6	0.8	-0.1	-3.1
Ce-140	1.8	5.3	-0.9	1.5	1.2	-4.4
Ce-142	-0.4	-0.4	-2.4	-2.1	-2.8	-3.8
Ce-144	19.0	23.6	21.0	24.7	21.9	
Sm-147	-2.1	-1.5	4.0	-0.6	-10.7	
Sm-148	3.8	2.5	0.7	-4.1	-12.3	-12.2
Sm-149	-0.1	0.9	12.5	26.6	29.9	16.2
Sm-150	5.3	3.8	6.1	5.5	9.4	-1.6
Sm-151	23.8	36.9	38.8	32.7	37.1	30.2
Sm-152	26.7	30.9	34.2	35.4	30.7	28.5
Sm-154	6.4	17.9	22.8	13.7	-4.5	-5.2
Eu-153	-7.1	-3.3	-4.0	2.1	-0.5	
Eu-154	5.6	11.2	18.8	43.1	8.0	
Eu-154	-24.8	-29.2	-26.0	-16.3	-15.6	
Gd-154	41.3	24.4	51.8	37.7	10.5	35.5
Gd-155	-9.3	-17.1	-7.4	-11.8	6.9	
Gd-156	9.1	5.6	6.3	2.7	2.9	-8.6
Gd-158	27.4	29.6	39.0	40.7	40.0	25.4
Gd-160	-6.5	10.8	13.7	15.2	-0.8	-2.6
Ru-106	-17.3	-6.3	-6.5	-0.5	1.4	
La-139	5.6		11.4	6.3		8.1
Rh-103						8.0
Tc-99	6.9					2.9

43

5.3 Data Evaluation Criteria

Prior to applying the experimental data for isotopic validation, the data were examined to identify potential systematic measurement problems or isolated errors associated with fuel samples or specific isotopes. Systematic biases can occur as a result of radiochemical analysis techniques. The root cause of the bias will determine if the bias is correlated with a specific measurement campaign, certain samples, or individual isotopes. Biases are also introduced by the computational model and modeling approximations, uncertainties in the fuel design description and reactor operating information, and deficiencies in nuclear data. Errors associated with the experiment will ultimately be manifest as code bias and uncertainty and may lead to inaccurate conclusions about the accuracy of the calculations.

The aggregate measurement data from each laboratory were examined to assess the general trends and behavior of all samples measured at each facility with respect to other laboratories. This assessment generally required knowledge of the measurement methods and accuracies. In several cases, laboratory results were observed to be clearly different than most other data obtained for comparable fuel samples. However, it was not always possible to conclude that these differences were caused by experimental problems and not by calculations. When the discrepancies were identified as probable experimental errors, further assessment was required to determine if other isotopic data in the same sample or data set would be subject to similar issues, or whether the discrepancies were isolated to a single isotope (e.g., due to a very low atomic concentration in the fuel). When widespread isotopic inconsistencies were observed, the evaluation needs to consider at what point to recommend removal of an entire set of measurements.

The following guidelines were used to evaluate the experimental data and corresponding code-predicted data, and also the intrinsic errors and uncertainties in each of these data sets:

- The results from each laboratory were evaluated for self-consistency in order to identify individual discrepant measurement data.

- The (C/E-1)% comparisons were tested for normality and to verify that the observed variations were consistent with the reported experimental errors.

- Consistency checks were performed for nuclides that are highly correlated at the time of measurement by the physics of parent-daughter relationships. For example, the concentration of ^{241}Am is produced mainly by the decay of ^{241}Pu, and consequently, the bias for these nuclides are expected to be very similar; a similar relationship is expected between ^{155}Gd and ^{155}Eu.

- Checks were performed to verify that the measured variation in the nuclide concentration as a function of burnup was consistent with the physics of isotope generation and depletion.

- Checks were also performed to examine the variation in the nuclide concentration with the axial location for samples obtained from the same fuel rod.

- Large discrepancies for individual nuclides within a set of laboratory data were examined to determine whether the errors were likely caused by isolated measurement problems for specific isotopes, or whether systematic deviations were observed for multiple isotopes in the same sample that might indicate larger issues with the sample itself.

- Measurements performed at a specific laboratory were compared with corresponding data from other independent laboratories. Agreement, particularly when different analytical methods were used that would reduce the likelihood of common bias in the measurements, provided a high level of confidence in the results; whereas, results exhibiting a clear and consistent bias with respect to other data sets are an indication of likely code model or measurement data issues.

Isotopic results identified in the review as nonconforming were generally retained in this study. It is important not to remove data without clear indication of a measurement error (e.g., on the basis on non-physical results), as problems may be associated with the computational model or the accuracy of the information used in the calculation. Removing potentially reliable measurements on this basis can lead to an underestimation of the computational uncertainties. Further evaluations were performed to examine and identify the root cause of discrepant data where possible, by looking at all aspects of the fuel irradiations, measurements, and calculations. The statistical analysis applied in the evaluations, described in the following section, provided an additional measure for assessing data quality.

5.4 Statistical Analyses

The results were statistically examined to provide a quantitative assessment of the data. The following statistical tests were applied:

- The mean and standard deviation of the data for each individual laboratory was calculated.

- The Shapiro-Wilk normality test[38] was used to determine whether the isotopic results from each laboratory had a normal distribution.

- The normality test was applied to the combined data from all laboratories and samples.

- A linear regression analysis was performed to determine the significance of the slope.

- The sample mean and standard deviation were calculated for the combined data of each isotope.

- The two-sided tolerance interval within which 95% of the data lie, with a 95% confidence ($p = 95\%$).

It is important to emphasize that acceptance or removal of data was not based on the results of the statistical analyses. It is possible that biases introduced by the models and nuclear data could result in statistical anomalies that, if applied in a strict statistical analysis, might lead to removal of good measurement data. The measurement data are not obtained from a random sampling of fuels, and many of the samples are highly correlated to one another. For example, the 11 samples measured by ANL were obtained from the same TMI-1 fuel rod (H6). Any bias attributed to either the calculations or the measurements will be highly correlated in these samples and could lead to anomalous distributions of results caused by over sampling of data analysed by one laboratory. The statistical tests, however, do provide insight into the behavior of the data but alone are not able to account for all of the complex relationships between the results obtained from different samples, analytical measurement methods, errors, and correlations in the calculations.

5.4.1 Normality Tests

The results of the Shapiro-Wilk normality tests are listed in Tables 5.8–5.11 for the isotopes of primary interest (see Table 5.1) to spent fuel applications. The tables list the total number of measurements available for each isotope and indicate whether the laboratory data and combined data set are normal. A large number of actinides and fission products do not meet a $p = 95\%$ acceptance criterion for normality when all data are included. This condition generally occurred when the results from one or more data sets showed large systematic differences with other results. Further evaluations were performed to identify problematic data (systematic discrepancies in either the measurements or calculations) that resulted in a combined dataset that was not normally distributed.

Several samples were removed from consideration before performing the normality tests. As discussed in more detail in Section 5.5, Takahama-3 samples SF95-1, SF96-1, and SF97-1 were obtained from axial rod positions very close to the active end of the fuel, causing results for many nuclides to be

systematically biased due to spectral effects that could not be accurately characterized by the code models. The bias is clearly evident in the isotopic results for plutonium, neptunium, americium, and curium, plotted in Figures A.5 – A.18.

Results obtained from different fuel rods and different laboratories may not necessarily lead to a normally distributed data set when combined, even when the results from each laboratory are normal. Laboratories and measurement campaigns may be subject to different sources of systematic (nonrandom) bias due to variations in fuel sample preparation, separations chemistry, analytical methods, standards, and instrumentation errors. Also, the calculations for samples from different fuels may also exhibit systematic computational bias due to errors, uncertainties, or approximations in reactor data, operating conditions, computational methods, and models. This effect is evident in some of the isotopic results plotted in Appendix A. For example, the distribution of data for ^{240}Pu is generally very consistent within each reporting laboratory; however, each laboratory set shows a different bias with respect to the other measurement sets. Results for ^{242m}Am and ^{243}Am are observed to be normally distributed by laboratory; however, the combined data sets are not normal. In general, this can often be attributed to large systematic bias in one or more individual data sets. This is not necessarily a definitive indication of experimental error, and further evaluation of the data is required.

The individual laboratory's results are generally found to have a normal distribution. Some exceptions are, for example, the Takahama-3 fuel samples, for which the ^{237}Np and ^{134}Cs results are not normally distributed. Further evaluation indicated that the observed discrepancies are due to the data corresponding to the SF96 gadolinium poison rod, and the cause is likely associated with the calculations. This is discussed further in the next section.

Laboratory data sets that exhibited a standard deviation significantly larger than the estimated measurement error, or showed a clear bias with respect to other data sets in the combined data, were examined to identify the possible cause of the large observed variation.

5.4.2   Linear Regression Analysis

A linear regression analysis of the calculated and measured data comparisons was performed to identify statistically significant trends in the results as a function of sample burnup. The following nuclides have a significant (p = 95%) slope: ^{143}Nd, ^{234}U, ^{236}U, ^{240}Pu, ^{242}Pu, ^{242}Cm, ^{133}Cs, ^{137}Cs, ^{152}Sm, ^{153}Eu, ^{154}Eu, and ^{155}Gd. However, further analysis of the results suggests that some trends are associated with the inclusion of measurement data with large biases compared to most other data. For example, removal of the TMI-1 data measured by ANL produced a non-significant slope in the remaining ^{240}Pu and ^{242}Pu data, i.e., no significant trend with burnup. Based on these observations, trending analysis based on statistical considerations alone may lead to inaccurate conclusions due to isolated biases in some data.

5.4.3   Bias and Uncertainty Analysis

The mean and standard deviation of the results from each analytical laboratory are listed in Tables 5.12–5.17. The tables show the number of samples measured by each laboratory, average result for each laboratory ($\bar{x}$), and the standard deviation (σ). Only the isotopes previously identified as being important to spent fuel application areas are included in the statistical analysis tables. The sample mean of the final combined data set, $\bar{x}$, was calculated as

$$\bar{x} = \frac{1}{n} \sum_{i}^{n} \left(\frac{C}{E} - 1 \right)_i \, ,$$

where n is the total number of measurements for isotope i, and C/E is the ratio of the calculated-to-experimental isotopic concentration.

The experimental uncertainties depend on the radiochemical analysis techniques and instrument precision and vary considerably between laboratories. Consideration was given to weighting the measurements in order to account for the different accuracies of the measurements using a weighting factor $\omega_i = 1 / \sigma_i^2$, where σ_i is the standard deviation associated with each data set. However, due to the nonstandard approach of the different laboratories in reporting uncertainties and the inconsistency between reported uncertainties and observed variance of the data, no weighting was performed to avoid potentially incorrectly biasing the mean using arbitrary weights.

The variance of results was calculated as

$$\sigma^2 = \frac{1}{(n-1)} \sum_i^n \left[\left(\frac{C}{E} - 1 \right)_i - \bar{x} \right]^2 ,$$

and the relative standard error was estimated as σ.

The data were also examined to identify potential trends with burnup. The existence of trends in the computation bias would mandate a regression analysis rather than determining the mean and variance of the results. However, no significant trends with burnup were observed for the results. Trends in the bias certainly do exist because the sensitivity of the nuclide concentrations to the neutron cross sections in the transmutation chains is not constant as a function of burnup.[39] However, in most cases, these trends are not statistically significant due to the scatter of the data as a result of experimental and computational uncertainties.

5.4.4 Confidence Intervals

The expression for the variance assumes that the value of the mean, $\bar{x}$, is known precisely. However, in practice, the mean is estimated from a finite number of measurements. For small sample sizes, the error in the mean can be large, and this error must be included in any realistic estimate of the isotopic uncertainty obtained from the experimental data. The tolerance interval is a commonly used statistical measure that defines a range that includes a specified fraction of the population with a given likelihood (e.g., p = 95% probability). Tolerance limits define the end points of the tolerance interval. Tolerance limits can be calculated from tolerance factors, multipliers on the standard deviation σ, to include the added uncertainty associated with small sample sizes.

Two-sided tolerance factors are used to define a range within which a specified fraction of the population is estimated to reside; one-sided tolerance factors are used to determine a value above or below which that sample population is likely to reside.

Table 5.8. Normality test results for actinides (U, Pu, Am, Np, Cm)

Laboratory	U-234	U-235	U-236	Pu-238	Pu-239	Pu-240	Pu-241	Am-241	Am-243	Np-237	Cm-242	Cm-244	Cm-246
PNNL + KRI	Y	Y	Y	Y	Y	Y	Y	Y		Y			
JAERI	N	Y	Y	Y	Y	Y	Y	Y	Y	N	Y	Y	Y
GE-VNC	Y	Y	Y	Y	Y	Y	Y	Y	Y	Y	Y	N	
ANL	Y	Y	Y	Y	Y	Y	Y		Y	Y			
SCK•CEN[a]	Y	Y	Y	Y	Y	Y	Y	Y	Y		Y	Y	
Studsvik	Y	N	Y	Y	N	Y	N	Y	Y	Y			Y
Combined set	N	N	N	N	N	N	N	Y	N	N	Y	N	Y

[a] Includes SCK•CEN, ITU, PSI, and CEA measurements of Gosgen and GKN II fuel samples.

Table 5.9. Normality test results for fission products (Cs, Ce, Nd)

Laboratory	Cs-133	Cs-134	Cs-137	Ce-144	Nd-143	Nd-145
PNNL + KRI	Y	Y	Y		Y	Y
JAERI		N	N	Y	Y	Y
GE-VNC		Y	Y		Y	Y
ANL			N		Y	Y
SCK•CEN[a]	Y		Y	Y	Y	Y
Studsvik	Y	N	Y	Y	Y	Y
Combined set	Y	N	N	Y	N	N

[a] Includes SCK•CEN, ITU, PSI, and CEA measurements of Gosgen and GKN II fuel samples.

Table 5.10. Normality test results for fission products (Sm, Eu, Gd)

Laboratory	Sm-147	Sm-149	Sm-150	Sm-151	Sm-152	Eu-151	Eu-153	Eu-154	Eu-155	Gd-155
PNNL + KRI	Y		Y	Y	Y		Y	Y	Y	Y
JAERI	Y	Y	Y	Y	Y			Y		
GE-VNC	Y	Y	Y	Y	Y	Y	Y			Y
ANL	Y	Y	Y	Y	Y	Y	Y		Y	
SCK•CEN[a]	Y	Y	Y	Y	Y	Y	Y	Y	Y	Y
Studsvik	Y	Y	Y	Y	Y	Y	Y	Y	Y	Y
Combined set	Y	Y	N	N	Y	N	N	N	Y	Y

[a] Includes SCK•CEN, ITU, PSI, and CEA measurements of Gosgen and GKN II fuel samples.

Table 5.11. Normality test results for other fission products (metallics)

Laboratory	Sr-90	Mo-95	Tc-99	Ru-101	Ru-106	Rh-103	Ag-109	Sb-125
PNNL + KRI	Y		Y					
JAERI					Y			Y
GE-VNC								
ANL		Y	Y	Y		Y	Y	
SCK•CEN[a]	Y	Y	Y	Y		Y	Y	Y
Studsvik			Y		Y			
Combined set	N	Y	Y	Y	N	Y	Y	Y

[a] Includes SCK•CEN, ITU, PSI, and CEA measurements of Gosgen and GKN II fuel samples.

Table 5.12. Calculated-to-experimental differences (%)—Major actinides

Reactor	Laboratory	U-234 #	U-234 $\bar{x}$	U-234 σ	U-235 #	U-235 $\bar{x}$	U-235 σ	U-236 #	U-236 $\bar{x}$	U-236 σ	Pu-238 #	Pu-238 $\bar{x}$	Pu-238 σ	Pu-239 #	Pu-239 $\bar{x}$	Pu-239 σ	Pu-240 #	Pu-240 $\bar{x}$	Pu-240 σ	Pu-241 #	Pu-241 $\bar{x}$	Pu-241 σ	Pu-242 #	Pu-242 $\bar{x}$	Pu-242 σ
Calvert Cliffs	PNNL, KRI	0			3	-1.7	0.7	3	2.1	0.3	3	-7.8	1.6	3	4.1	1.9	3	0.3	0.4	3	-1.6	1.3	3	-1.1	0.9
Takahama-3	JAERI	13	4.0	11.9	13	2.1	1.0	13	-0.6	0.5	13	-3.4	5.5	13	4.5	2.9	13	6.5	1.3	13	-0.5	2.5	13	1.1	3.2
TMI-1	GE-VNC	8	0.2	1.3	8	3.5	1.2	8	-3.3	0.5	8	-16.8	3.7	8	2.0	3.9	8	-2.3	1.6	8	-7.6	2.8	8	-11.2	1.5
TMI-1	ANL	11	3.6	3.9	11	4.6	11.0	11	3.3	2.1	11	-2.5	19.4	11	14.9	3.7	11	15.4	6.1	11	4.3	2.8	11	3.2	7.4
Gösgen + GKN II	SCK•CEN[a]	7	16.7	17.3	7	-0.3	3.9	7	-0.2	1.0	7	-6.1	3.3	7	3.0	4.3	7	3.1	0.7	7	-3.2	2.8	7	-1.6	2.0
Vandellós II	Studsvik	5	9.6	10.5	5	-5.5	5.3	5	3.9	3.7	6	-0.3	10.7	6	1.2	3.7	6	5.6	4.7	6	-1.1	4.4	6	5.4	7.9
Combined set		44	5.9	11.1	47	1.5	6.4	47	0.6	2.9	48	-5.7	11.5	48	5.8	6.1	48	6.1	6.9	48	-1.1	4.7	48	-0.5	7.1

[a] The Gosgen and GKN II results measured by SCK•CEN, ITU, PSI, and CEA are grouped in the analysis.

Table 5.13. Calculated-to-experimental differences (%)—Minor actinides

Reactor	Laboratory	Am-241 #	Am-241 $\bar{x}$	Am-241 σ	Am-243 #	Am-243 $\bar{x}$	Am-243 σ	Np-237 #	Np-237 $\bar{x}$	Np-237 σ	Cm-242 #	Cm-242 $\bar{x}$	Cm-242 σ	Cm-244 #	Cm-244 $\bar{x}$	Cm-244 σ
Calvert Cliffs	PNNL, KRI	3	-7.5	2.7	0			3	9.6	5.1	0			0		
Takahama-3	JAERI	0			13	19.4	6.3	9	25.2	29.4	13	-14.3	17.6	13	2.3	7.2
TMI-1	GE-VNC	8	3.5	14.4	8	12.5	17.9	8	-3.5	3.4	8	-28.4	9.5	8	-6.8	16.9
TMI-1	ANL	11	-1.3	22.7	11	26.9	24.8	11	4.7	4.7	0			0		
Gösgen + GKN II	SCK•CEN[a]	7	5.7	14.1	7	19.9	12.2	6	1.8	18.4	5	-8.6	20.2	7	-5.9	4.8
Vandellós II	Studsvik	6	21.1	6.4	6	25.0	17.2	6	-5.2	5.8	0			0		
Combined set		35	4.5	17.6	45	20.8	16.7	43	6.0	18.3	26	-17.5	17.3	28	-2.4	11.0

[a] The Gosgen and GKN II results measured by SCK•CEN, ITU, PSI, and CEA are grouped in the analysis.

49

Table 5.14. Calculated-to-experimental differences (%)—Fission products (Cs, Ce, Nd)

Reactor	Laboratory	Cs-133			Cs-134			Cs-137			Ce-144			Nd-143			Nd-145		
		#	$\bar{x}$	σ	#	$\bar{x}$	σ	#	$\bar{x}$	σ	#	$\bar{x}$	σ	#	$\bar{x}$	σ	#	$\bar{x}$	σ
Calvert Cliffs	PNNL, KRI	3	1.9	1.2	3	-13.5	8.1	3	-0.7	0.3	0			3	1.2	0.9	3	-0.8	0.2
Takahama-3	JAERI	0			13	-10.1	8.0	13	-3.4	1.9	13	2.6	7.8	13	-1.1	1.2	13	0.5	0.6
TMI-1	GE-VNC	0			8	-21.8	1.9	8	-5.0	1.4	0			8	2.5	0.5	8	1.7	0.3
TMI-1	ANL				0			11	-2.1	7.5	0			11	8.2	5.2	11	4.5	2.9
Gösgen + GKN II	SCK•CEN[a]	7	4.9	2.1	6	-11.3	3.1	7	1.7	3.6	7	-2.5	5.5	7	1.8	3.4	7	0.0	2.2
Vandellós II	Studsvik	5	6.4	7.4	6	-15.2	5.1	6	-1.5	2.3	5	22.0	2.2	6	2.2	3.1	6	1.6	2.0
Combined set		15	4.8	4.5	36	-14.0	7.2	48	-2.2	4.4	25	5.1	10.9	48	2.6	4.5	48	1.6	2.4

[a]The Gosgen and GKN II results measured by SCK•CEN, ITU, PSI, and CEA are grouped in the analysis.

Table 5.15. Calculated-to-experimental differences (%)—Fission products (Pm, Sm)

Reactor	Laboratory	Sm-147			Sm-149			Sm-150			Sm-151			Sm-152		
		#	$\bar{x}$	σ	#	$\bar{x}$	σ	#	$\bar{x}$	σ	#	$\bar{x}$	σ	#	$\bar{x}$	σ
Calvert Cliffs	PNNL, KRI	3	-1.5	6.4	0			3	6.5	1.7	3	34.6	7.0	3	26.2	4.0
Takahama-3	JAERI	5	-1.4	1.4	5	-0.3	6.4	5	5.2	0.7	5	31.9	2.8	5	27.9	3.2
TMI-1	GE-VNC	8	-3.9	1.3	8	15.9	6.0	8	1.6	0.5	8	26.4	4.5	8	15.4	1.6
TMI-1	ANL	11	11.3	7.4	11	19.1	9.5	11	11.8	6.7	11	43.6	10.6	11	36.4	4.2
Gösgen + GKN II	SCK•CEN[a]	7	-3.2	6.0	7	10.4	7.5	7	3.8	4.8	7	31.6	6.4	7	28.8	4.8
Vandellós II	Studsvik	5	-2.2	5.4	6	14.3	12.6	6	4.7	3.6	6	33.3	5.6	6	31.1	3.3
Combined set		39	1.2	8.2	37	13.4	10.4	40	6.1	5.6	40	34.4	9.2	40	28.2	8.1

[a]The Gosgen and GKN II results measured by SCK•CEN, ITU, PSI, and CEA are grouped in the analysis.

Table 5.16. Calculated-to-experimental differences (%)—Fission products (Eu, Gd)

Reactor	Laboratory	Eu-151			Eu-153			Eu-154			Eu-155			Gd-155		
		#	$\bar{x}$	σ	#	$\bar{x}$	σ	#	$\bar{x}$	σ	#	$\bar{x}$	σ	#	$\bar{x}$	σ
Calvert Cliffs	PNNL, KRI	0			3	3.2	0.2	3	2.5	6.8	3	-30.6	1.0	3	-34.6	12.2
Takahama-3	JAERI	0			0			13	-2.5	3.3	0			0		
TMI-1	GE-VNC	8	25.9	8.8	8	-7.4	1.3	0			0			8	-42.8	4.1
TMI-1	ANL	11	-11.3	27.7	11	7.8	3.6	0			11	-56.4	6.1	11	-48.7	7.3
Gösgen + GKN II	SCK•CEN[a]	4	-1.4	37.5	7	6.3	3.1	7	6.0	7.7	7	-33.4	6.1	7	-30.2	11.0
Vandellós II	Studsvik	0			5	-2.6	3.5	5	17.3	15.3	5	-22.4	6.1	5	-7.8	8.9
Combined set		23	3.4	29.3	34	2.0	6.9	28	6.0	9.3	26	-40.7	15.3	34	-36.2	15.9

[a]The Gosgen and GKN II results measured by SCK•CEN, ITU, PSI, and CEA are grouped in the analysis.

Table 5.17. Calculated-to-experimental differences (%)—Fission products (metallics)

Reactor	Laboratory	Sr-90			Mo-95			Tc-99			Ru-101			Ru-106			Rh-103			Ag-109			Sb-125		
		#	$\bar{x}$	σ	#	$\bar{x}$	σ	#	$\bar{x}$	σ	#	$\bar{x}$	σ	#	$\bar{x}$	σ	#	$\bar{x}$	σ	#	$\bar{x}$	σ	#	$\bar{x}$	σ
Calvert Cliffs	PNNL, KRI	3	2.2	1.1	0			3	8.7	4.7	0			0			0			0			0		
Takahama-3	JAERI	0			0			0			0			13	24.0	26.6	0			0			13	87.3	40.1
TMI-1	GE-VNC	0			0			0			0			0			0			0			0		
TMI-1	ANL	0			11	2.0	4.6	11	-0.3	11.5	11	4.4	6.7	0			11	11.6	6.0	11	111.4	55.1	0		
Gösgen + GKN II	SCK•CEN[a]	6	-4.8	9.4	7	-2.3	7.2	7	10.8	12.0	7	7.6	12.9	6	-1.8	10.5	7	8.3	12.6	6	77.4	73.5	5	45.5	19.7
Vandellós II	Studsvik	0			0			2			0			5	-5.8	7.3	1			0			0		
Combined set		9	-2.5	8.3	18	0.3	6.0	23	4.7	11.3	18	5.7	9.4	24	11.3	24.5	19	10.2	8.7	17	99.4	62.2	18	75.7	40.0

[a]The Gosgen and GKN II results measured by SCK•CEN, ITU, PSI, and CEA are grouped in the analysis.

5.5 Review of Laboratory Measurements

A qualitative review of the results from each laboratory was first performed. This served two purposes:

- the measurements reported by each laboratory were reviewed for self-consistency;

- laboratory results were reviewed by group with respect to results from other laboratories that measured similar fuel types.

With the exception of the Gösgen and GKN II samples, most laboratories performed measurements for multiple samples obtained from the same fuel rod, having very similar properties. These measurements are useful for checking measurement data for self-consistency by analyzing measurements as a function of sample burnup and axial position in the fuel rod. For the Gösgen samples, the experimental programs used independent laboratory cross checks to confirm the accuracy of the measurements.

5.5.1 PNNL-KRI

The Calvert Cliffs ATM-104 samples evaluated in this work were measured at PNNL, and extended lanthanide measurements were performed at KRI. All three fuel samples were obtained from the MKP109 fuel rod. The PNNL results are generally very consistent and within the range of other laboratory results. Lanthanide measurements made at KRI are less consistent and exhibit much larger deviations compared to other laboratory data. A notable inconsistency is observed for ^{149}Sm, an important burnup credit fission product. The ^{149}Sm concentration does not follow a consistent trend with the burnup of the samples and shows high variability when compared to calculations, from about -40% to +30%, indicating a serious measurement problem. A review of ^{149}Sm results from other laboratories suggests that the KRI result for sample 87-72 (104-MKP109-CC) is likely in error. Similar erratic behavior was observed for ^{151}Eu in the 87-72 sample.

Further review of the experiments indicates that the KRI measurements for nuclides with very low isotopic concentrations in the fuel samples are unreliable. Based on this observation, the KRI results for ^{149}Sm and ^{151}Eu were not considered reliable for use in code validation.

5.5.2 JAERI

The JAERI results for the Takahama samples are observed to be very consistent, the exception of the fuel rod end samples SF95-1, SF96-1, and SF97-1, excluded from this study. The RSD of the calculated-to-experiment comparisons is 1% for ^{235}U and about 3% for the major plutonium isotopes. The results for ^{241}Am are very erratic. The JAERI measurement data for all isotopes, except for samarium nuclides, were back-calculated to the time of discharge. Since most of the ^{241}Am at the time of measurement is attributed to ^{241}Pu decay, the procedure to correct measured ^{241}Am for the large ^{241}Pu contribution introduces extremely large errors in the reported ^{241}Am concentration. These additional errors were not completely considered and have been dramatically underestimated by the laboratory. Consequently, the ^{241}Am measurements are not considered reliable.

Measurement results for Takahama-3 samples SF95-1, SF96-1, and SF97-1 were excluded from consideration in this study because of systematic bias associated with the calculations. These three low burnup samples exhibit large systematic discrepancies for many isotopes. It is observed that Pu, Am, and Cm isotopes are systematically overpredicted in the current study for these samples, as illustrated in the plots in Appendix A. These three samples were located very close to the active fuel ends and were exposed to a different neutron spectrum than the rest of the fuel. These samples were previously studied,

and it was determined that three-dimensional models are required to accurately simulate the spectrum near the fuel end region.[40]

The SF96 UO_2-Gd_2O_3 rod samples exhibit a larger systematic bias for [237]Np and [134]Cs than the results for SF95 and SF97 rod samples that did not contain gadolinium poison. The bias was not observed for other isotopes, suggesting that the source of the bias could be a high sensitivity of the cross sections to changes in the neutron energy spectrum caused by the poison or self shielding calculations of resonance cross sections in the presence of a strong neutron absorber. The SF96 fuel samples were the only samples containing gadolinium poison. The present calculations were performed without spatial subdivision (radial rings) of the gadolinium-bearing fuel rod due to limitations of the NITAWL code used to perform the resonance self shielding calculations.

The JAERI measurements did not include separate analysis for any undissolved material. The measured metallic fission products [106]Ru and [125]Sb showed extremely large variability and were overpredicted in the calculations, which may indicate incomplete recovery of these isotopes in the fuel dissolver solution.

5.5.3 ANL

The TMI-1 samples measured by ANL had relatively large experimental uncertainties compared to most other laboratories due to the extensive use of lower-precision ICPMS methods and a systematic bias observed between two sets of replicate measurements. The data also exhibited a large variability in comparisons of calculations against measurements. However, the observed variability is generally consistent with the reported measurement error.

The results for several nuclides are observed to be systematically biased compared to other laboratory data for similar fuels, particularly for the plutonium isotopes. The calculated results for [239]Pu, [240]Pu, [241]Pu, and [242]Pu in the 11 TMI-1 samples measured at ANL exhibit a consistent bias (overprediction) relative to the experimental data. In the case of [239]Pu, for example, the average bias is about 15% (±3.7%); whereas, the results for [239]Pu corresponding to all other experimental data sets combined (34 samples) have a mean bias of only 2.5% (±4.2%). The RSDs of [240–242]Pu data are 6.1%, 2.8%, and 7.4%, respectively, which is generally consistent with the reported experimental errors.

The root cause of the positive bias in the plutonium data is unknown. It may be due to experimental measurement problems, uncertainties in the sample burnup (discussed below) that are not included in the error bars in the plots, and errors in the calculations and nuclear cross-section data, or it may be due to fuel configuration or operating conditions that are not accurately documented or modeled in the calculations. A potential source of uncertainty, which may have contributed to uncertainties in reactor operating conditions, was operational anomalies and fuel failure that occurred during cycle 10.[17] Some of the affected fuel rods were the source of fuel for the isotopic analysis measurements used in this study, and measured rod O12 is known to have breached clad integrity. The Electric Power Research Institute (EPRI) performed detailed fuel examinations following the cycle 10 failures to identify the root causes of fuel phenomena. The affected fuel was subject to elevated crud buildup on the fuel rods, likely localized boiling and precipitation of soluble boron on the fuel rods, and elevated fuel temperatures. Fuel rod bowing measurements were also made, and distortions of more than 0.3 mm were measured. However, biases were not observed in the TMI-1 measurements made at GE-VNC involving similar fuel that was also exposed during cycle 10, suggesting that abnormal operating conditions are not a probable cause of the discrepancy, although this cannot be altogether eliminated as a potential source of the errors. The large bias in the ANL Pu isotopes is also not observed in any other measurements involving similar fuel, indicating that the calculations are an unlikely source of the observed bias.

In the case of ^{235}U, as illustrated in Figure A.2, a very large variance in the TMI-1 results is observed. The difference between calculation and measurement is 4.7 ± 11.0%. The variance is considerably larger than that observed in other laboratories and much larger than the reported measurement uncertainty of 3.7%. Inconsistency of the ANL measurement data is revealed by a plot of the ^{235}U concentration as a function of burnup, illustrated in Figure 5.3(a), for the Phase I and Phase II measurements performed at ANL on samples from the same H6 fuel rod. These results are based entirely on the experimental data and do not involve calculations. The burnup values are those based on the measured ^{148}Nd concentration in each sample. The expect result is a gradual decrease in the ^{235}U content with increasing burnup. Samples A2, B2, C1, C3, and D2 were measured in Phase I, and samples A1B, B1B, B3J, C2B, D1A2, and D1A4 were measured in Phase II. The bias between the Phase I and II results is clearly evident. Several samples with nearly identical burnup have measured ^{235}U contents that differ by 10%. However, the same measurement data, plotted in Figure 5.3(b) as a function of axial height of the sample in the rod, exhibits an expected behavior, with an axial variation in ^{235}U concentration that is consistent with a typical burnup profile for a PWR assembly. This result clearly indicates a significant error in the sample burnup as determined by ^{148}Nd.

The reported measurement error of ^{148}Nd is about 7%, confirming that the sample burnup is not known precisely. Including the effect of the burnup uncertainty in the plots in Appendix A would significantly increase the size of the experimental error bars. The error in sample burnup for the TMI-1 samples measured at ANL will increase the calculation errors for all nuclides and result in larger differences between calculations and experiment.

A large number of nuclides from the ANL measurements exhibited significant biases that were identified as potential cause of the observed non-normal distribution of the combined data set (10 out of 38 considered isotopes), an indication of possible systematic problems with the ANL data. The problems associated with the lower-precision measurements, uncertainties in the sample burnup, bias observed between some Phase I and II results, and the operational uncertainties and fuel failures that occurred during cycle 10 could justify not recommending use of the ANL measurements for application to code validation. However, in this study, all TMI-1 results were used because of the extensive fission product measurements made by ANL that provide an opportunity to evaluate uncertainty for isotopes, which previously had very few measurements.

For burnup credit using both actinides and fission products, inclusion of the ANL data will lead to larger uncertainties for many actinides, but this increase in actinide uncertainty will be partially offset by the increase in the number of fission product measurements and a reduction in associated uncertainty due to the larger sample size.

54
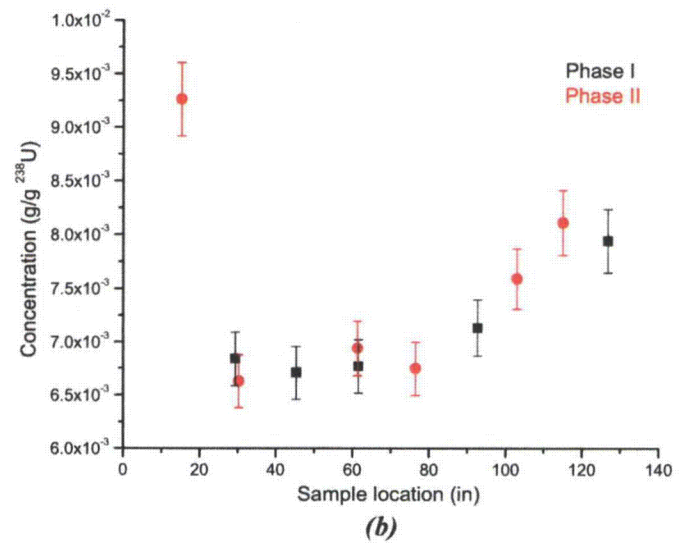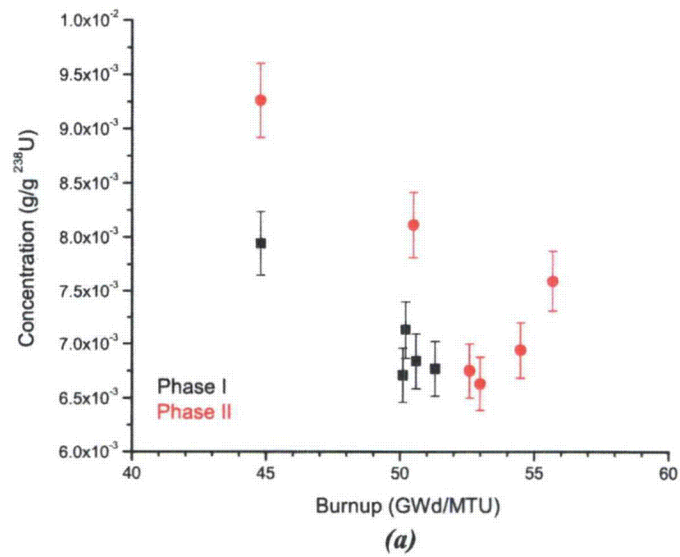
Figure 5.3. ^{235}U concentration for TMI-1 samples measured at ANL (Phase I and II) shown as a function of *(a)* estimated burnup and *(b)* axial height of the sample in the fuel rod. The stated uncertainty in the sample burnup based on measured ^{148}Nd is about 8% (50 ± 4 GWd/MTU), large enough to account for the observed deviation from an expected linear decrease in the ^{235}U with increasing burnup.

5.5.4   GE-VNC

The TMI-1 fuel samples measured at GE-VNC were made with extensive use of high-precision TIMS methods with isotopic dilution. The fuel rods from assembly NJ070G measured by GE-VNC had a lower burnup than the ANL samples from assembly NJ05YU and did not include measurements for metallic fission products. One of the measured fuel rods, O12, was identified as having failed during cycle 10, and the other rods were subject to elevated crud deposits. However, these anomalies do not appear to have adversely affected the quality of the data for validation. The uranium and plutonium results are consistent with results for other similar fuels, even though samples were obtained from several different fuel rods and are, therefore, subject to larger computational uncertainty. The RSD of the ^{235}U results is 1.2% and less than 4% for the plutonium isotopes. The plutonium results exhibit a negative bias, although the data are generally within the range of other laboratory data.

The root cause of the differences observed between the TMI-1 results for the samples measured at ANL and GE-VNC has not been clearly identified. Assemblies NJ070G and NJ05YU resided in adjacent core locations and were therefore likely subjected to similar operating conditions.

5.5.5   SCK•CEN

Four samples measured at SCK•CEN included fuel from four different fuel rods, each rod from a different assembly irradiated in either the Gösgen or GKN II reactors. Therefore, these samples will not be highly correlated to one another compared to other experiments involving more similar fuels. The SCK•CEN results are observed to be self-consistent and exhibit variability similar to that seen in other experimental results. Sample GU1 was measured at both SCK•CEN and ITU, and cross-check measurements generally confirm the accuracy of the reported measurement uncertainties.

An exception to the consistent behavior is observed for the metallic fission product species that exhibit high variability, particularly for ^{106}Ru, ^{109}Ag, and ^{125}Sb. The variance for these isotopes is significantly larger than the estimated error of the measurements. The SCK•CEN measurements included separate analysis of the undissolved residues. These results point to the significant difficulty in obtaining accurate measurements for the metallic species, even when careful analysis of the residues is performed.

The SCK•CEN fuels measured in the ARIANE program (GU1, GU3 and GU4) were obtained from a rebuilt assembly, whereby fuel rods in the assembly were reconfigured at some point during irradiation. Although this is identified as a potential source of additional computational uncertainty, the results are observed to be well within the range of other commercial UO$_2$ fuels, indicating that any uncertainty introduced by the reconfiguration of fuel rods is small. In the case of the GU1 rod, the effect of reconfiguration was judged to be sufficiently small that it was ignored. However, the reconfiguration of rod GU3/4 was explicitly modeled in this study. Also, the Gösgen samples GGU1, GGU2/1 and GGU2/2 measured in the MALIBU program were irradiated in a MOX core. Previous studies have indicated that this would not have a significant effect on the isotopic predictions, and the results in the current study confirm this assessment.

5.5.6   ITU

ITU measured Gösgen fuel sample GU4 used in this study. In general, the ITU results are observed to be well within the range of other data. ITU used high-precision TIMS measurements with isotopic dilution for the uranium and plutonium isotopes, and lower-precision ICPMS methods were used for neodymium and most other fission products. A reported measurement uncertainty of 6.7% for the ^{148}Nd concentration resulted in large burnup uncertainty and is believed to have contributed to some variability between

calculations and measurements. An anomalous overprediction of the burnup indicator ^{137}Cs by 9.1% suggests that the sample burnup based on ^{148}Nd may be too high (measurement error for ^{137}Cs was 1.5%). However, no other systematic discrepancies were observed for any other isotopes that would support a burnup discrepancy of this magnitude. Reference measurements for sample GU3 were based on a combination of measurement data from ITU and SCK•CEN. ITU measurements of ^{148}Nd in the GU3 sample were considered out-of-trend in comparisons with independent SCK•CEN measurements. The ITU data for neodymium were not recommended by the ARIANE program.[20]

ITU also performed separate analysis of the metallic elements in undissolved residues. The ITU result for ^{99}Tc in GU3 is observed to be highly discrepant as compared to the SCK•CEN result. However, the results for ^{106}Ru are very consistent, although both results indicate large discrepancies (>80%) compared to calculations and results for similar samples made at other laboratories. It is extremely difficult to reconcile these observed anomalies. The relatively short half-life of ^{106}Ru (1.023 years) makes the calculations highly sensitive to the cooling time of the samples. However, an error in the reported cooling time was not corroborated by other nuclide results.

5.5.7   *Studsvik Nuclear AB*

The Vandellós samples measured at Studsvik represent the highest burnup samples evaluated in this study. In general, the Studsvik results are observed to be consistent with samples measured at the other laboratories. The Studsvik measurements were carried out using ICPMS methods that resulted in larger uncertainties in some data. However, in most cases, the reported uncertainty of the measurements was consistent with the observed variability in results. Measurement of metallic fission product ^{103}Rh was only reported for one sample, 160-800, and ^{99}Tc was reported for two samples, E58-88 and 160-800.

Measurements were carried out in two experimental phases. The second phase provided measurements for one sample and cross-check measurements designed to confirm first phase results and reduce the experimental uncertainty. The results for ^{244}Cm were observed to be inconsistent with all other data (deviations up to 100%), but the measurements had a large relative standard error of about ±20%. The very large uncertainty makes these measurements of limited value for code validation, and the Studsvik results for this nuclide are not recommended.

5.6   *Analysis of Selected Isotopic Data*

An evaluation of the isotopic results is discussed for the following element groups: U, Pu, Np, Am, Cm, lanthanides (La, Ce, Pr, Nd, Sm, Eu, Gd), Cs, and metallic species (Tc, Mo, Ru, Rh, Ag, Sb, Sr).

The evaluations are restricted to the isotopes listed in Table 5.1 as being important to burnup credit and radiological safety applications. The results discussed in this section refer to the percent differences between the calculated and measured isotopic concentrations.

Comparisons of calculated and experimental data shown in Appendix A include the results for all samples included in this study. The plots include the three Takahama-3 samples, identified as SF95-1, SF96-1, and SF97-1, that were removed from consideration in the uncertainty analysis because of their proximity to the active ends of the fuel rods. The figures include the results for all samples.

5.6.1   *Uranium Isotopes*

Results for the uranium isotopes, ^{234}U, ^{235}U, ^{236}U, and ^{238}U, are plotted in Figures A.1 to A.4.

5.6.1.1 U-235

The results for ^{235}U are observed to be predicted on average within about 5% of the measurement for most samples. The largest deviations are observed for the TMI-1 samples measured at ANL. The deviations are directly attributed to the uncertainty in the experimental determination of the sample burnup caused by a large uncertainty in the measured ^{148}Nd content as discussed in Section 5.5.3. The sample burnup uncertainty is not included in the error bars shown in the plots. Burnup uncertainty will impact the calculated isotopic results by different amounts. Uranium-235 concentration, particularly for high burnup fuel, is extremely sensitive to the burnup value.

Analysis of all measurement data for ^{235}U resulted in a mean bias of 1.6 ± 6.2%. Removal of the ANL data from the set would result in a significantly reduced mean and standard deviation: 0.7 ± 3.7%. All ^{235}U data were included in the uncertainty analysis for this study.

5.6.1.2 U-238

Several laboratories (ANL, GE-VNC, and Studsvik) reported measured isotopic data as isotopic mass relative to ^{238}U mass in the sample. In these cases, the nuclide concentrations were adjusted to mass relative to uranium mass initially present in the fuel (unirradiated) using the combined heavy metal mass measured in the sample, adjusted for heavy metal mass loss caused by fission using measured ^{148}Nd as a measure of integral fissions. For these measurements absolute ^{238}U mass was not reported. Although it is possible to derive ^{238}U content from the other isotopic measurements, such a procedure was not used in this study.

All calculated results for ^{238}U were within 1% of the measurement. The PNNL results for the Calvert Cliffs sample showed the largest variations and had the largest uncertainty. The GU1 sample had a deviation slightly larger than the reported uncertainty.

5.6.1.3 U-234

The discrepancies in the ^{234}U results are significantly larger than for the other uranium isotopes analyzed. One possible explanation is uncertainty in the specified initial concentration of ^{234}U in the fuel. The precision of the initial uranium isotopic vector is generally not given and may be subject to error since the ^{234}U concentrations in fresh fuel are very low (typically <0.05 wt % ^{234}U/U). In experiments where the initial concentration of the minor isotopes ^{234}U and ^{236}U were not specified, the calculations applied approximate values derived from other similar experiments. However, the concentrations of ^{234}U and ^{236}U in unirradiated fuel are dependent on the origin and enrichment of the fuel, and there is considerable uncertainty in derived estimates that may contribute to observed discrepancies. The final ^{234}U content is highly dependent on the initial concentration in the unirradiated fuel.

Therefore, experiments that did not provide measured initial ^{234}U content should not be used to validate calculated ^{234}U content in spent fuel. The only experiment that did not document the initial ^{234}U concentration was Calvert Cliffs 1.

5.6.1.4 U-236

The concentration of initial ^{236}U was only documented for some of the samples considered. It is present from the use of some recycled fuel in the fuel manufacturing process, since it does not occur naturally. However, the concentration of ^{236}U in spent fuel is not very dependent on the initial concentration. The results for ^{236}U are well predicted for most samples.

58

5.6.2 *Plutonium Isotopes*

The results for the plutonium isotopes are plotted in Figures A.5 to A.9.

5.6.2.1 *Pu-238*

The calculated ^{238}Pu results exhibit an average negative bias. The ANL results have a variance that is larger than the reported experimental uncertainty and larger than the variance of other data sets. The ^{238}Pu measurements are generally made by α-spectrometry (other plutonium isotopes were measured by ICPMS) and may be subject to larger experimental errors. As the concentration of ^{238}Pu is very sensitive to the fuel burnup, it may have been affected by errors in the sample burnup similar to the ^{235}U case, as discussed previously.

5.6.2.2 *Pu-239*

The ^{239}Pu data are generally calculated within the range of experimental error and are overpredicted on average. The ANL data are observed to be inconsistent with respect to other data. The variance of the ANL results, however, is consistent with the reported measurement uncertainty. The results show a positive bias not observed with other data sets. The bias is not explained on the basis of the burnup uncertainty because the concentration of ^{239}Pu is not highly sensitive to burnup and all samples are biased to a similar extent. All ^{239}Pu measurements were used in the uncertainty analysis in this study because the bias could not be clearly associated with experimental errors. However, use of the TMI-1 data measured by ANL significantly altered the mean bias and increased the standard deviation of the data as compared to the case when the ANL data were not considered.

5.6.2.3 *Pu-240*

The results for ^{240}Pu are very similar to those obtained for ^{239}Pu. The TMI-1 data measured by ANL are again observed to be systematically overpredicted as compared to all other laboratory measurements.

5.6.2.4 *Pu-241*

The ^{241}Pu results from each laboratory exhibit very similar behavior to the other plutonium data. Calculations are generally within the experimental uncertainties. The ANL results exhibit a positive bias with respect to other data, but the scatter is consistent with the reported measurement uncertainty.

5.6.2.5 *Pu-242*

The ^{242}Pu results exhibit larger variability than the other plutonium isotopes. The TMI-1 data measured by ANL exhibit large variations, but the results generally lie within the range of other measurements. The calculated results for the TMI-1 fuel are consistently underpredicted relative to GE-VNC measurements and do not agree within experimental uncertainty with the TMI-1 fuel measured at ANL.

5.6.3 *Neptunium-237*

Neptunium-237 is a minor actinide in burnup credit calculations. Results for ^{237}Np (illustrated in Figure A.10) show good agreement between calculations and measurements for all samples, with the exception of the Takahama-3 data for the samples from gadolinium-bearing fuel rod SF96. This deviation is likely associated with the calculations and the evaluated nucldear data (SF96 is the only measured rod that contained gadolinium). The ITU result for sample GU4 and the Studsvik results exhibit a negative bias relative to the other laboratory results.

The discrepancy in ^{237}Np requires further investigation. Since many modern fuel designs make extensive use of burnable poison rods, additional work is needed to fully understand the nature of the observed errors in predicted ^{237}Np content for gadolinium rods. The systematic deviations cannot be dismissed as erratic data. Until the issue is resolved, it is recommended that ^{237}Np data not be used in burnup credit calculations for fuel assemblies containing integral burnable poison rods, unless the bias observed in the calculated results for the poison rod is conservatively addressed in the uncertainty analysis.

5.6.4   Americium

The results for the americium isotopes are plotted in Figures A.11–A.13.

5.6.4.1   Am-241

The ^{241}Am results exhibit large deviations that are difficult to evaluate. The concentration of ^{241}Am at the time of measurement is attributed almost entirely to formation of ^{241}Am from decay of ^{241}Pu after discharge. The Takahama-3 results, as previously indicated, were back calculated to the time of discharge, and this procedure introduced large errors in the adjusted measurements for ^{241}Am. The Takahama results are therefore not considered for validation in this study.

The ^{241}Am results for other samples (reported at the time of measurement) are expected to mirror very closely the results for ^{241}Pu. However, the ^{241}Am results are observed to exhibit much larger deviations than its decay parent. The calculated ^{241}Am concentrations are biased consistently higher than measurement for samples measured by SCK•CEN and Studsvik results, by >20%. The bias in the Studsvik results may be attributed in part to the relatively large uncertainty in the measurements. The SCK•CEN data has much lower reported uncertainty; however, the observed ^{241}Am bias is inconsistent with ^{241}Pu, and inconsistent with other laboratory results, CEA and ITU included.

The discrepancy in the SCK•CEN data for ^{241}Am may be caused by a systematic bias in the measurements made using α-spectrometry that results in values of the ^{241}Am content that are about 20% low. Additionally, the bias likely extends to other americium isotopes determined by TIMS using the ^{241}Am concentration to determine the absolute contents of the other isotopes. It is observed that ^{242m}Am and ^{243}Am are also overpredicted relative to the SCK•CEN data by about 20%. The GE-VNC and ITU results do not exhibit a significant bias, and the agreement between the biases seen for ^{241}Am and ^{241}Pu is a good indication of the quality of the GE-VNC and ITU ^{241}Am measurements.

Better estimates of ^{241}Am uncertainty and bias may be obtained indirectly by using the results for ^{241}Pu, which are generally measured with much higher precision. Since ^{241}Am is formed primarily from the decay of ^{241}Pu at most cooling times of interest to transportation and interim storage (and at the time of measurements), any bias in ^{241}Pu will be reflected directly in the ^{241}Am results. For shorter cooling times, however, this cannot be assumed.

5.6.4.2   Am-243

The calculated ^{243}Am results for most samples are overpredicted relative to the measurements. The ANL results exhibit clear systematic bias between the Phase I and Phase II measurements, as seen in Figure 5.4. Calculated results are within the Phase I experimental results, whereas the Phase II results exhibit a positive bias of about 50%, indicating significant ^{243}Am measurement problems in Phase II. The TMI-1 data for ^{243}Am measured by ANL are nevertheless included in this study as the deviations in the ANL data are similar to those observed in several other experiments. Similar measurement problems were observed for ^{242m}Am. These discrepancies highlight the difficulty in obtaining reliable americium measurements.
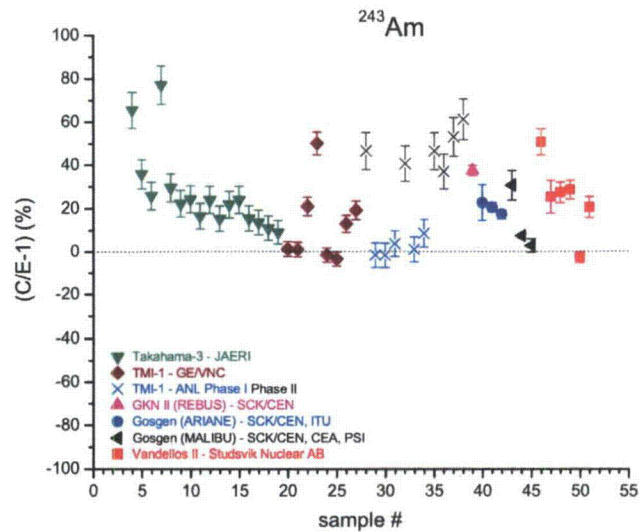
Figure 5.4. Comparison of measurements and calculations for ^{243}Am. The ANL results for the Phase I and II measurements are shown separately.

5.6.5 Curium Isotopes

The curium isotopic results are plotted in Figures A.14 to A.19.

The results for the ^{242}Cm and ^{244}Cm isotopes, both important neutron emitters, exhibit relatively large variability, which may be partially attributed to the relatively low accuracy of many curium measurements made by α-spectrometry. The observed variance is generally larger than the uncertainties cited for the measurements.

The calculated results for the Studsvik data of ^{244}Cm (shown in Figure A.16) exhibit very large deviations compared to the measured values. The large uncertainty of the measurements makes these data of limited value for code validation. These results are highly inconsistent with other laboratory measurements of similar samples. The Studsvik results for ^{244}Cm were therefore not considered in this study.

5.6.6 Lanthanides

Results for the neodymium isotopes $^{142-148}$Nd and ^{150}Nd are plotted in Figures A.27–A.33. Other lanthanides ^{144}Ce, $^{147-152}$Sm, ^{154}Sm, ^{151}Eu, $^{153-155}$Eu, $^{154-156}$Gd, ^{158}Gd, and ^{160}Gd are plotted in Figures A.24–A.26 and A.35–A.50.

5.6.6.1 Nd-143

The calculated results for ^{143}Nd, one of the six fission products most important for burnup credit, are observed to be predicted within the experimental uncertainty. The calculations are generally within about 5% of experiment, with the exception of the ANL measurements, which exhibit relatively large scatter and are biased high on average. The reported uncertainty of the ANL measurements of ^{143}Nd is ±6%.

61

5.6.6.2 Nd-145

The results for ^{145}Nd are observed to be very similar to ^{143}Nd. The isotope is generally well predicted for all experimental data.

5.6.6.3 Nd-148

For most samples evaluated in this study, the calculational procedure used a sample burnup value that yielded a calculated ^{148}Nd value that was consistent with the measured value. Consequently, the ^{148}Nd results for these samples, as shown in Figure A.32, exhibit good agreement between calculation and experiment. Larger variations were observed for some samples that used ^{148}Nd and other indicators of burnup, such as ^{137}Cs, to estimate the sample burnup. Additional measures of burnup were used in instances where there was some indication of ^{148}Nd measurement problems.

5.6.6.4 Ce-144

The results for ^{144}Ce are observed to be well predicted in most samples, although the scatter of data is relatively large due likely to uncertainties in the measurements. The decay daughter of ^{144}Ce ($T_{1/2} = 285$ days) is ^{144}Pr ($T_{1/2} = 17$ minutes), an important gamma-emitting nuclide and a dominant gamma source in shielding for decay times less than about 5 years.

5.6.6.5 Sm-149

The samarium isotopes have large absorption cross sections, and ^{147}Sm, ^{149}Sm, ^{150}Sm, ^{151}Sm, and ^{152}Sm are important to burnup credit criticality calculations that consider fission product absorption. The results for the samarium isotopes are plotted in Figures A.35–A.47.

The results for ^{149}Sm, one of the six most important fission products in burnup credit calculations that credit fission products, are shown in Figure A.36. Calculated concentrations are overpredicted on average, and the observed bias appears to be dependent on the measurement laboratory. The ^{149}Sm results for the Calvert Cliffs samples are highly discrepant and were not recommended in this study based on the observed experimental problems previously discussed.

5.6.6.6 Sm-147 and Sm-150

Calculated results for ^{147}Sm and ^{150}Sm are predicted within experimental uncertainty for most samples, with the exception of the ANL data, which are biased with respect to the other data sets. However, the deviations in the ANL data are generally consistent with the reported uncertainty of the measurements. The behavior of the ANL data is similar to that observed for many of the neodymium isotopes; the data are clearly biased, resulting in a non-normal distribution of the combined data in some cases, but generally, the data exhibit a variance that is consistent with the experimental uncertainty.

5.6.6.7 Sm-151 and Sm-152

Results for ^{151}Sm and ^{152}Sm exhibit a positive bias of about 30% for all data sets. The variance in these results is also large.

5.6.6.8 Europium Isotopes

The europium isotopic results are plotted in Figures A.42–A.45. The ^{153}Eu isotope, and to a lesser extent ^{151}Eu, are fission products important to burnup credit. Europium-154 ($T_{1/2} = 8.6$ years) is moderately

important to decay heat calculations and is a dominant nuclide in gamma ray shielding in the timeframe 10 to 30 years after discharge. Results for [155]Eu are also indirectly important to burnup credit, because [155]Gd is produced in significant quantities by the decay of [155]Eu after discharge. Therefore, any bias in [155]Eu will directly affect [155]Gd.

The [154]Eu results are generally calculated within the range of experimental uncertainty, although the SCK•CEN, Studsvik, and Calvert Cliffs data exhibit relatively large variance. No large discrepant bias was observed in the data sets.

Calculated [153]Eu is generally predicted to within 10% of measurement, although a different bias is evident in each of the laboratory data sets. The GE-VNC and Studsvik results are uniformly low, and the KRI, SCK•CEN, and ANL results are all high.

Evaluation of [151]Eu, plotted in Figure 5.5, was more problematic because the results for most data sets exhibited large deviations. Data from ANL, KRI, and SCK•CEN exhibited inconsistent behavior and deviations much larger than the estimated measurement uncertainties. The results from these laboratories ranged from about -40% to +30%. The variability is inconsistent with results of all other europium isotopes. The concentration of [151]Eu in fuel is very low, and this may have contributed to experimental errors. The deviations of the ANL and KRI data for samples obtained from the same fuel rod measurements are a strong indicator of measurement problems. Based on the erratic behavior of the KRI, SCK•CEN, and ANL data, these measurements were not recommended for use in this study.

5.6.6.9 Gd-155

The results for the gadolinium isotopes are plotted in Figures A.46–A.50. The calculated results for [155]Gd are consistently underpredicted relative to measurement for all samples, by about 15 to 50%. The concentration of [155]Gd at the time of the measurement is attributed entirely to the decay of the parent [155]Eu ($T_{1/2} = 4.75$ years). The bias observed for [155]Eu is very similar to that of [155]Gd, confirming that the source of the bias in [155]Gd results from errors in the predicted concentration of the [155]Eu.

5.6.7 Cesium Isotopes

The results for the cesium isotopes are plotted in Figures A.20–A.23.

5.6.7.1 Cs-133

The [133]Cs isotope is one of the six most important fission products in burnup credit calculations. The measured results are observed to be well predicted, within 7% of measurement for all 13 samples. No measurements of [133]Cs were made by ANL, GE-VNC, or JAERI.

5.6.7.2 Cs-134

The calculated results for [134]Cs are systematically underpredicted in all samples by about 15–20%, with the exception of the Takahama-3 gadolinium poison rod SF96 samples that are not recommended in this study. Cesium-134 ($T_{1/2} = 2.06$ years) is a dominant nuclide in decay heat and shielding calculations for decay times less than about 10 years (see Figure 5.2), where [134]Cs can represent more than 25% of the decay heat. The production route for [134]Cs is from [133]Cs neutron capture.
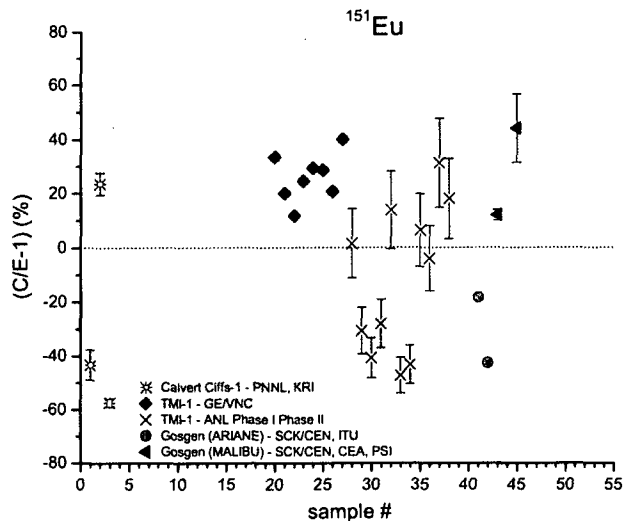
Figure 5.5. Comparison of measurements and calculations for ^{151}Eu. The ANL results for the Phase I and II measurements are indicated separately.

5.6.7.3 Cs-137

The isotope ^{137}Cs ($T_{1/2}$ = 30 years), an important gamma source, is generally predicted within about 5% of experiment. The variation of the data is generally consistent with the reported measurement uncertainties, with the exception of the ANL measurements that exhibit differences that range from -14% to +17%, discrepancies likely associated with uncertainties in sample burnup as previously discussed.

The 662 keV gamma rays, commonly associated with ^{137}Cs decay, are actually due to the decay progeny ^{137m}Ba ($T_{1/2}$ = 2.5 minutes). Gamma rays and decay energy associated with ^{137m}Ba make this nuclide an important decay heat and radiological isotope. The isotopic validation results for ^{137}Cs are directly applicable to validating the predictions for ^{137m}Ba because these nuclides are in secular equilibrium at the time of the measurements.

5.6.8 Metallic Fission Product Isotopes

The results for the metallic fission products ^{90}Sr, ^{95}Mo, ^{99}Tc, ^{101}Ru, ^{106}Ru, ^{103}Rh, ^{125}Sb, and ^{109}Ag are plotted in Figures A.51–A.58.

5.6.8.1 Mo-95, Tc-99, Ru-101, Rh-103, and Ag-109

The nuclides ^{95}Mo, ^{99}Tc, ^{101}Ru, ^{103}Rh, ^{109}Ag are often considered in burnup credit calculations that credit fission products. Rhodium-103 is one of the six most important burnup credit fission products. The metallic elements are known to be difficult to dissolve in nitric acid (usually employed to dissolve uranium fuels) and are commonly associated with undissolved residues in high concentrations. The Gösgen and GKN II fuel measurements performed by SCK•CEN, ITU, PSI, and CEA in the Belgonucleaire experimental programs evaluated undissolved material separately to ensure recovery of all fission product material in the reported concentrations. Other laboratories that reported results for some metallic species (PNNL and ANL) did not evaluate undissolved material but also did not indicate the

64

presence of any significant quantity of residue in the dissolver. Any significant amount of unaccounted material would incorrectly appear as an overprediction by the code. In general, the results for many of these metallic species exhibit relatively large deviations, likely to be associated with the complexity and difficulty of performing accurate measurements.

Results for ^{95}Mo are well predicted in all samples. The calculated data are within about 10% of the measured values for most samples.

The variations in the ^{99}Tc data are similar to ^{95}Mo for most samples; however, the ITU result for GU4 is clearly discrepant relative to the other data, and one of the TMI-1 samples measured at ANL is also discrepant.

Results for ^{101}Ru exhibit large deviations for the samples measured at SCK•CEN, for which the observed variation of the results is about 16%. The REBUS sample is discrepant (30% overpredicted) as compared to the other three samples measured at SCK•CEN. The ANL results are well within the range of results reported by SCK•CEN and ITU.

The ^{103}Rh results are overpredicted on average by about 13%. Measurements of ^{103}Rh were only performed at ANL, SCK•CEN, and ITU. It was noted that one measurement of ^{103}Rh made by KRI for an ATM-106 sample evaluated previously (but not used in this study) indicated an underprediction of ^{103}Rh rather than the overprediction seen in the samples evaluated here.[41]

Results for ^{109}Ag are highly erratic and overpredicted. The results give little confidence in the ability to accurately measure ^{109}Ag. The results for samples GU3 and GGU2 are well predicted (<10%), whereas GU1, measured at ITU, is overpredicted by more than 100% and the GKN II sample is overpredicted by 31%. The data for the four samples measured at SCK•CEN have an RSD of 56%. The ANL results are overpredicted from 34% to 205%, and the data have a relative standard deviation of 55%. The experimental problems with measurements of ^{109}Ag performed at ANL are probably biased because of dissolution chemistry problems associated with loss of silver in precipitates, resulting in poor reproducibility.

5.6.8.2 Ru-106 and Sb-125

Measurements of ^{106}Ru and ^{125}Sb are reported by JAERI and SCK•CEN, and ^{106}Ru was also measured by ITU and Studsvik. Although the GU3 and GU4 sample results for ^{106}Ru, measured by SCK•CEN and ITU, respectively, are similar, the data are clearly problematic, and there is probably an issue common to the samples, error in the measurements or data used in the calculations. These particular measurements for samples GU3 and GU4 were removed in this evaluation, although the results for the other samples measured by SCK•CEN were retained.

The Takahama results are also very erratic and exhibit a systematic positive bias consistent with a potential loss of the metallic species in the residue. However, the source of the variability is not confirmed. The Takahama results for ^{106}Ru and ^{125}Sb were therefore not used because of the erratic behavior and variability of the data.

5.6.8.3 Sr-90

Strontium-90 ($T_{1/2}$ = 28.8 years) isotope and its decay progeny ^{90}Y ($T_{1/2}$ = 2.7 days) are fission products important in decay heat calculations, and ^{90}Y is an important radiological gamma source. The results for ^{90}Sr have important implications on radiological dose assessments involving fission product release. The ^{90}Sr results are also directly applicable to validating ^{90}Y because these isotopes are in secular equilibrium.

Only six measurements of ^{90}Sr were available. The result for the Gösgen GU1 sample measured by SCK•CEN is low compared to the other two samples, GU3 and GGU2, also measured by SCK•CEN, and compared to the results for the three Calvert Cliffs samples measured at PNNL.

5.6.9 *Isotopic Bias and Uncertainty Results*

The mean and relative standard deviation of the validation results for the combined data sets, with the discrepant data removed from the population of isotopic data, are listed in Table 5.18. Only the isotopes identified as being important to burnup credit, decay heat, and radiation source terms are shown. The table lists the total number of measurements used, the sample mean (bias), the RSD between calculation and experiment, and the p = 95% confidence interval for each nuclide.

It is important to emphasize that samples were removed only when there was clear evidence of experimental problems that yielded erratic and non-physical measurement results. The following list summarizes the experimental data that was not considered in the analysis of isotopic bias and uncertainty.

- Takahama samples SF95-1, SF96-1, SF97-1 (fuel end region samples)

- Takahama measurements of ^{241}Am (errors caused by back calculation to discharge)

- Vandellós results for ^{244}Cm (excessive measurement uncertainty)

- Calvert Cliffs results for ^{149}Sm (erratic experimental data associated with low isotopic concentrations)

- Gösgen, GKN II, and Calvert Cliffs results for ^{151}Eu (concentrations near detection limit)

- TMI-1 measurements of ^{242m}Am (experimental problems)

- Takahama measurements for ^{106}Ru and ^{125}Sb

Table 5.18. Summary of analysis results for all samples used in this study

Nuclide	No. of measurements	C/E–1 (%)	σ C/E–1 (%)	Tolerance interval (p = 95%/95%)	
				Lower (%)	Upper (%)
U-234	44	5.9	11.2	-21.1	33.0
U-235	47	1.5	6.4	-13.8	16.8
U-236	47	0.6	3.0	-6.5	7.8
U-238	27	-0.2	0.4	-1.2	0.8
Pu-238	48	-5.7	11.5	-23.1	11.8
Pu-239	48	5.8	6.1	-8.7	20.4
Pu-240	48	6.1	6.9	-10.4	22.6
Pu-241	48	-1.1	4.7	-12.3	10.1
Pu-242	48	-0.5	7.1	-17.5	16.5
Np-237	43	6.0	18.3	-38.3	50.3
Am-241	35	4.5	17.6	39.3	48.3
Am-243	45	20.8	16.7	-19.4	61.0
Cm-242	26	-17.5	17.3	-63.2	28.2
Cm-244	28	-2.4	11.1	-31.0	26.2
Cs-133	15	4.8	4.5	-8.5	18.1
Cs-134	36	-14.0	7.2	-31.8	3.9
Cs-137	48	-2.2	4.4	-12.7	8.3
Ce-144	25	5.1	10.9	-23.5	33.8
Nd-143	48	2.6	4.5	-8.1	13.4
Nd-145	48	1.6	2.4	-4.1	7.3
Sm-147	39	1.2	8.2	-18.9	21.3
Sm-149	37	13.4	10.4	-12.3	39.1
Sm-150	40	6.1	5.6	-7.6	19.8
Sm-151	40	34.4	9.2	11.9	56.9
Sm-152	40	28.2	8.1	8.4	48.0
Eu-151	23	3.4	29.3	-75.0	81.7
Eu-153	34	2.0	6.9	-15.2	19.3
Eu-154	28	6.0	9.3	-18.0	30.0
Eu-155	26	-40.7	15.3	-80.7	-0.7
Gd-155	34	-36.2	15.9	-74.5	2.1
Sr-90	9	-2.5	8.38	-32.2	27.2
Mo-95	18	-0.3	6.0	-17.2	16.6
Tc-99	23	4.7	11.3	-25.5	34.9
Ru-101	18	5.7	9.4	-20.8	32.2
Ru-106	24	11.3	24.5	-53.7	76.3
Rh-103	19	10.2	8.7	-14.0	34.4
Ag-109	17	99.4	62.2	-78.4	277.2
Sb-125	18	75.7	40.0	-37.1	188.5

5.7 Observations and Recommendations

Observations from the isotopic data validation performed using the high burnup spent fuel samples analyzed in this study are summarized. Several lessons learned from the evaluation process and recommendations for future studies that will be performed as new experimental data are made available and analyzed are included.

- There is no physical standard that can be used to calibrate measurement techniques and instruments for spent fuel isotopic measurements; the accuracy of measurements can be assessed only by careful analysis and intercomparison of data.

- No single measure or criterion appears to be reliable for assessing experimental data quality. The evaluation process requires careful consideration of the analytical techniques used for each isotope, and correlations caused by modeling approximations and nuclear data issues, and it involves comparison of data with other established measurement laboratories.

- Statistical tests are useful in evaluating data sets for consistent behavior but alone are not sufficient to assess the quality of measurement data.

- The measurement uncertainties should be used to weight the different measurements to account for experimental error in future studies, if possible, provided that realistic uncertainties can be assigned to the data. Uncertainties were not used quantitatively in this study because the values reported by several laboratories appear to be unrealistically small and did not account for uncertainties in all phases of the measurement process.

- Error in the burnup determined from the measurements should be included in the experimental error to provide more realistic error bars on the experimental data.

- Measurement accuracies for the metallic fission products appear to be problematic. Evaluation of undissolved residues for metallic fission products can be important to increase the accuracy for these nuclides, as previous studies have indicated that the fraction of these nuclides recovered in the dissolver solution can vary widely. However, the results for the metallic species exhibit very large variance even for laboratories that separately measured these species in undissolved residues; measurement errors for these nuclides are likely to be underestimated.

- Isotopic data acquired from standard commercial reactor fuel assemblies should be used whenever possible. However, the reality is that isotopic measurements on spent fuel have frequently not been performed for standard fuel, but for fuels intended for other purposes. In this study, measurements for high burnup spent fuel were obtained from
    o Assemblies that were rebuilt (reconstituted) during irradiation;
    o Assemblies that experienced abnormal operations and fuel rod failures; and
    o Assemblies irradiated in reactors operating with MOX fuels.

An assessment of these fuels indicated that they were highly applicable for validation of standard commercial UO_2 fuel. The results observed in this study confirm that assessment, although the nonstandard fuels likely contributed to additional uncertainty.

- An important consideration is the number of fuel samples obtained from each rod. While cost factors may favor acquiring a large number of samples from a single rod, it must be recognized that such samples, alone, do not represent an accurate measure of the uncertainty because the computational bias due to reactor operating conditions and position of the fuel rod in the assembly are highly correlated. Nevertheless, acquisition and analysis of multiple samples from the same fuel rod are desirable for the purposes of experimental error analysis.

- The validation data analyzed in this study are generally representative of modern fuels. The database includes fuel samples covering a broad range of enrichments and burnups that are representative of the fuel assembly inventory, a representative selection of rods within an assembly (include gadolinium poison rods), different assembly designs, and different reactor types.

6 CONCLUSIONS

An extensive isotopic validation database has been compiled and analyzed to provide a basis for evaluating the uncertainties in calculations involving spent nuclear fuel. The bias and uncertainties in the isotopic predictions documented in this report are applicable to establishing margins for uncertainty for applications including burnup credit criticality calculations, decay heat calculations, and radiation source terms. The calculations described in this report were performed using the two-dimensional TRITON/NEWT depletion analysis sequence in SCALE 5.1. This sequence supersedes the one-dimensional SAS2H sequence, widely used by industry for spent fuel isotopic calculations. The two-dimensional sequence is more rigorous for modeling modern heterogeneous fuel assembly designs and for modeling some of the more complex fuel reconfigurations that have occurred in some experimental programs. The validation results presented in this study are not directly applicable to validating other depletion analysis sequences in SCALE.

The high burnup spent fuel samples evaluated in this study were selected on the basis of having extensive actinide and fission product nuclide measurements. The selected samples, obtained from assemblies irradiated in six different PWR plants operated in Germany, Japan, Spain, Switzerland, and the United States, have enrichments from 2.6 to 4.7 wt % ^{235}U and cover a large burnup range, from 14 to 78 GWd/MTU. The database therefore covers fuel with burnup levels up to, and beyond, the current licensing peak rod limit of 62 GWd/MTU.

The isotopic validation data in this report provide the technical basis for performing application-specific uncertainty assessments. Realistic estimates of application bias and uncertainty can be obtained by identifying the relative contribution of the dominant nuclides to the fuel property being calculated, and by propagating the isotopic bias and the uncertainties using either bounding or best-estimate methods.

The calculated isotopic results are generally found to be within the range of the experimental data for many important isotopes in spent fuel. It was observed that the calculation bias does not depend to any significant extent on the burnup of the samples, and there are no significant trends observed for very high burnup fuel. Although the bias in the calculated nuclide concentrations is not observed to depend to a measurable extent on burnup, the bias associated with the application will change as the relative importance of different isotopes changes as a function of fuel enrichment, burnup, and cooling time.

It is recognized that inclusion of some of the more problematic data in this analysis will yield relatively large and conservative estimates of isotopic uncertainty. Reducing isotopic uncertainties in the future will likely require additional measurements performed using high-precision measurement techniques and instruments. As additional isotopic measurement data are acquired, the database evaluated in this study will also provide a basis for assessing the quality of new experimental data.

7   REFERENCES

1. *SCALE: A Modular Code System for Performing Standardized Computer Analyses for Licensing Evaluations*, ORNL/TM-2005/39, Version 5.1, Vols. I–III, Oak Ridge National Laboratory, Oak Ridge, TN, November 2006. Available from the Radiation Safety Information Computational Center at Oak Ridge National Laboratory as CCC-725.

2. G. Ilas, I. C. Gauld, F. C. Difilippo, and M. B. Emmett, *Analysis of Experimental Data for High Burnup PWR Spent Fuel Isotopic Validation–Calvert Cliffs, Takahama, and Three Mile Island Reactors*, NUREG/CR-6968, ORNL/TM-2008/071, prepared for the Nuclear Regulatory Commission by Oak Ridge National Laboratory, Oak Ridge, TN (2008).

3. G. Ilas, I. C. Gauld, and B. D. Murphy, *Analysis of Experimental Data for High Burnup PWR Spent Fuel Isotopic Validation–ARIANE and REBUS Programs (UO2 Fuel)*, NUREG/CR-6969, ORNL/TM-2008/072, prepared for the Nuclear Regulatory Commission by Oak Ridge National Laboratory, Oak Ridge, TN (2008).

4. G. Ilas and I. C. Gauld, *Analysis of Experimental Data for High Burnup PWR Spent Fuel Isotopic Validation–Vandellós II Reactor*, NUREG/CR-7013, ORNL/TM-2009/321, prepared for the Nuclear Regulatory Commission by Oak Ridge National Laboratory, Oak Ridge, TN (2010).

5. *MALIBU Program–Radiochemical Analysis of MOX and UOX LWR Fuels Irradiated to High Burnup*, Belgonucleaire Technical Proposal, MA 2001/02, Belgonucleaire, Brussels, Belgium (September 2001).

6. R. J. Guenther et al., *Characterization of LWR Spent Fuel MCC-Approved Testing Material ATM-104*, PNL-5109-104, Pacific Northwest Laboratory, Richland, WA (1991).

7. S. R. Bierman and R. J. Talbert, *Benchmark Data for Validating Irradiated Fuel Compositions Used in Criticality Calculations*, PNL-10045, Pacific Northwest Laboratory, Richland, WA, October 1994.

8. "Standard Test Method for Atom Percent Fission in Uranium and Plutonium Fuel (Neodymium-148 Method)," American Society for Testing and Materials, ASTM E 321 (1996).

9. M. D. DeHart, M. C. Brady, and C. V. Parks, *OECD/NEA Burnup Credit Calculational Criticality Benchmark Phase I-B Results*, NEA/NSC/DOC(96)-06 (ORNL-6901) Oak Ridge National Laboratory, Oak Ridge, TN, June 1996.

10. H. Mochizuki, K. Suyama, Y. Nomura, H. Okuno, *Spent Fuel Composition Database System on WWW - SFCOMPO on WWW Ver.2*, JAERI-Data/Code 2001-020, Japan Atomic Energy Research Institute (2001), from http://www.nea.fr/sfcompo/.

11. Y. Nakahara, Y. Suyama, and T. Suzaki, *Technical Development on Burnup Credit for Spent LWR Fuels*, JAERI-Tech 2000-071 (ORNL/TR-2001/01), English Translation, Oak Ridge National Laboratory, Oak Ridge, TN (2002).

12. K. Suyama, H. Mochizuki, and T. Kiyosumi, "Revised Burnup Code System SWAT: Description and Validation Using Postirradiation Examination Data," *Nucl. Technol.* **138(2)**, 97–110 (2002).

13. J. M. Scaglione, *Three Mile Island Unit 1 Radiochemical Assay Comparisons to SAS2H Calculations*, Yucca Mountain Project Report, CAL-UDC-NU-000011, Rev. A, April 2002.

14. S. F. Wolf, D. L. Bowers, and J. C. Cunnane, *Analysis of Spent Nuclear Fuel Samples from Three Mile Island and Quad Cities Reactors: Final Report*, Argonne National Laboratory, Argonne, IL, November 2000.

15. S. F. Wolf, D. L. Bowers, and J. C. Cunnane, "Analysis of High Burnup Spent Nuclear Fuel by ICPMS," *J. Radioanal. Nucl. Chem.* **263**, 581–586 (2005).

16. R. D. Reager and R. B. Adamson, *TRW Yucca Mountain Project, Test Report, Phase 1 and Phase 2*, Ref. TRW Purchase Order No. A09112CC8A, GE Nuclear Energy.

17. TMI-1 Cycle 10 Fuel Rod Failures, Volume 1: Root Cause Failure Evaluations, EPRI, Palo Alto, CA; GPU Nuclear, Parsippany, NJ; and Duke Power Company, Charlotte, NC: 1998. EPRI Report TR-108784-V1.

18. M. Lippens et al., "Source Term Assessment: The ARIANE Program," The 8th International Conference on Radioactive Waste Management and Environmental Remediation (ICEM), Bruges, Belgium, September 30–October 4, 2001.

19. J. Basselier et al., "Validation for Computer Codes for Source Term and Burnup Credit Evaluations," IAEA Technical Meeting on Optimization of Cask/Container Loading for Long-Term Spent Fuel Storage, Vienna, Austria, March 2003.

20. *ARIANE International Programme–Final Report*, ORNL/SUB/97-XSV750-1, Oak Ridge National Laboratory, Oak Ridge, TN, May 1, 2003.

21. D. Boulanger et al., "High Burnup PWR and BWR MOX Fuel Performance: A Review of Belgonucleaire Recent Experimental Programs," ANS International Meeting on LWR Fuel Performance, Orlando, Florida, September 19–22, 2004.

22. P. Baeten, K. Van der Meer, S. Van Winckel, M. Gysemans, L. Sannen, D. Marloye, B. Lance, and J. Basselier, "The Burnup Credit Experimental Programme REBUS," *Practices and Developments in Spent Fuel Burnup Credit Applications, Proceedings of a Technical Committee Meeting,* Madrid, April 22–26, 2002, IAEA-TECDOC-1378 (2003).

23. J. M. Conde, C. Alejano, and J. M. Rey, "Nuclear Fuel Research Activities of the Consejo de Seguridad Nuclear," *Proceedings of the Top Fuel 2006 International Meeting on LWR Fuel Performance,* Salamanca, Spain, October 22–26, 2006.

24. J. M. Alonso, J. M. Conde, J. A. Gago, P. González, M. Novo, and L. E. Herranz, "Spanish R&D Program on Spent Fuel Dry Storage," *Proceedings of the Top Fuel 2006 International Meeting on LWR Fuel Performance,* Salamanca, Spain, October 22–26, 2006.

25. J. C. Tait, I. Gauld, and A. H. Kerr, "Validation of the ORIGEN-S Code for Predicting Radionuclide Inventories in Used CANDU Fuel," *J. Nucl. Mater.* 223, 109–121 (1995).

26. R. J. Guenther, D. E. Blahnik, T. K. Campbell, U. P. Jenquin, J. E. Mendel, L. E. Thomas, and C. K. Thornhill, *Characterization of Spent Fuel Approved Testing Material ATM-103,* PNL-5109-103 (UC-70), Pacific Northwest Laboratory, Richland, WA (1988).

27. M. C. Brady-Raap and R. J. Talbert, *Compilation of Radiochemical Analyses of Spent Nuclear Fuel Samples,* PNNL-13677, Pacific Northwest National Laboratory, Richland, WA, September 2001.

28. H. U. Zwicky and J. Low, *Fuel Pellet Isotopic Analyses of Vandellós 2 Rods WZtR165 and WZR0058,* Final Report, STUDSVIK/N(H)-03/069, Rev. 1 (2008).

29. H. U. Zwicky and J. Low, *Fuel Pellet Isotopic Analyses of Vandellós 2 Rods WZtR165 and WZR0058: Qualification of Method,* STUDSVIK/N(H)-04/002, Rev. 2 (2008).

30. H. U. Zwicky and J. Low, *Fuel Pellet Isotopic Analyses of Vandellós 2 Rods WZtR165 and WZR0058: Complementary Report,* STUDSVIK/N(H)-04/135, Rev. 1 (2008).

31. H. U. Zwicky, J. Low, and M. Granfors, *Additional Fuel Pellet Isotopic Analyses of Vandellós 2 Rods WZtR160 and WZR0058,* Final Report, STUDSVIK/N-07/140 (2008).

32. M. D. DeHart, I. C. Gauld, and M. L. Williams, "High-Fidelity Lattice Physics Capabilities of the SCALE Code System Using TRITON," *Proceedings of the Joint International Topical Meeting on Mathematics & Computation and Supercomputing in Nuclear Applications,* American Nuclear Society, Monterey, CA, April 15–19, 2007.

33. B. L. Broadhead, M. D. DeHart, J. C. Ryman, J. S. Tang, and C. V. Parks, *Investigation of Nuclide Importance to Functional Requirements Related to Transport and Long-Term Storage of LWR Spent Fuel,* ORNL/TM-12742, Oak Ridge National Laboratory, Oak Ridge, TN (1995).

34. I. C. Gauld and J. C. Ryman, *Nuclide Importance to Criticality Safety, Decay Heating, and Source Terms Related to Transport and Interim Storage of High Burnup LWR Fuel,* NUREG/CR-6700 (ORNL/TM-2000/284), prepared for the Nuclear Regulatory Commission by Oak Ridge National Laboratory, Oak Ridge, TN (2001).

35. International Atomic Energy Agency, "Implementation of Burnup Credit in Spent Fuel Management Systems," *Proceedings of a Technical Committee Meeting,* Vienna, July 10–14, 2000, IAEA-TECDOC-1241 (2001).

36. I. C. Gauld, "Spent Fuel Isotopic Validation Activities in the United States and Lessons Learned," in *Workshop Proceedings on the Need for Post Irradiation Experiments to Validate Fuel Depletion Calculation Methodologies*, OECD Nuclear Energy Agency, Prague, Czech Republic, May 11–12 2006, Nuclear Science WPNCS (December 2006).

37. I. C. Gauld, G. Ilas, B. D. Murphy, and C. F. Weber, *Validation of SCALE 5 Decay Heat Predictions for LWR Spent Nuclear Fuel*, NUREG/CR-6972 (ORNL/TM-2008/015), prepared for the U.S. Nuclear Regulatory Commission by Oak Ridge National Laboratory, Oak Ridge, TN (2008).

38. I. Guttman, S. S. Wilks, and J. S. Hunter, *Introductory Engineering Statistics*, Wiley Series in Probability and Mathematical Statistics–Applied, John Wiley & Sons (1971).

39. I. C. Gauld and D. E. Mueller, *Evaluation of Cross-Section Sensitivities in Computing Burnup Credit Fission Product Concentrations*, ORNL/TM-2005/48, Oak Ridge National Laboratory, Oak Ridge, TN (2005).

40. M. D. DeHart, I. C. Gauld, and K. Suyama, "Issues in Three-Dimensional Depletion Analysis of Measured Data Near the End of a Fuel Rod," 2008 ANS Winter Meeting and Nuclear Technology Expo, November 9–13, 2008, Reno, Nevada. *Trans. Amer. Nucl. Soc.* **99** (2008).

41. I. C. Gauld, *Strategies for Application of Isotopic Uncertainties in Burnup Credit*, NUREG/CR-6811 (ORNL/TM-2001/257), prepared for the U.S. Nuclear Regulatory Commission by Oak Ridge National Laboratory, Oak Ridge, TN (2003).

APPENDIX A

COMPARISON OF ISOTOPIC MEASUREMENTS AND CALCULATIONS FOR ALL DATA SETS
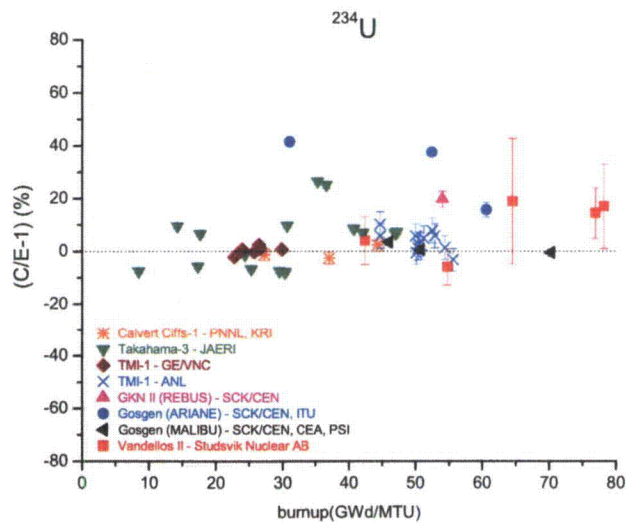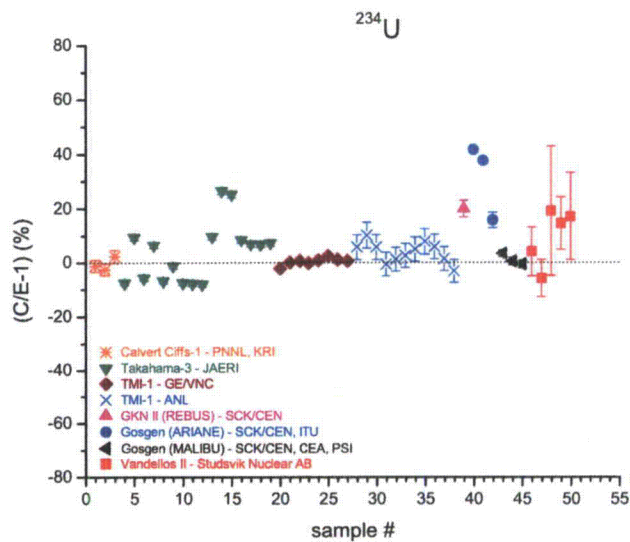
Figure A.1. Comparison of measurements and calculated values for ^{234}**U.**
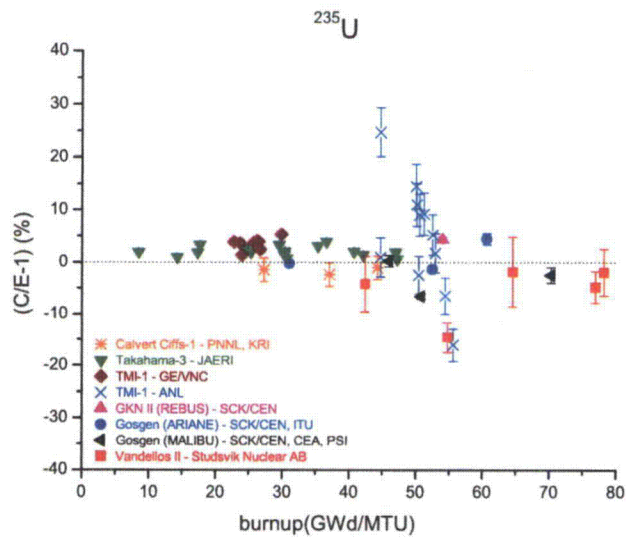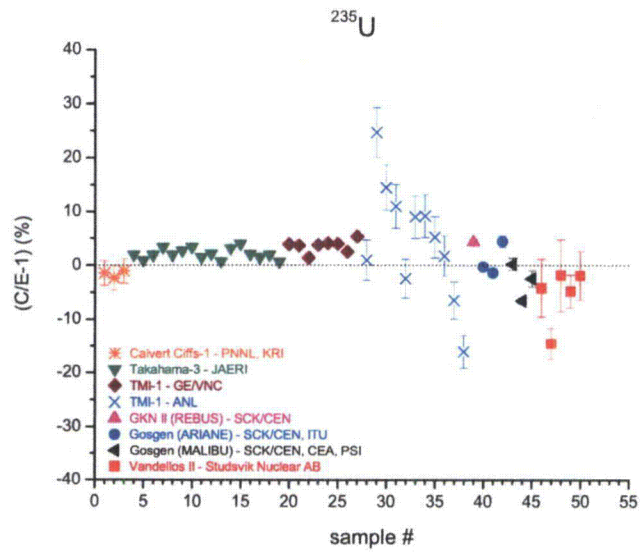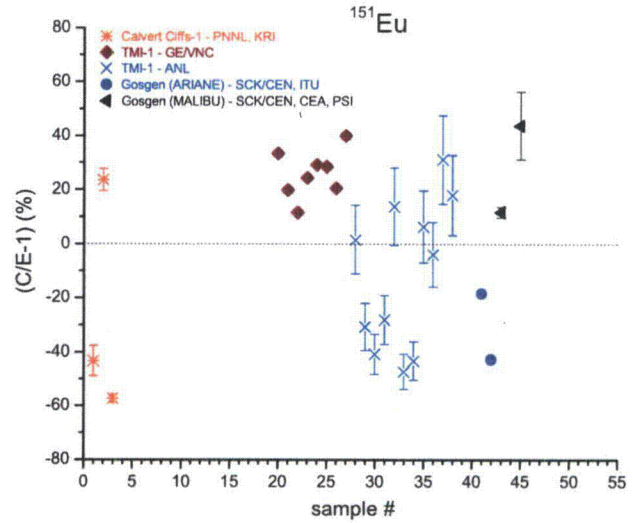
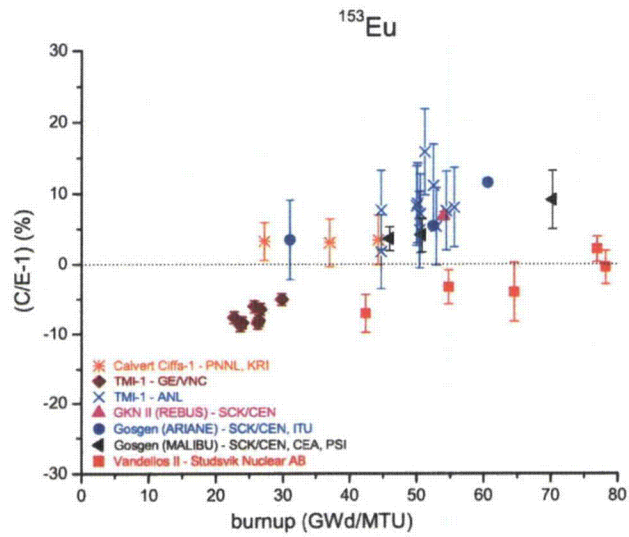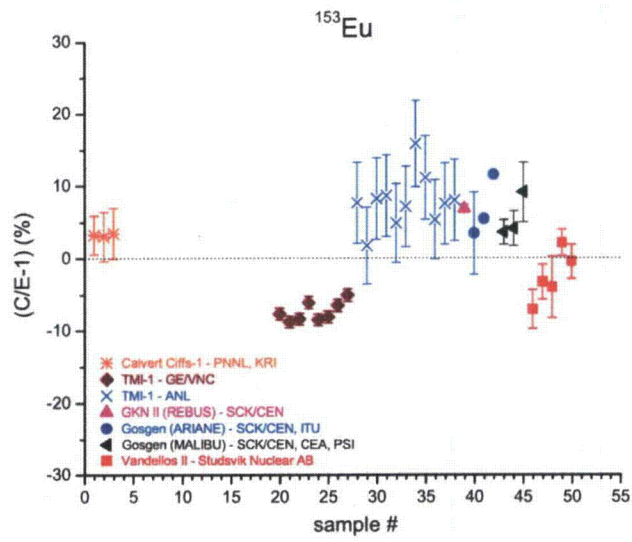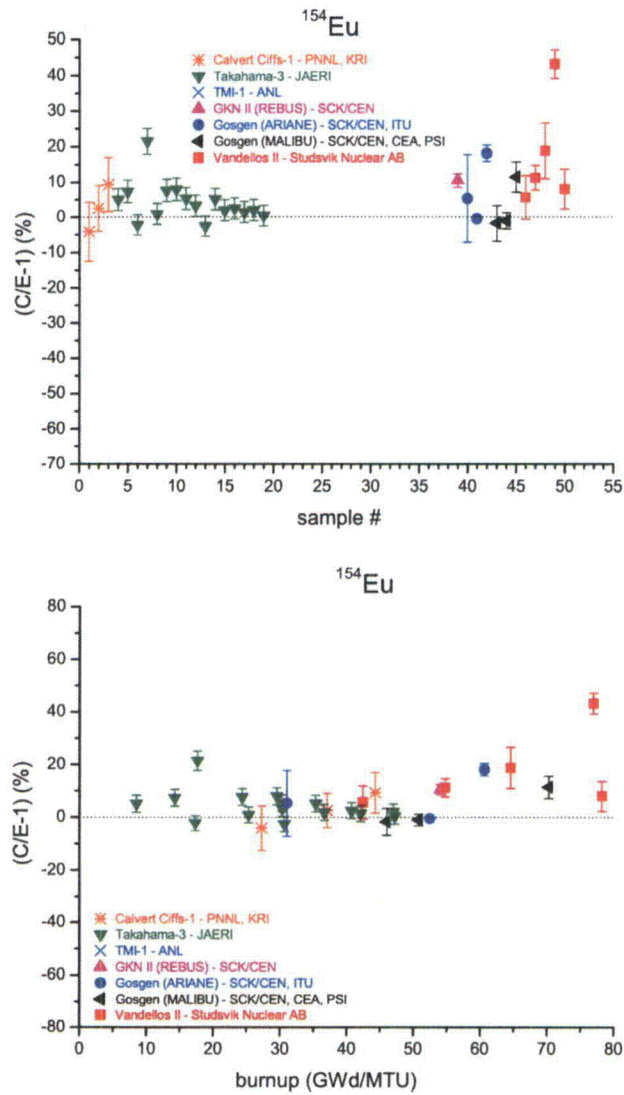**Figure A.2. Comparison of measurements and calculated values for ^{235}U.**
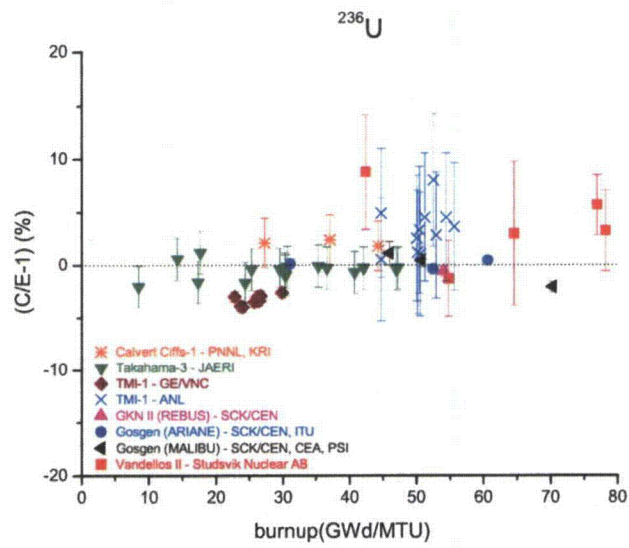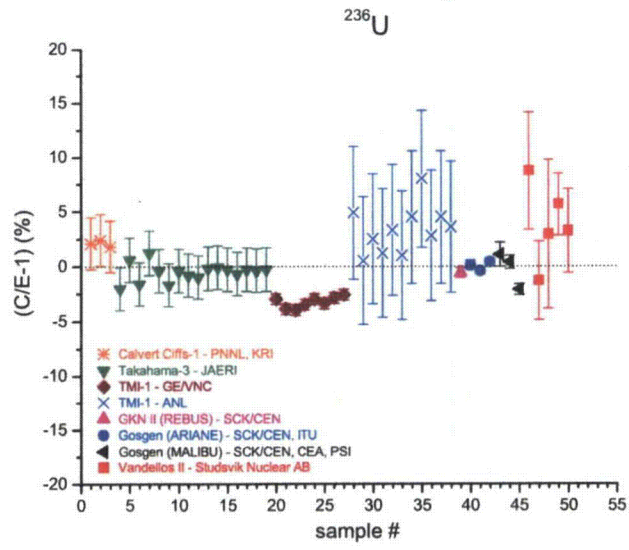
Figure A.3. Comparison of measurements and calculated values for ^{236}U.
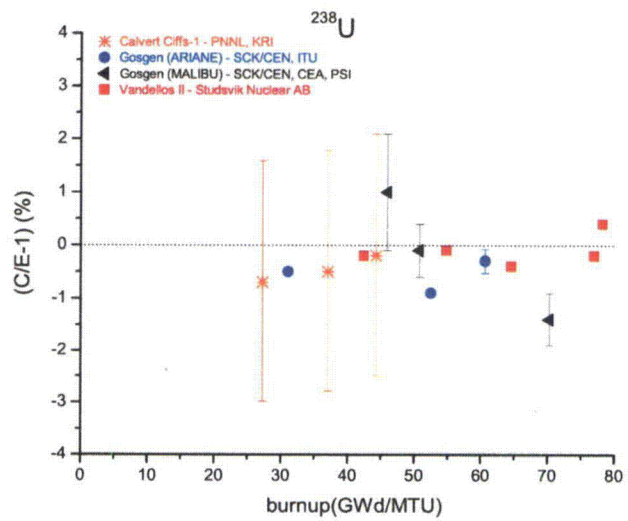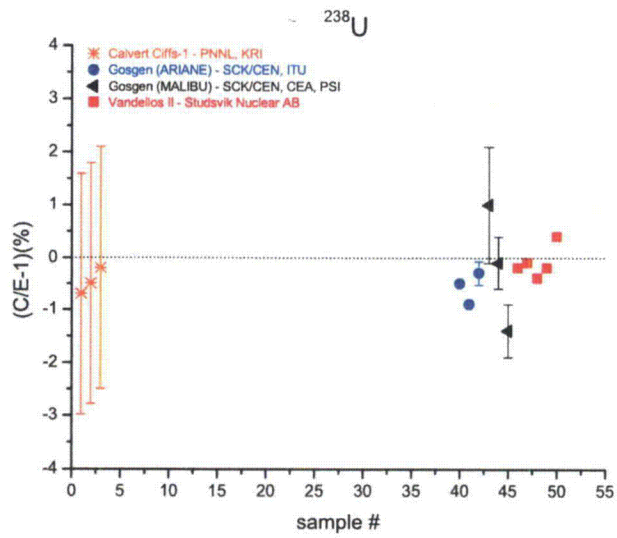
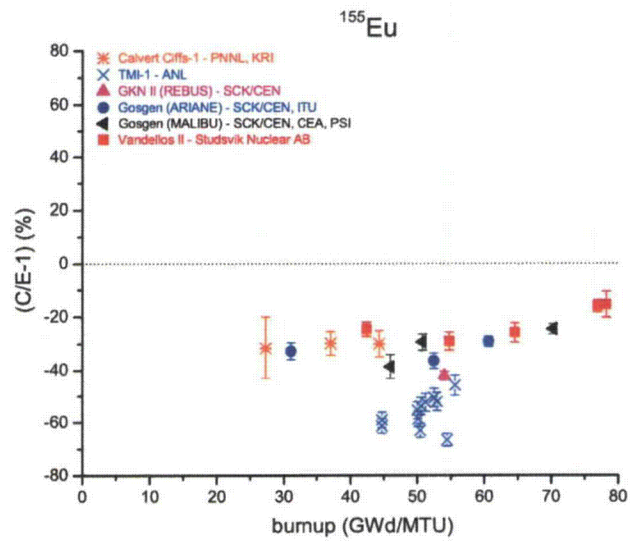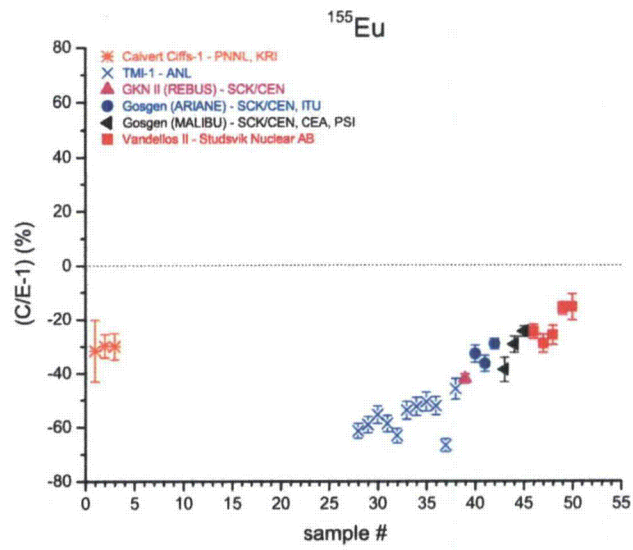Figure A.4. Comparison of measurements and calculated values for ^{238}U.
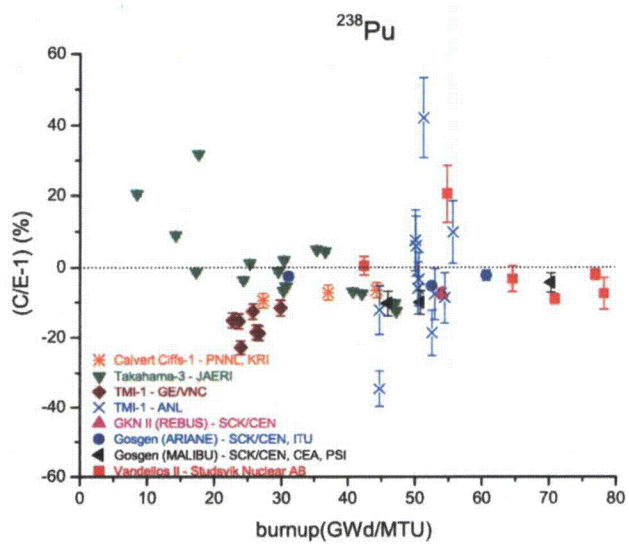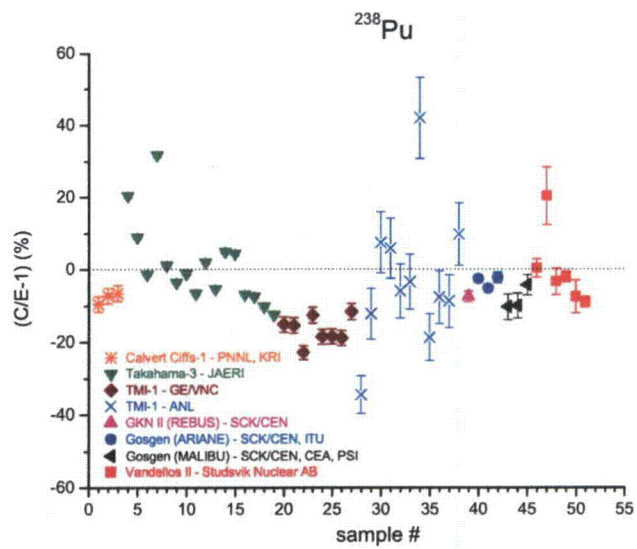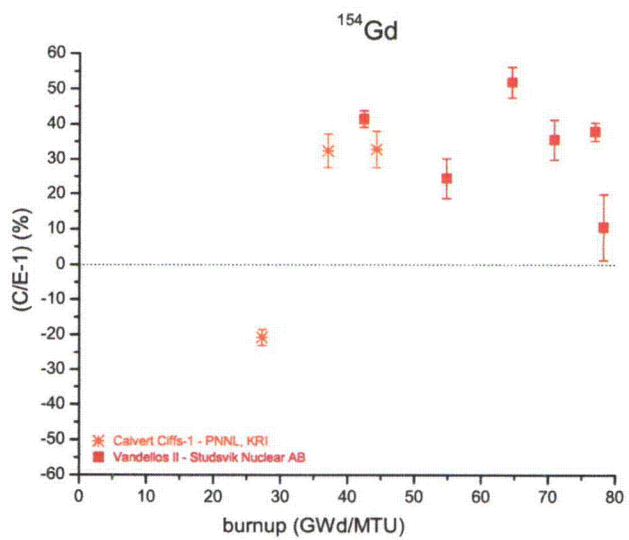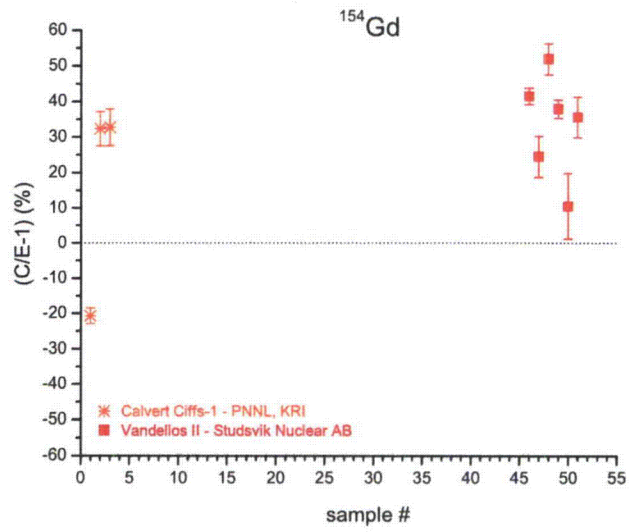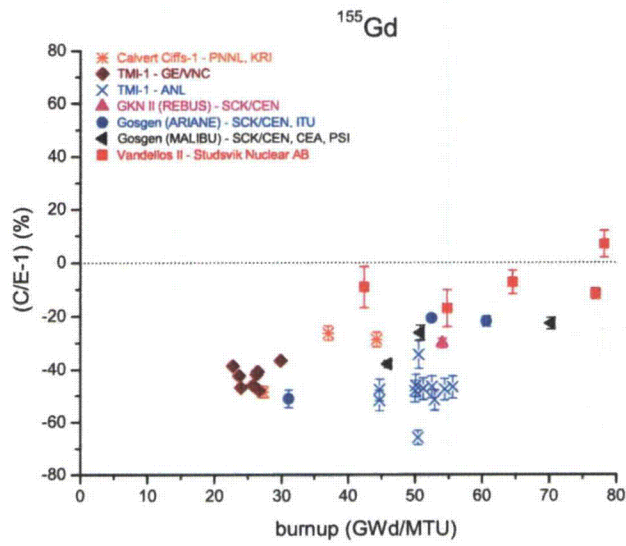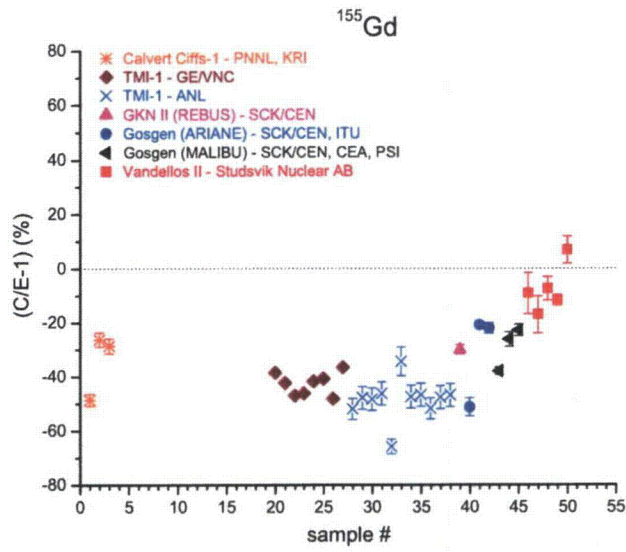
Figure A.5. Comparison of measurements and calculated values for ^{238}Pu.
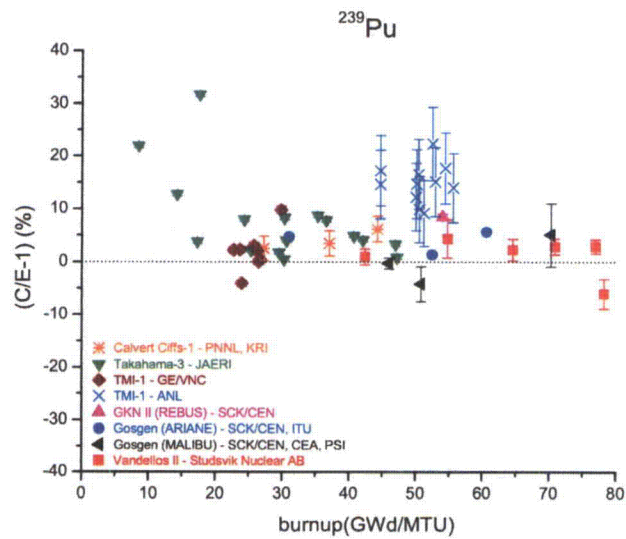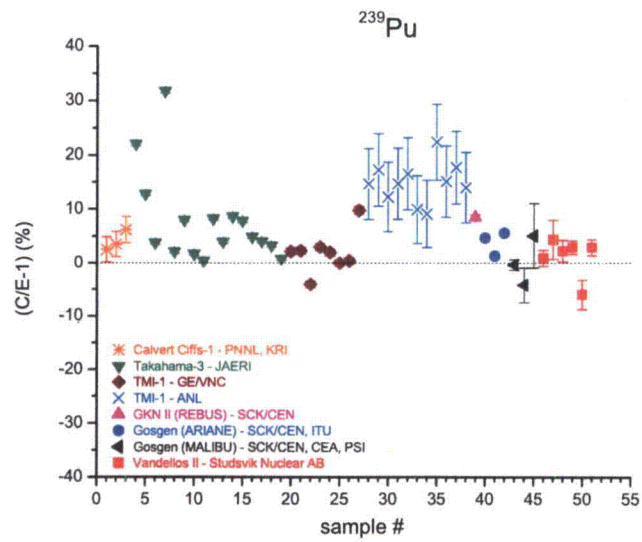
Figure A.6. Comparison of measurements and calculated values for ^{239}Pu.
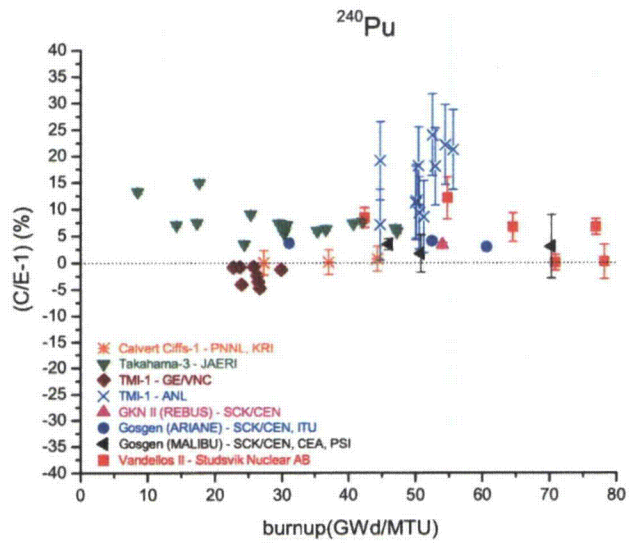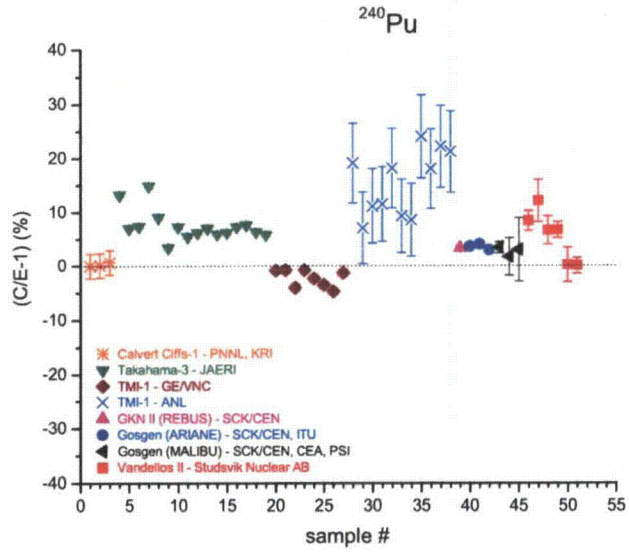
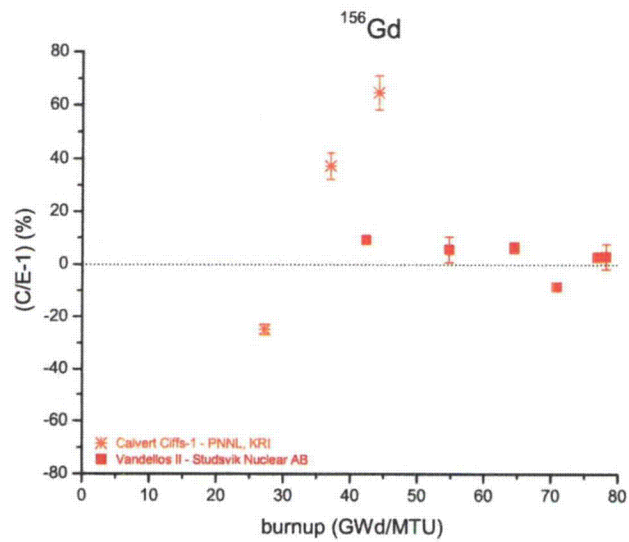Figure A.7. Comparison of measurements and calculated values for ^{240}Pu.
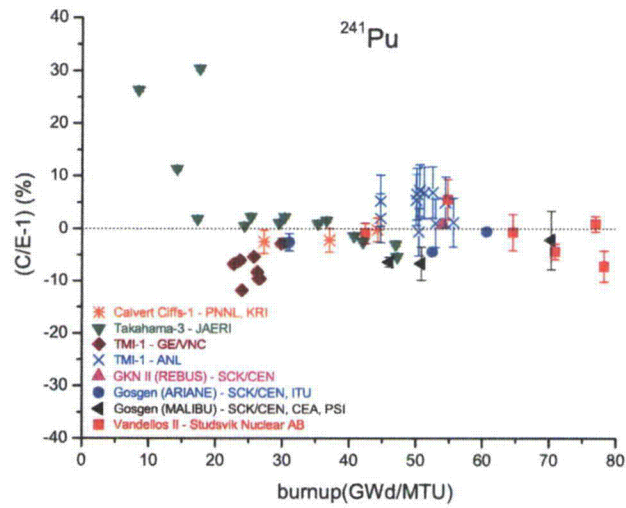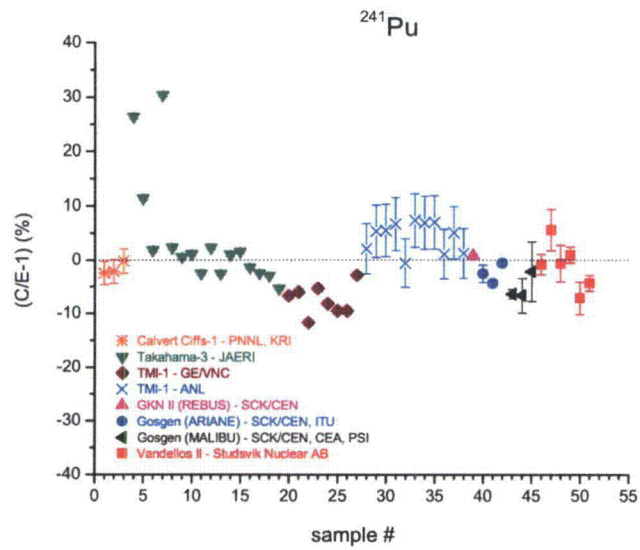
Figure A.8. Comparison of measurements and calculated values for [241]Pu.
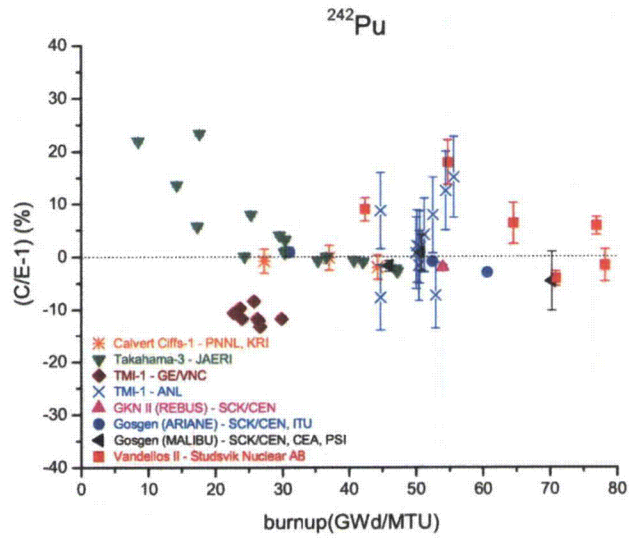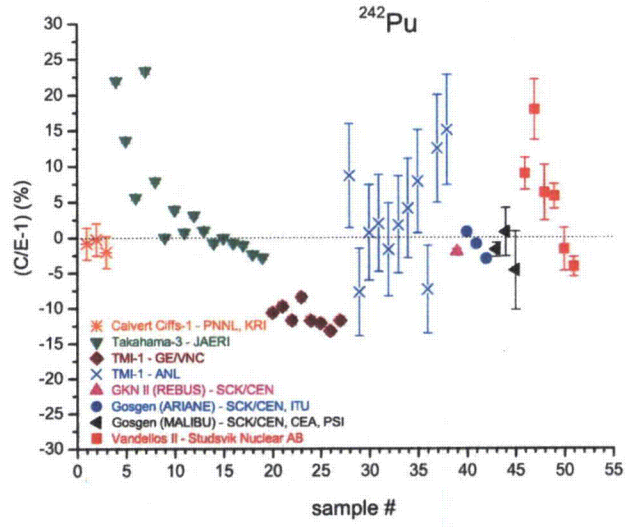
Figure A.9. Comparison of measurements and calculated values for ^{242}Pu.
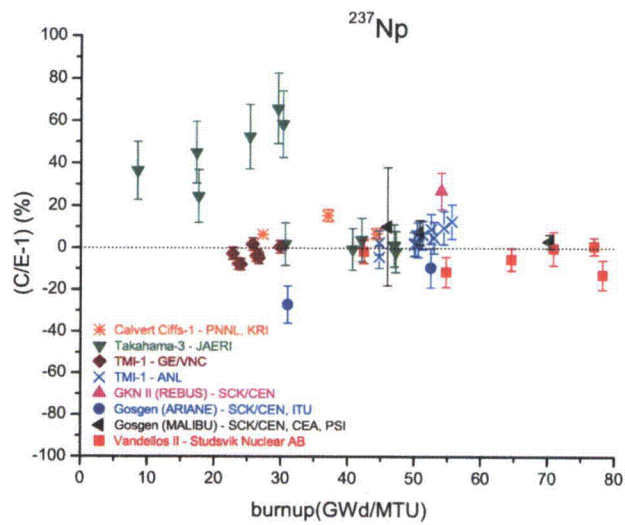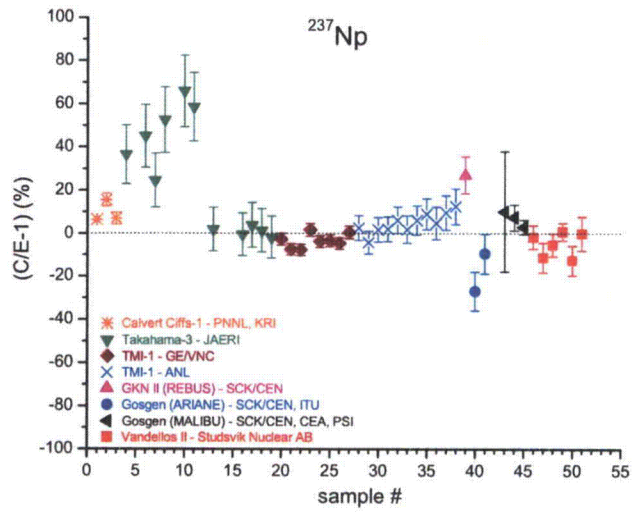
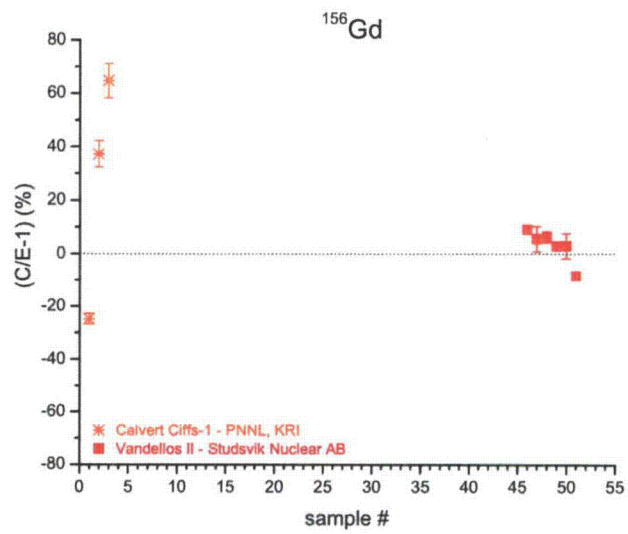**Figure A.10. Comparison of measurements and calculated values for ^{237}Np.**
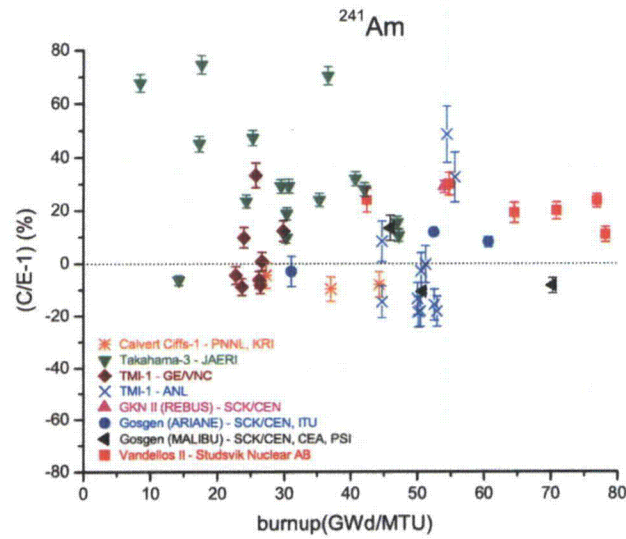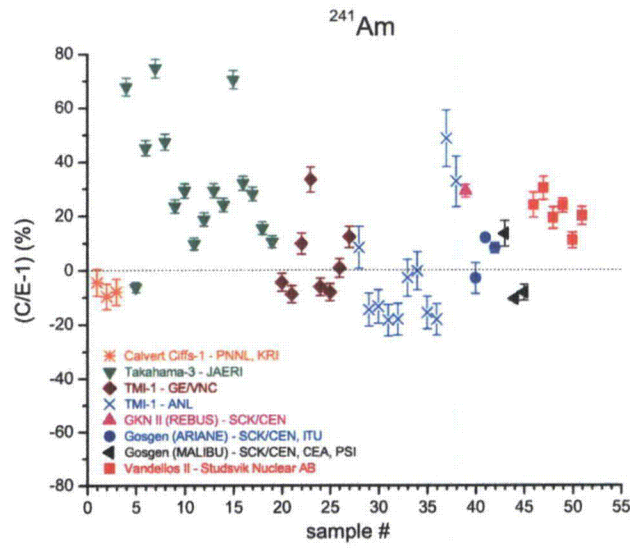
Figure A.11. Comparison of measurements and calculated values for ^{241}Am.
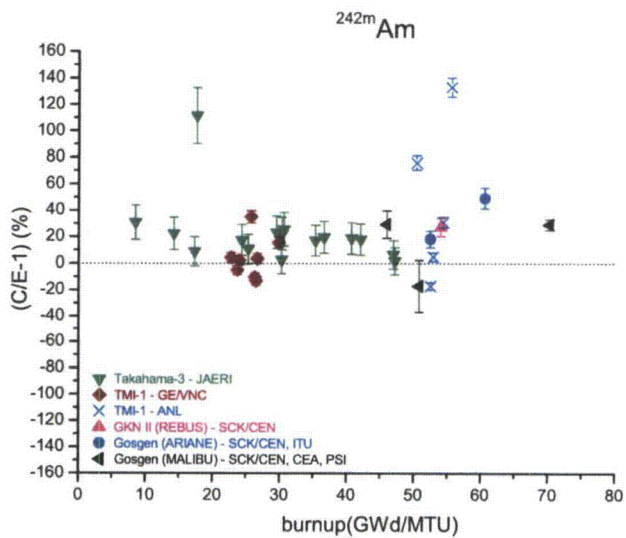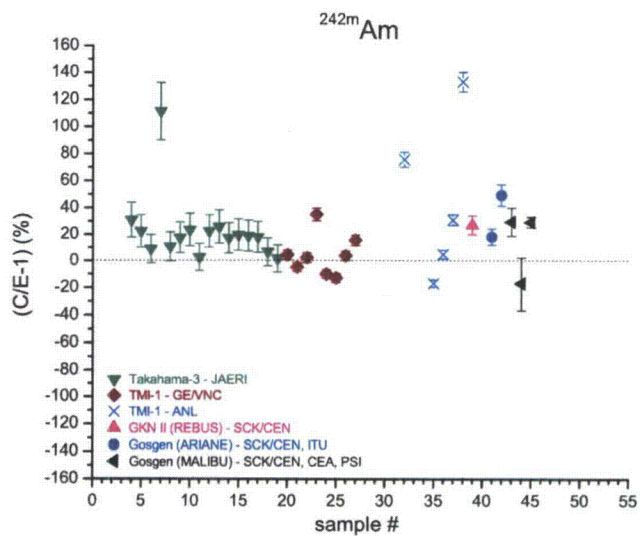
Figure A.12. Comparison of measurements and calculated values for ^{242m}Am.
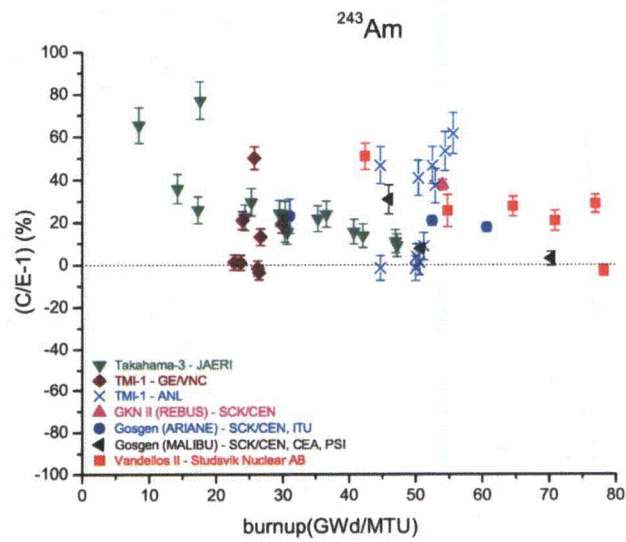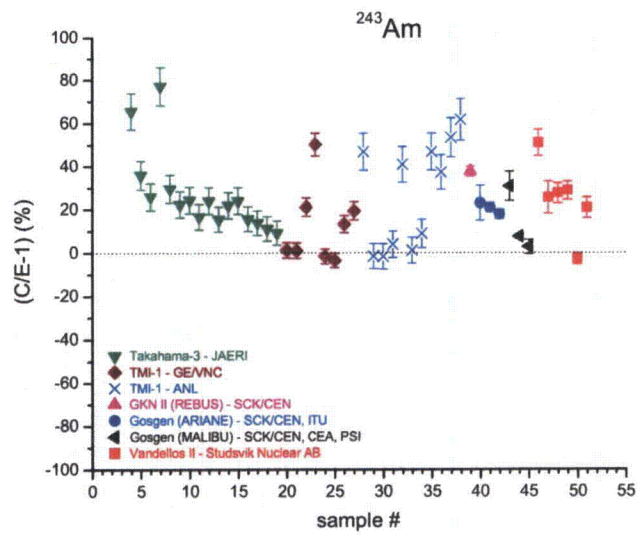
Figure A.13. Comparison of measurements and calculated values for ^{243}Am.
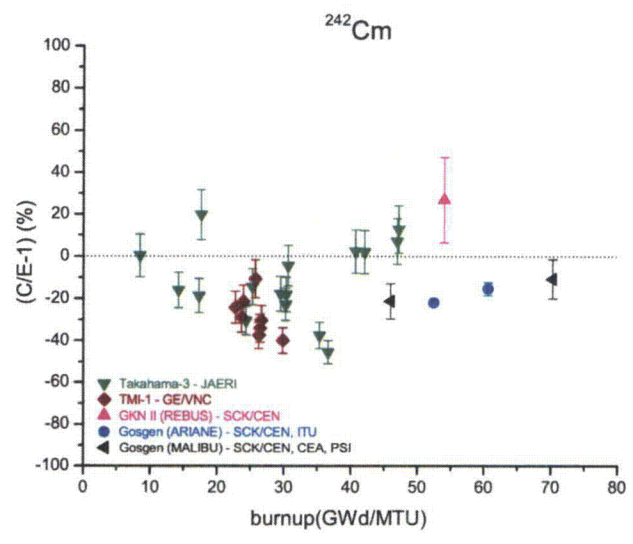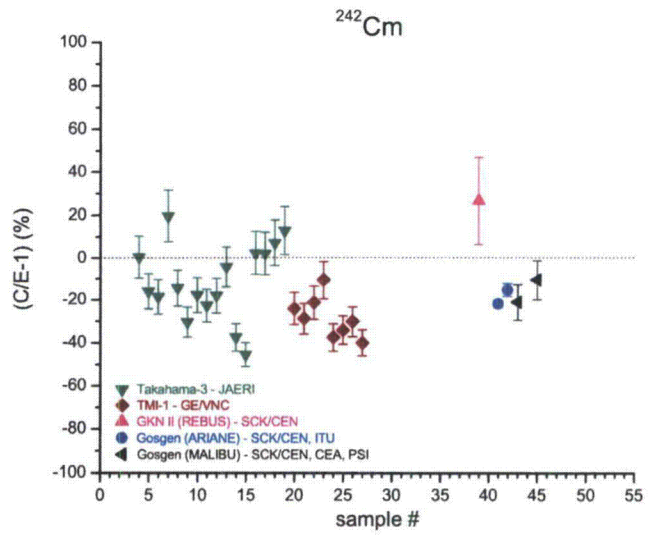
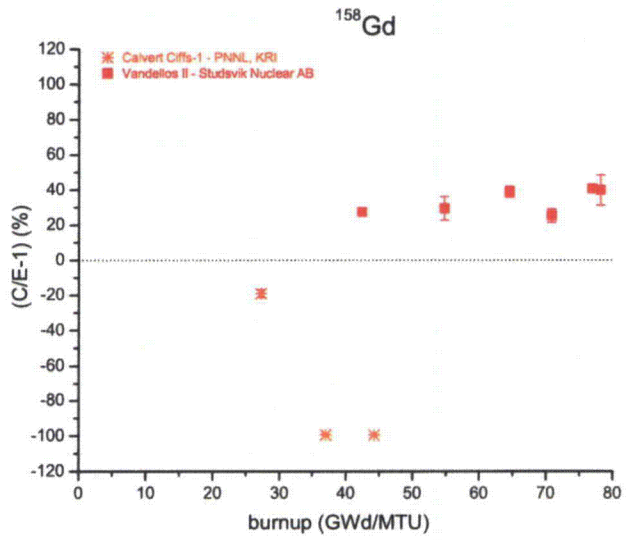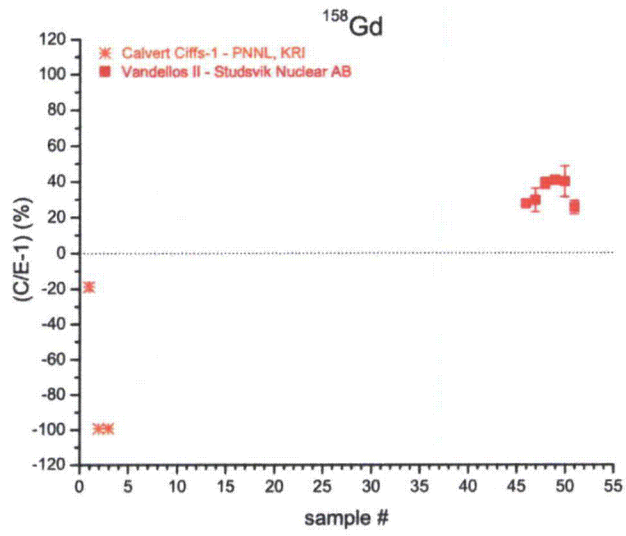**Figure A.14. Comparison of measurements and calculated values for ^{242}Cm.**
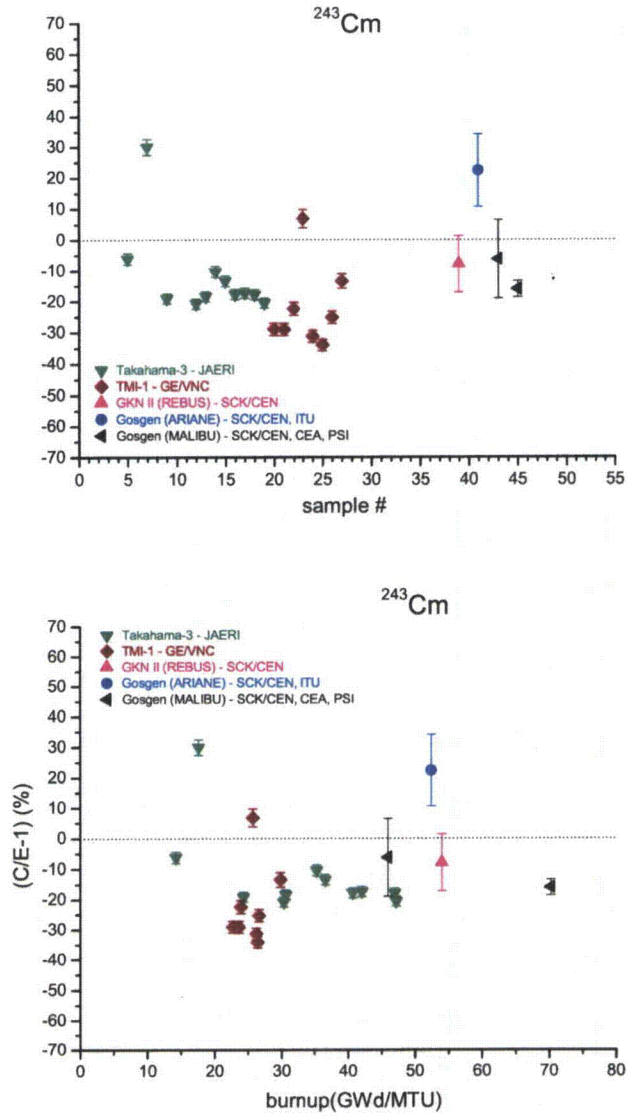
Figure A.15. Comparison of measurements and calculated values for ^{243}Cm.
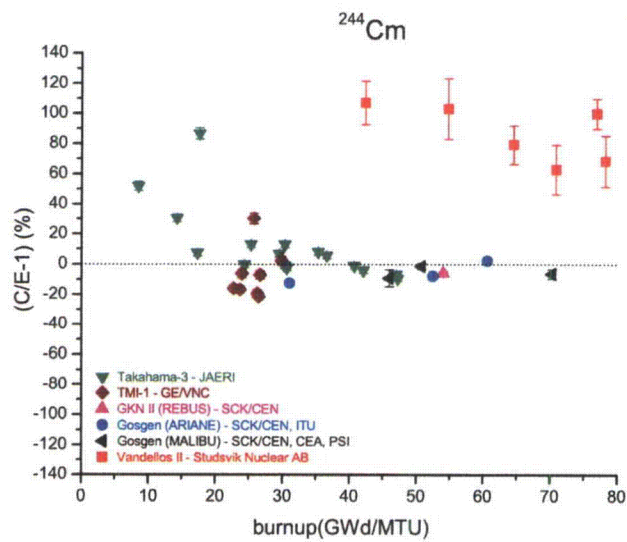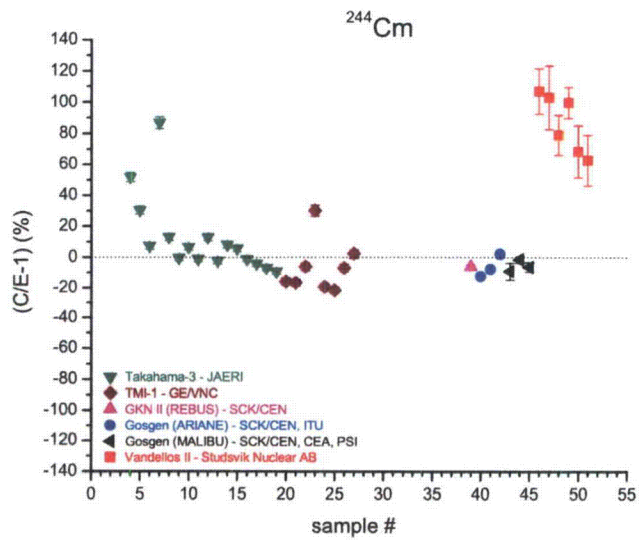
Figure A.16. Comparison of measurements and calculated values for ^{244}Cm.
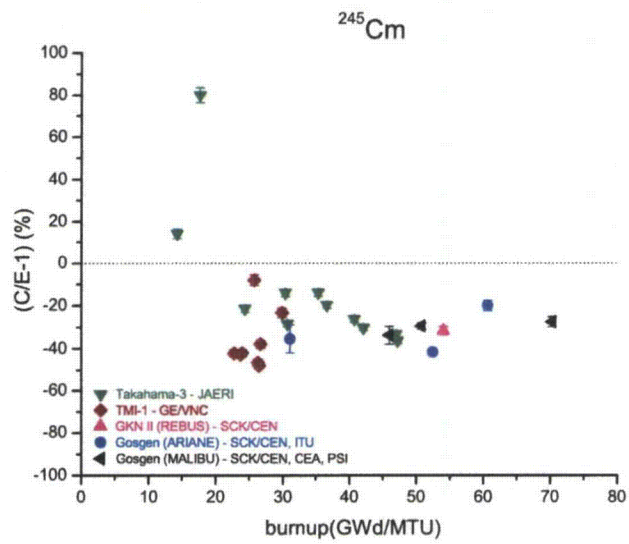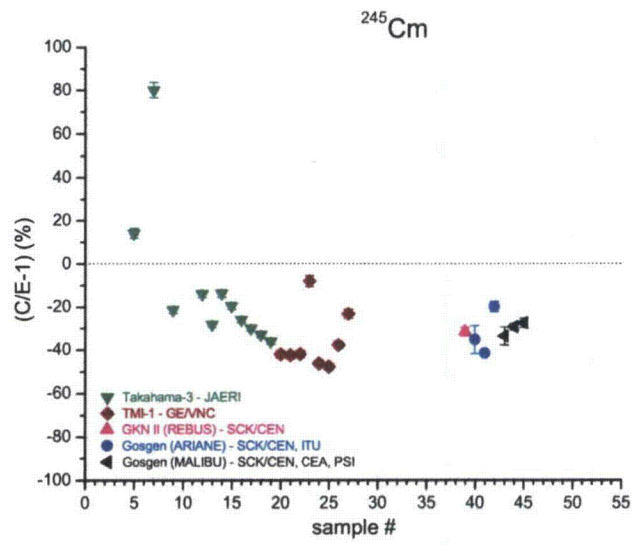
Figure A.17. Comparison of measurements and calculated values for ^{245}Cm.
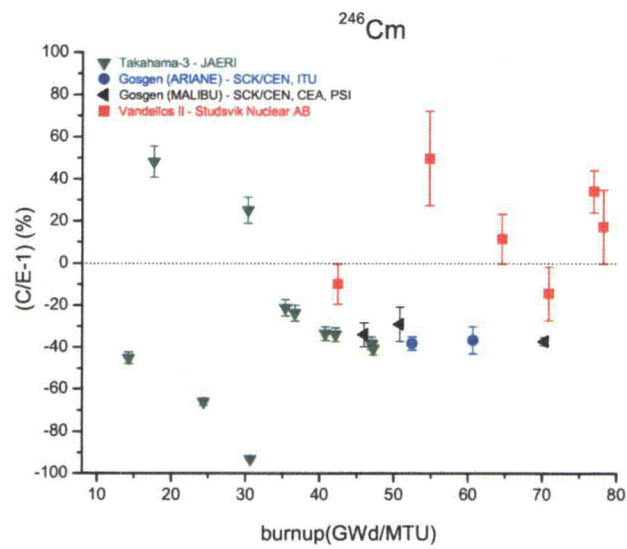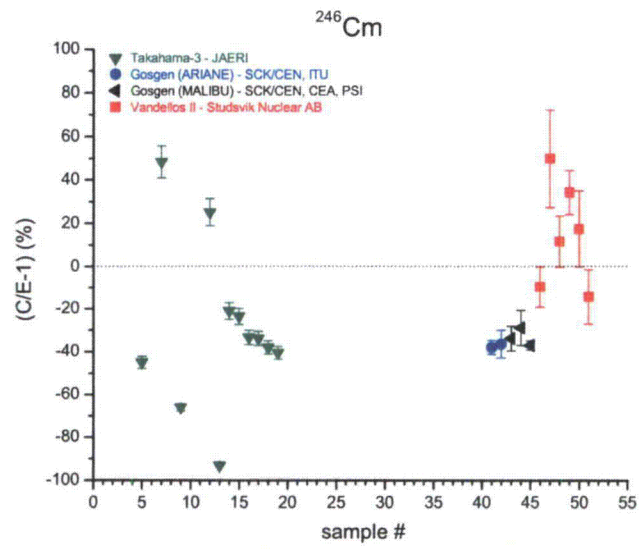
Figure A.18. Comparison of measurements and calculated values for ^{246}Cm.
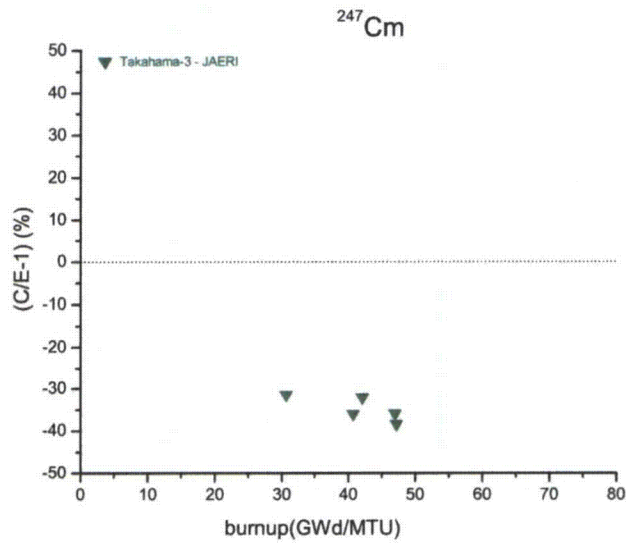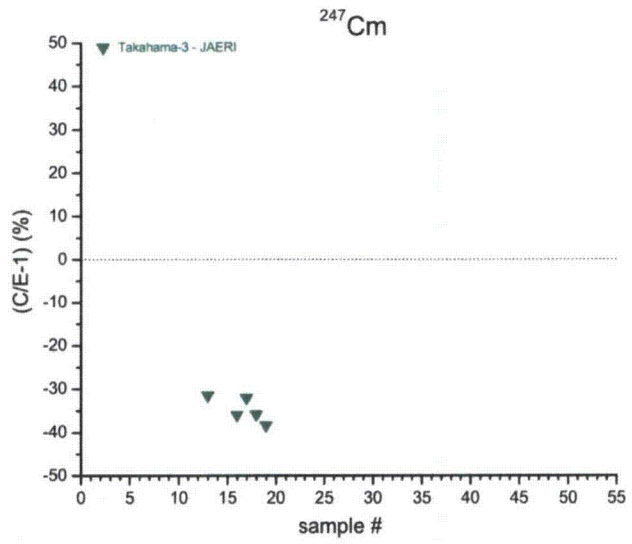
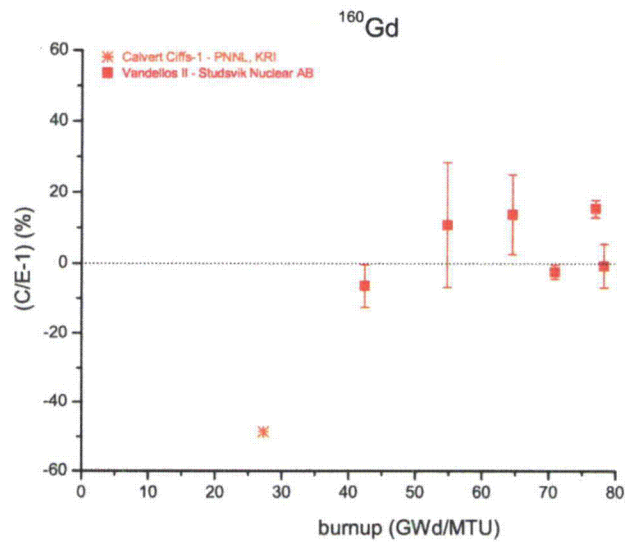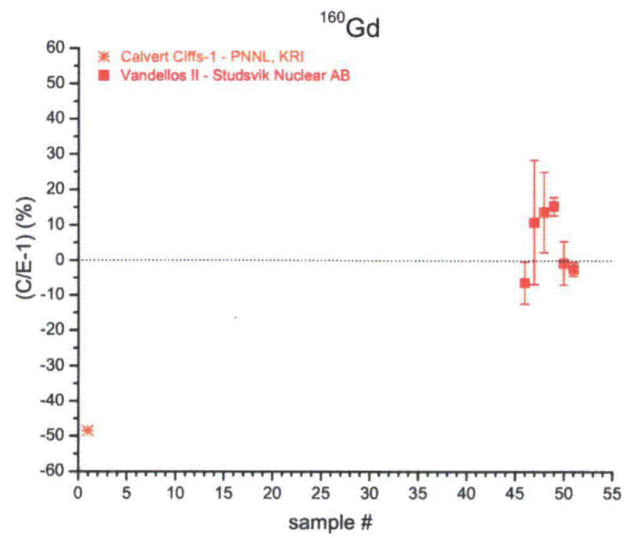Figure A.19. Comparison of measurements and calculated values for ^{247}Cm.
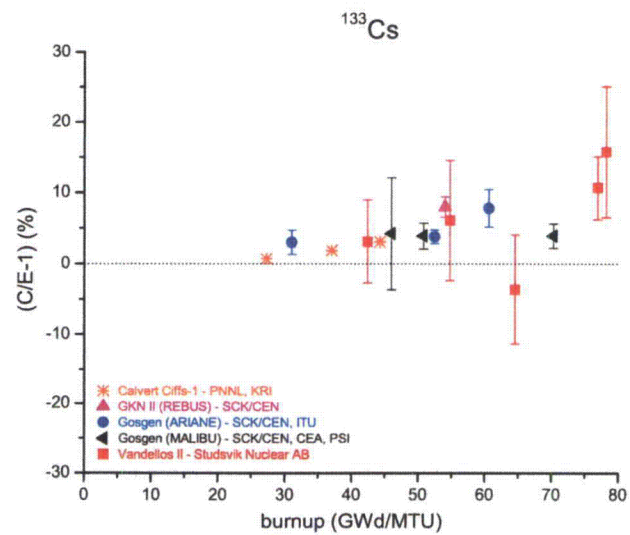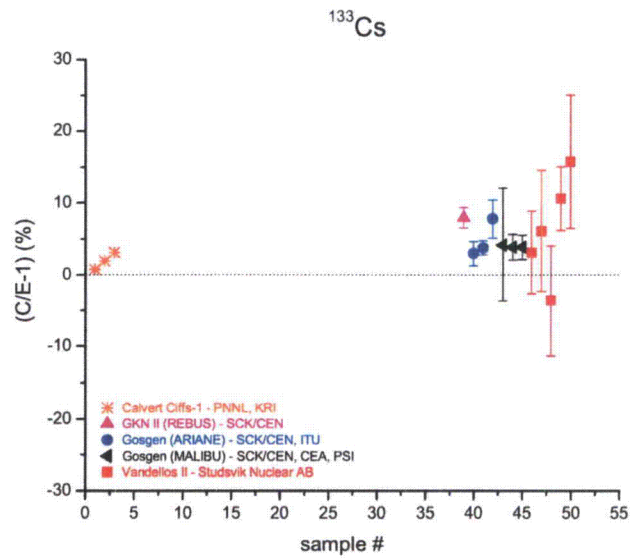
Figure A.20. Comparison of measurements and calculated values for ^{133}Cs.
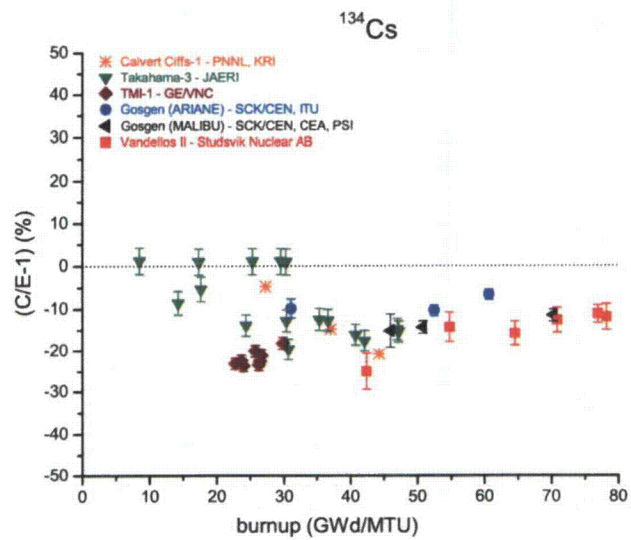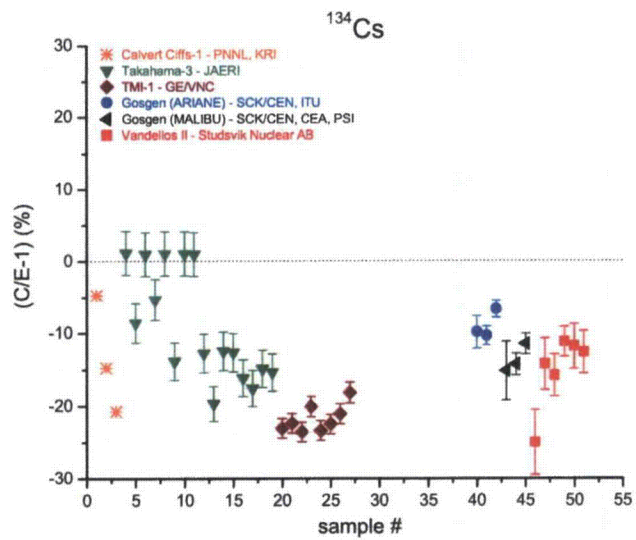
Figure A.21. Comparison of measurements and calculated values for ¹³⁴Cs.
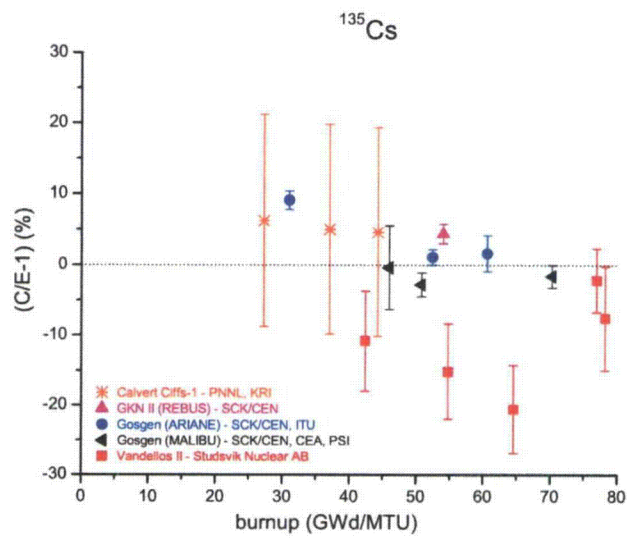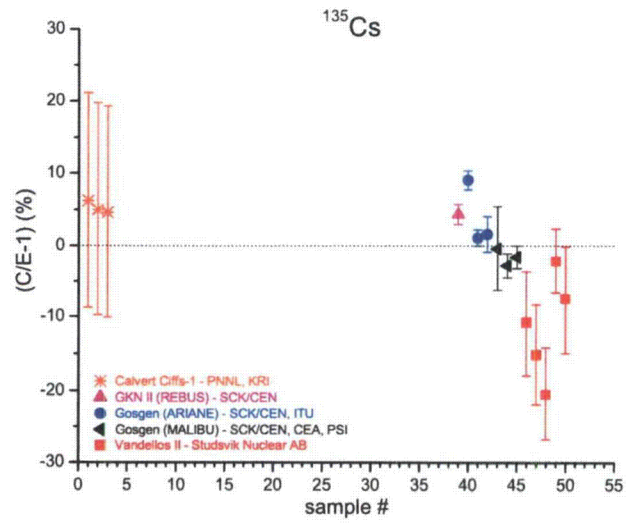
Figure A.22. Comparison of measurements and calculated values for ¹³⁵Cs.
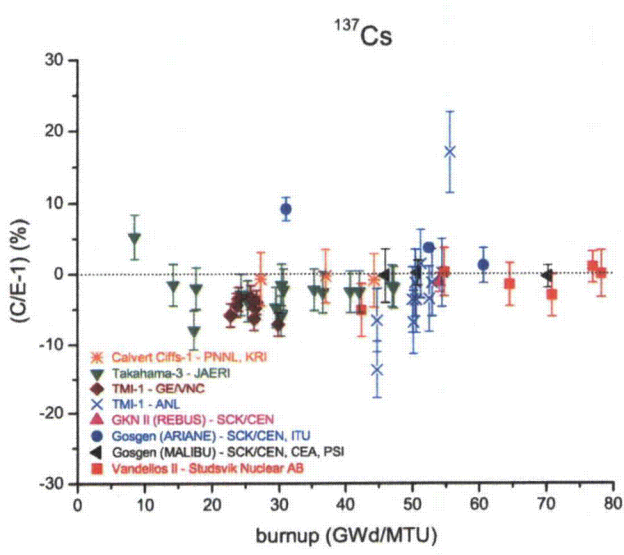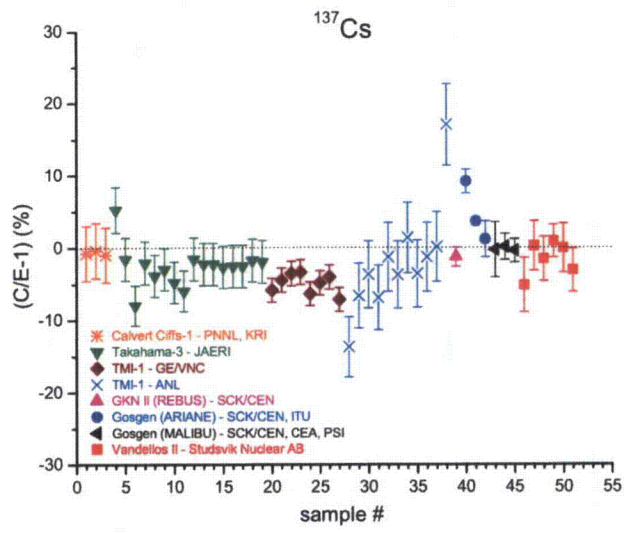
Figure A.23. Comparison of measurements and calculated values for ^{137}Cs.
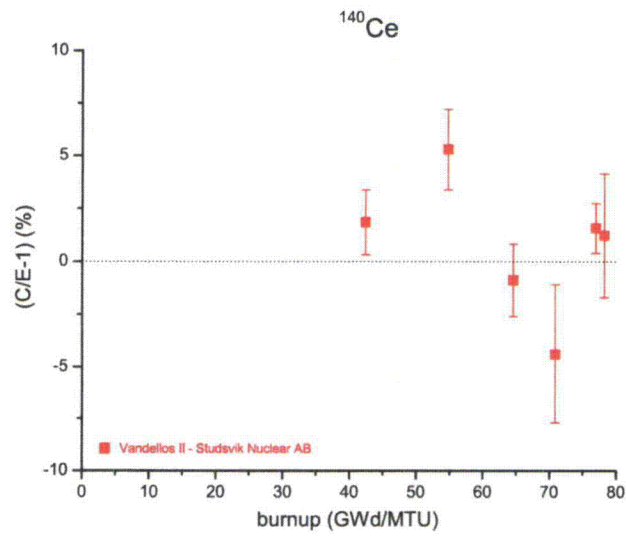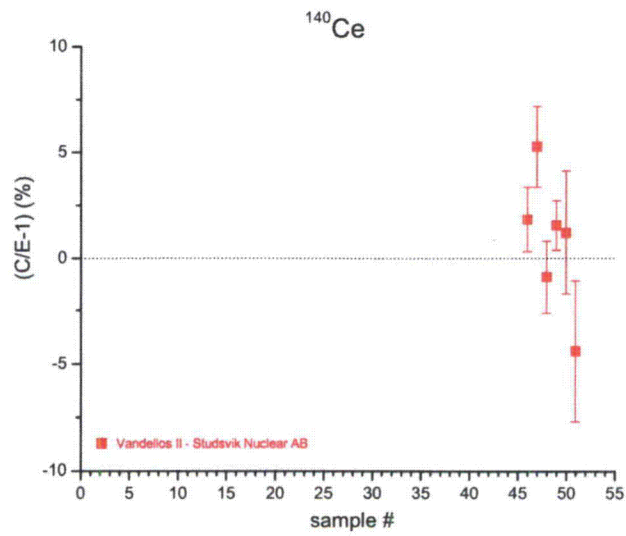
Figure A.24. Comparison of measurements and calculated values for ^{140}Ce.
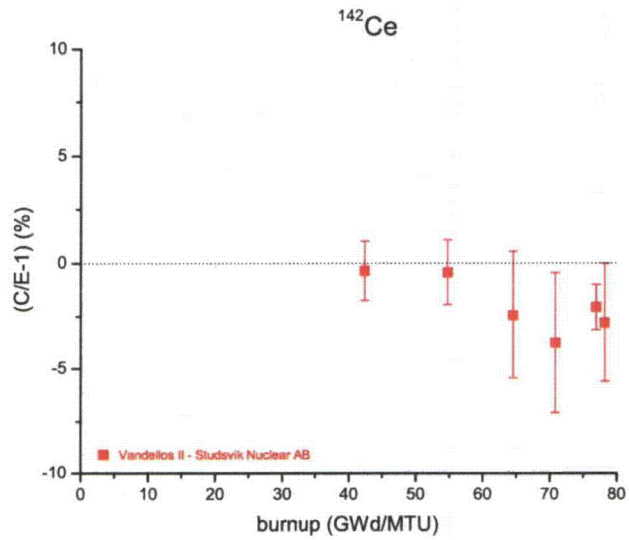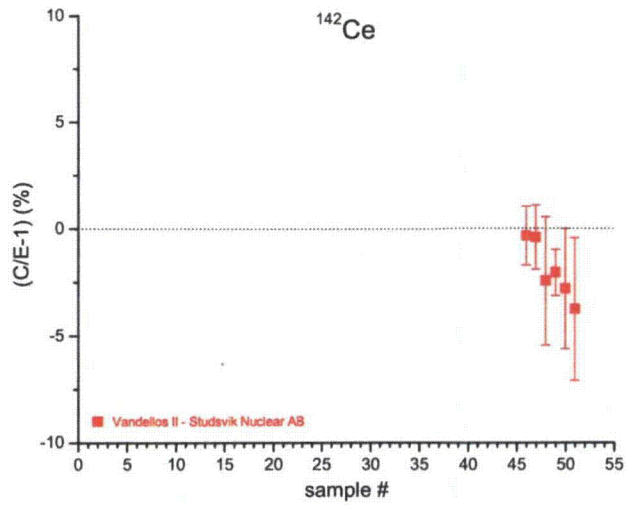
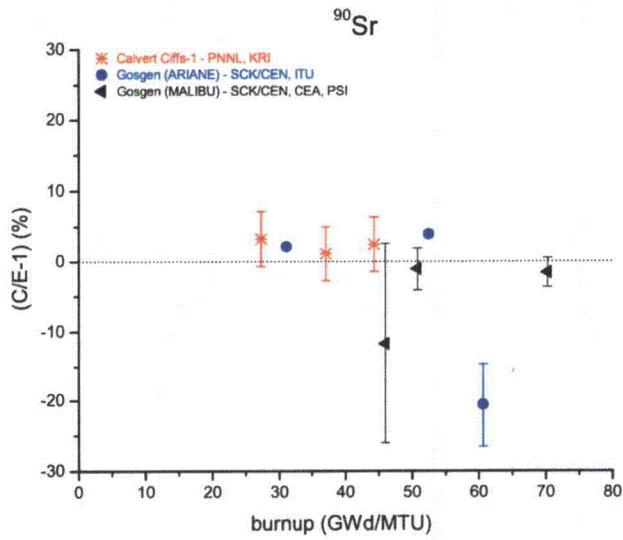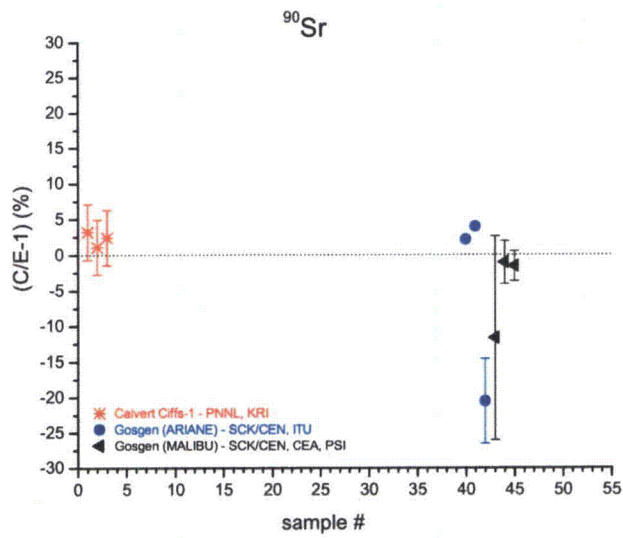**Figure A.25. Comparison of measurements and calculated values for ^{142}Ce.**
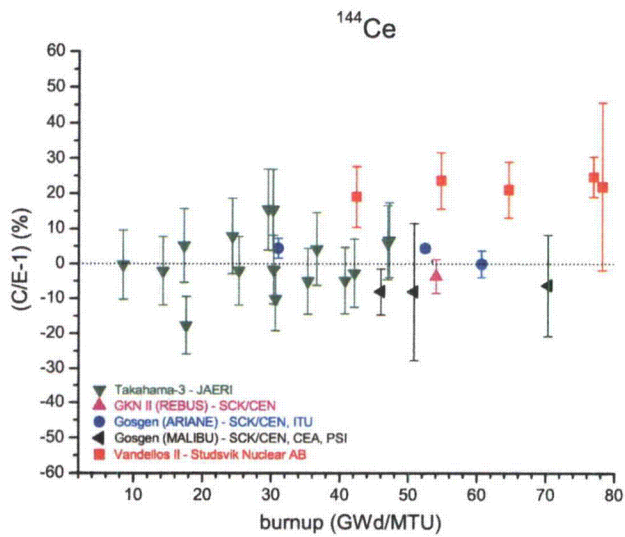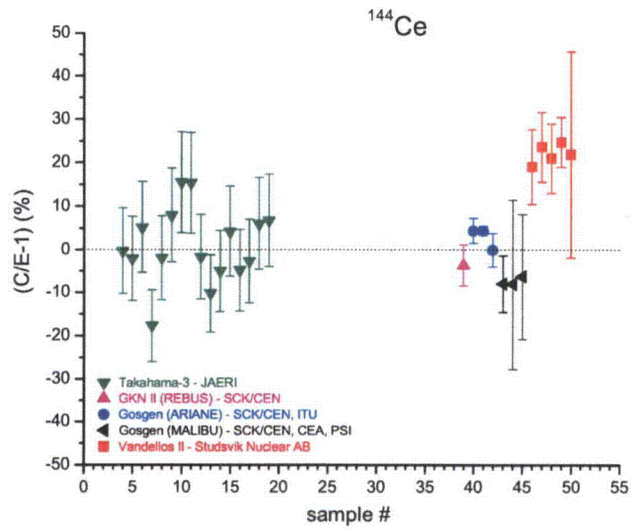
Figure A.26. Comparison of measurements and calculated values for ^{144}Ce.
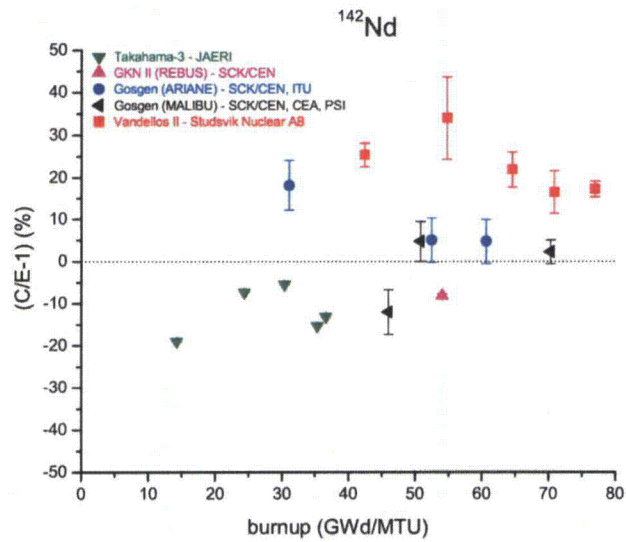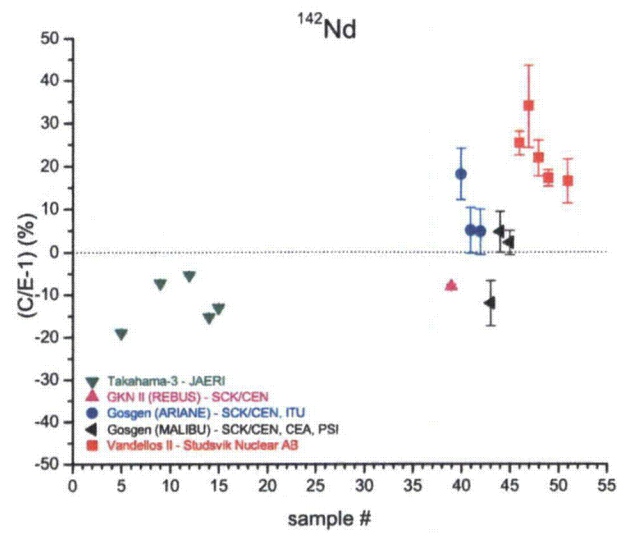
Figure A.27. Comparison of measurements and calculated values for ^{142}Nd.
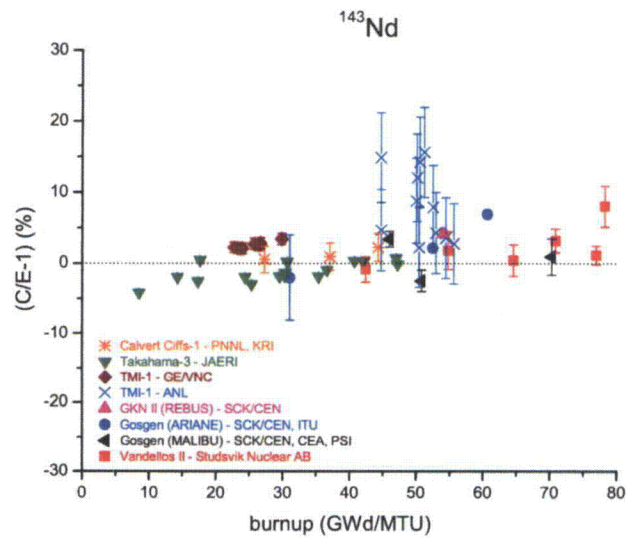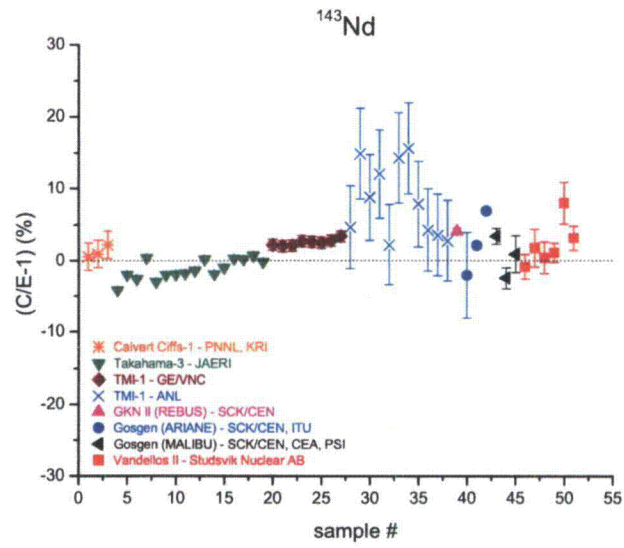
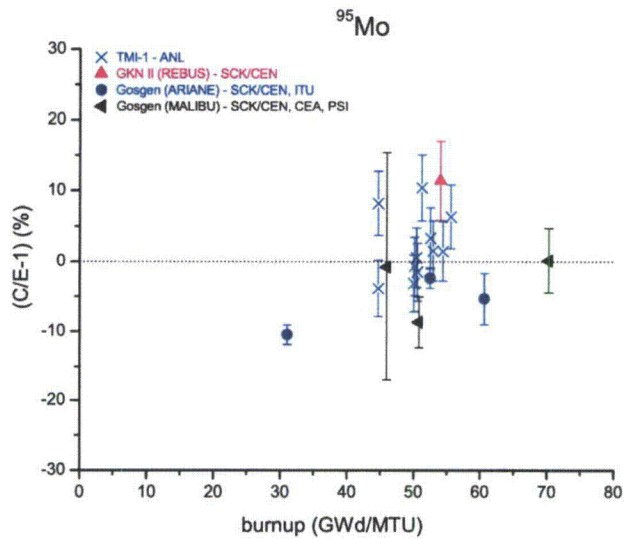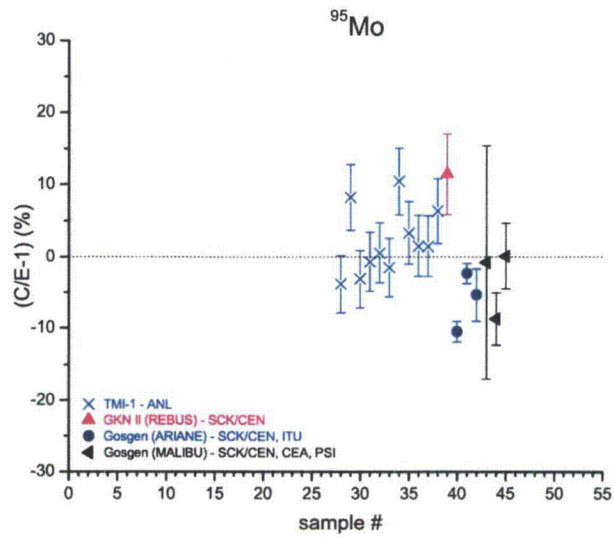**Figure A.28. Comparison of measurements and calculated values for ^{143}Nd.**
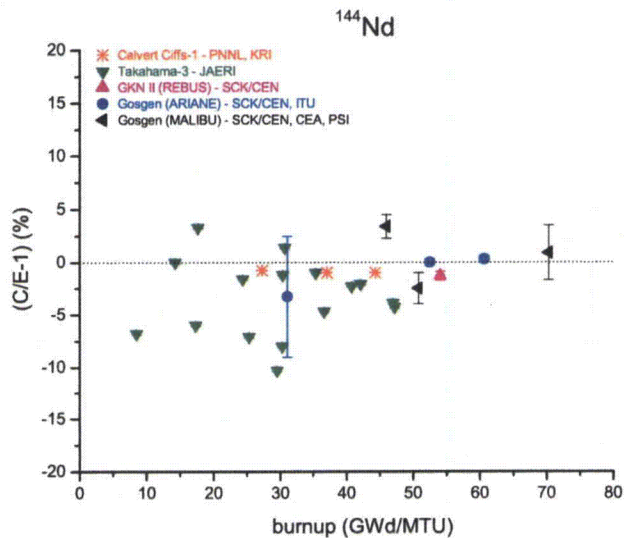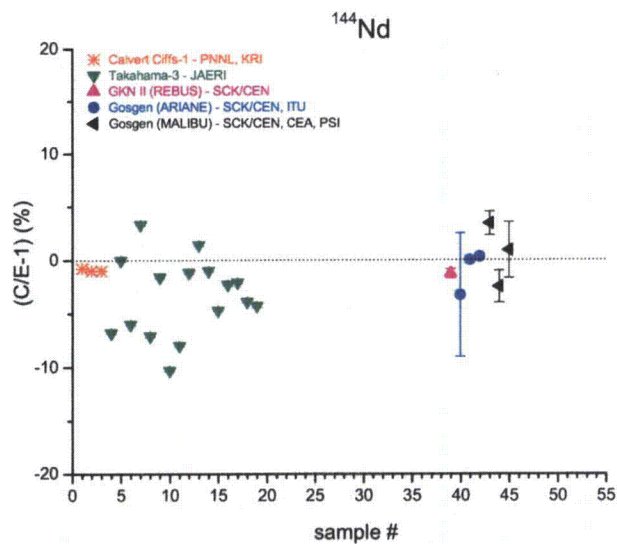
Figure A.29. Comparison of measurements and calculated values for [144]Nd.
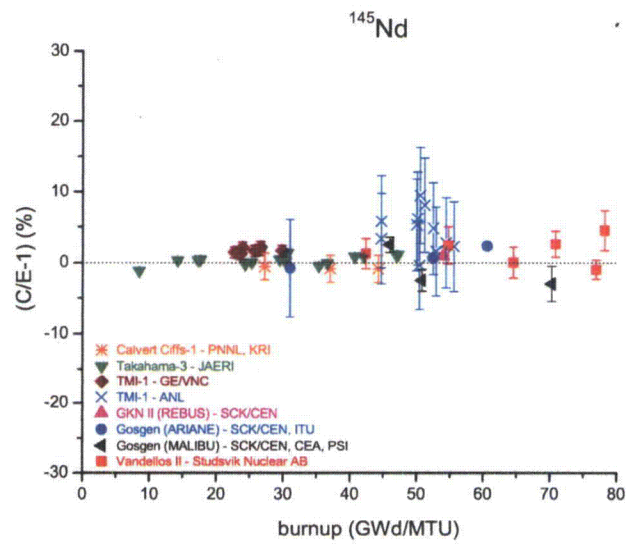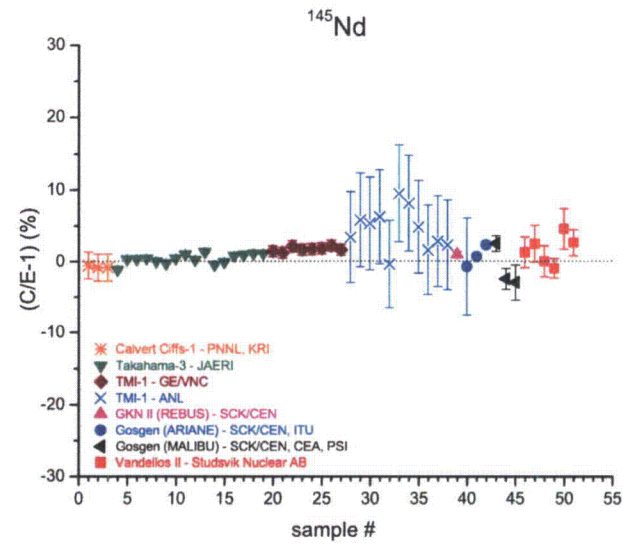
Figure A.30. Comparison of measurements and calculated values for ^{145}Nd.
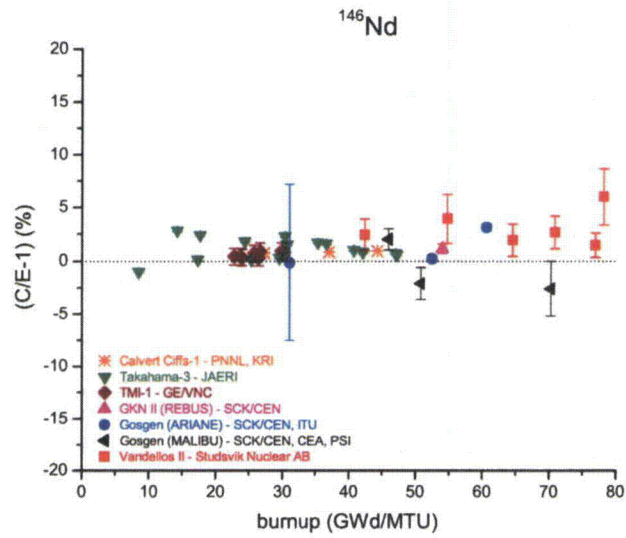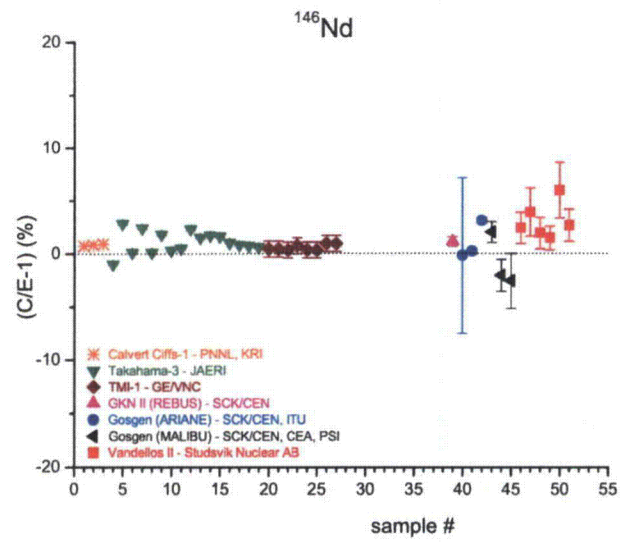
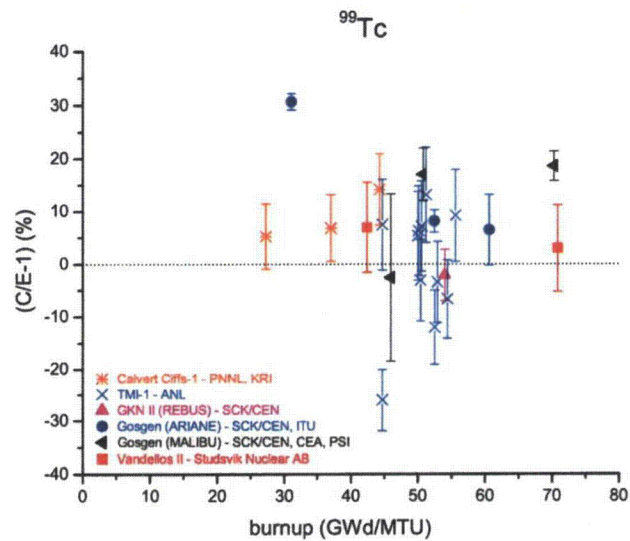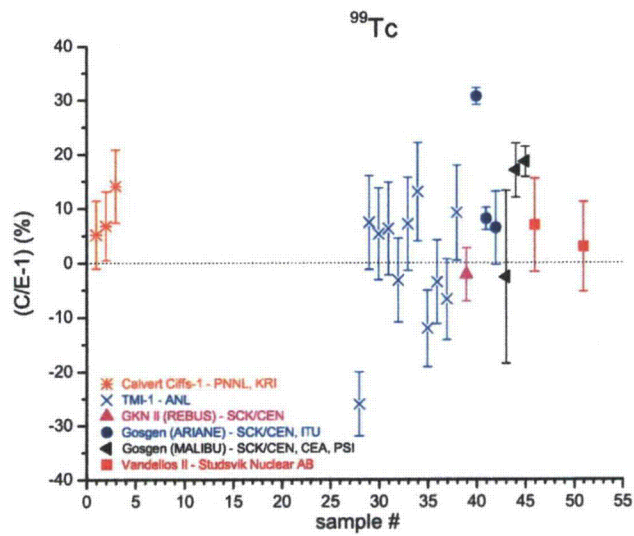**Figure A.31. Comparison of measurements and calculated values for [146]Nd.**
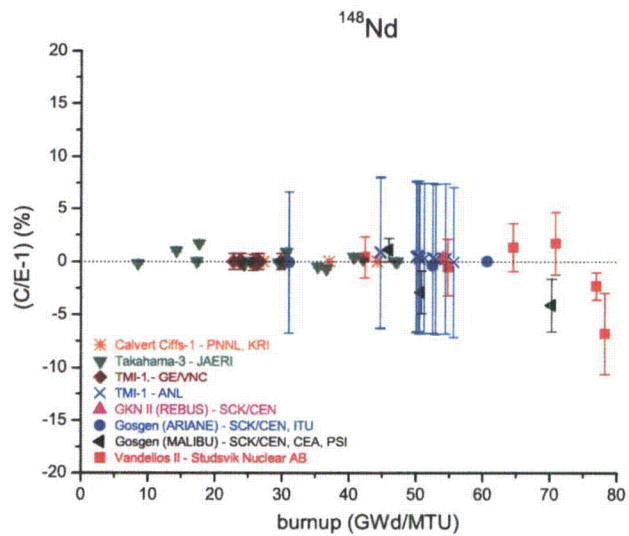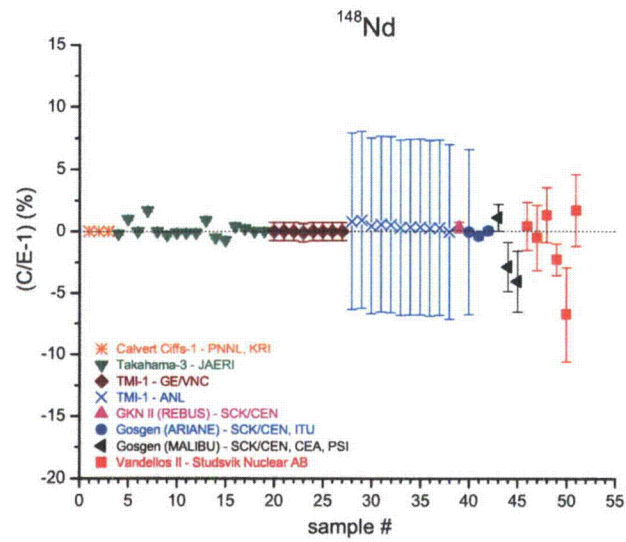
Figure A.32. Comparison of measurements and calculated values for ¹⁴⁸Nd.
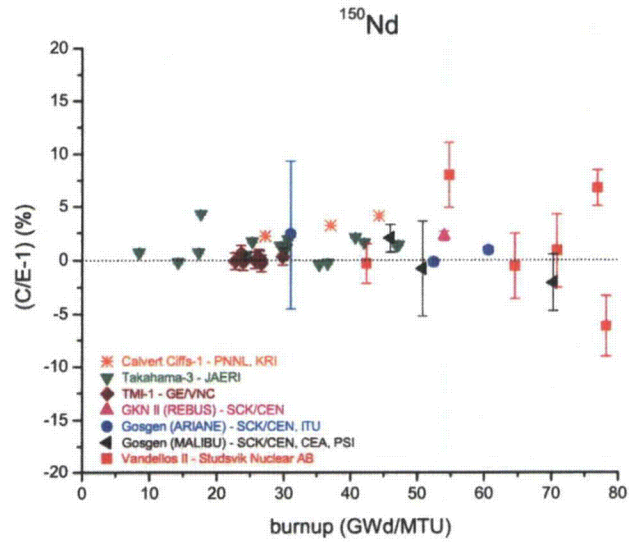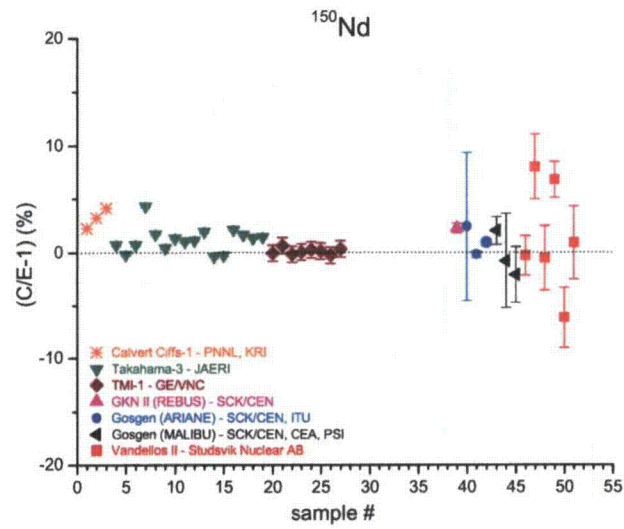
Figure A.33. Comparison of measurements and calculated values for ^{150}Nd.
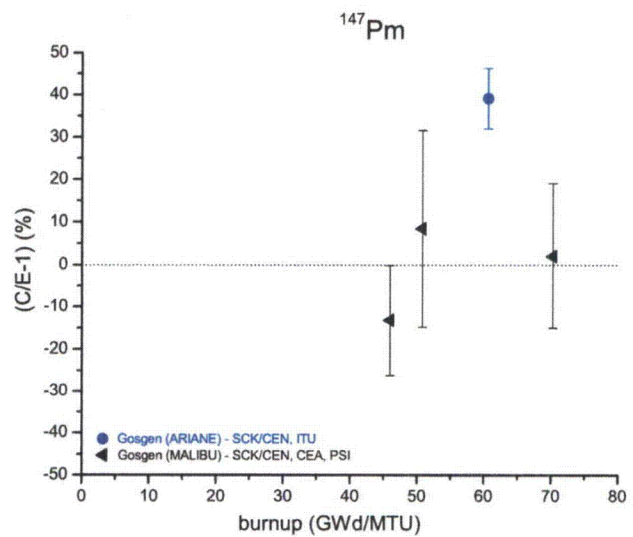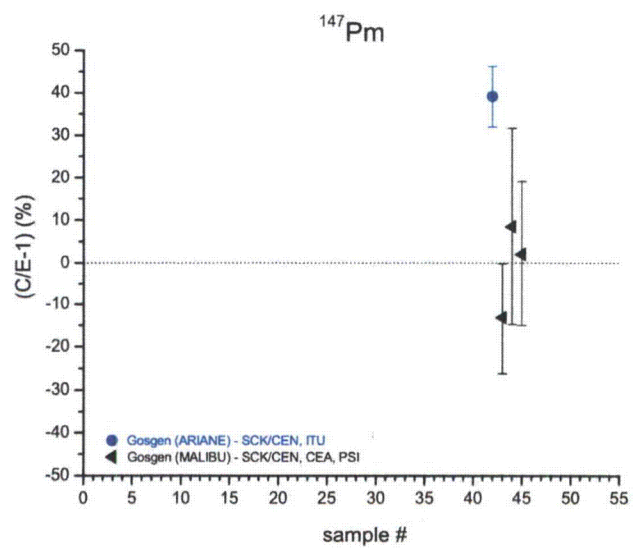
Figure A.34. Comparison of measurements and calculated values for [147]Pm.
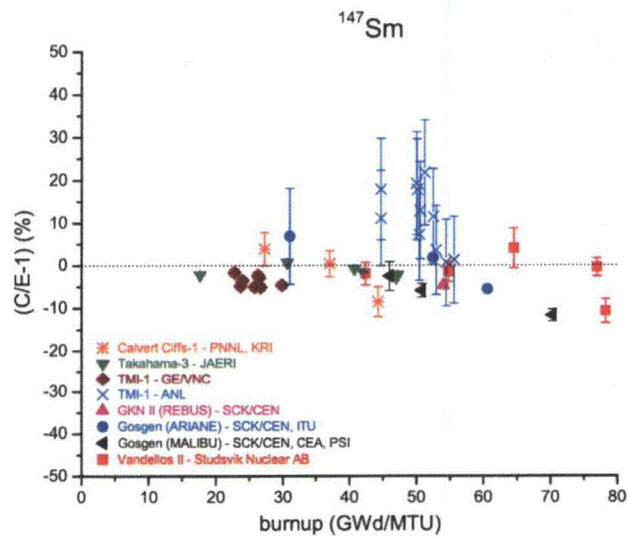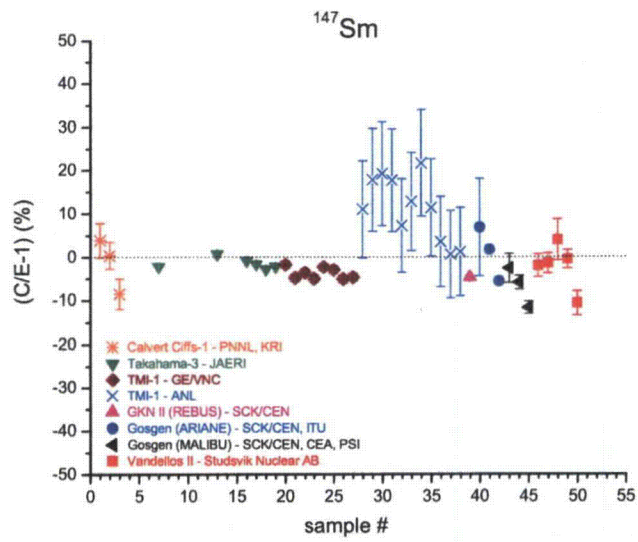
Figure A.35. Comparison of measurements and calculated values for ^{147}Sm.
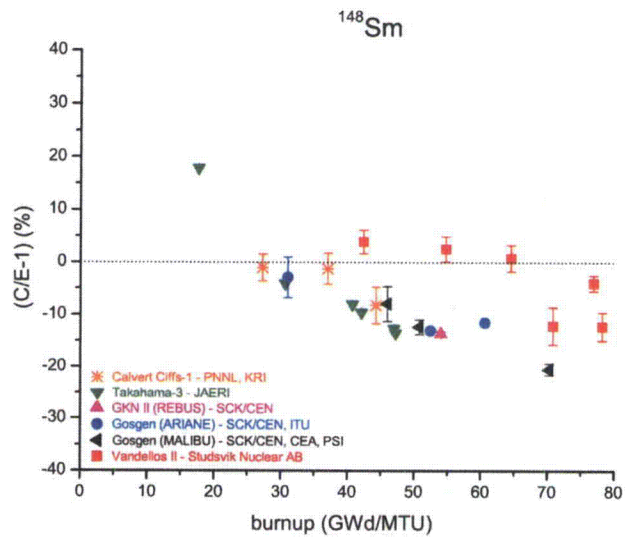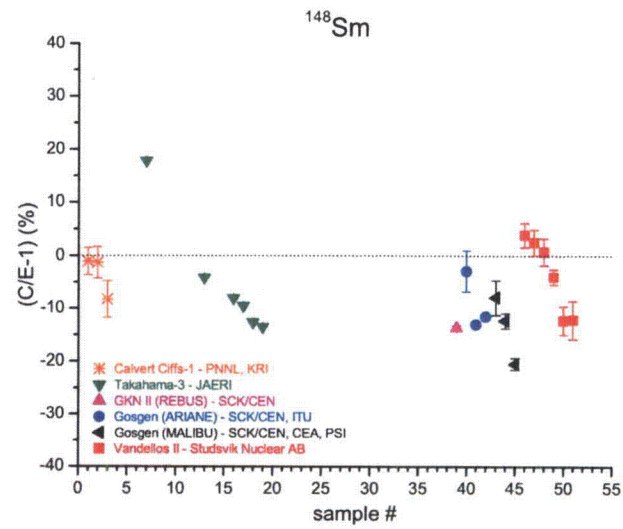
Figure A.36. Comparison of measurements and calculated values for [148]Sm.
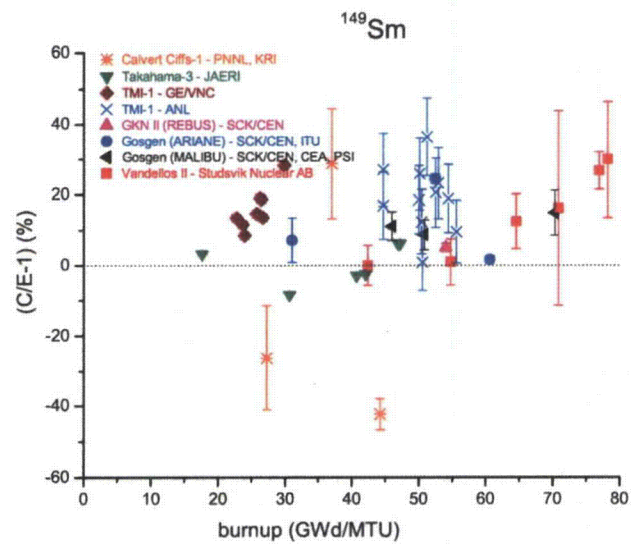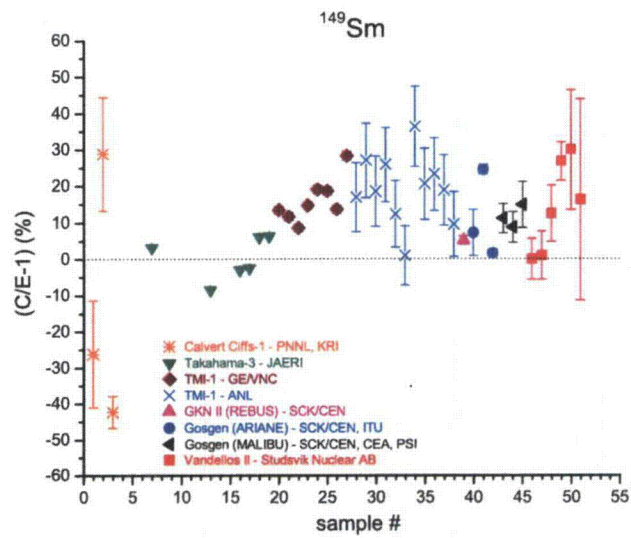
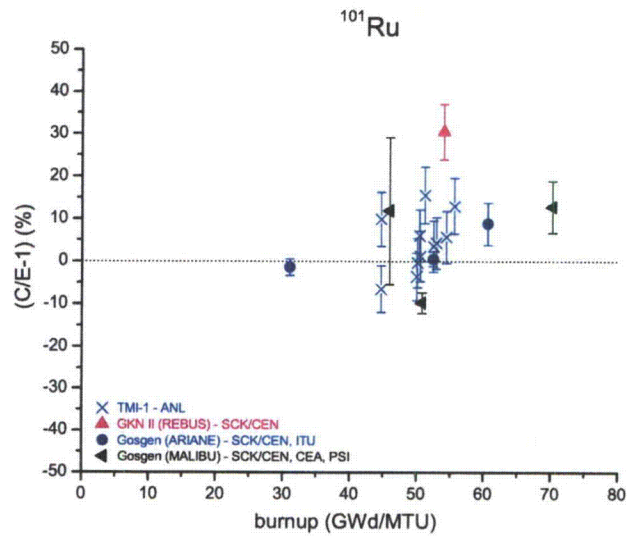Figure A.37. Comparison of measurements and calculated values for ^{149}Sm.
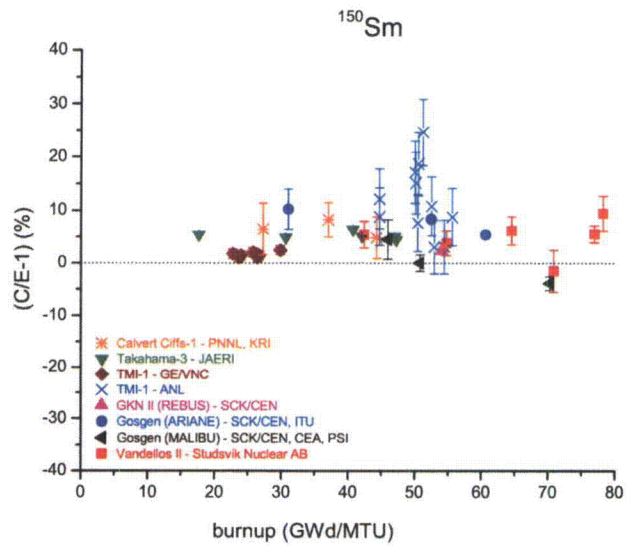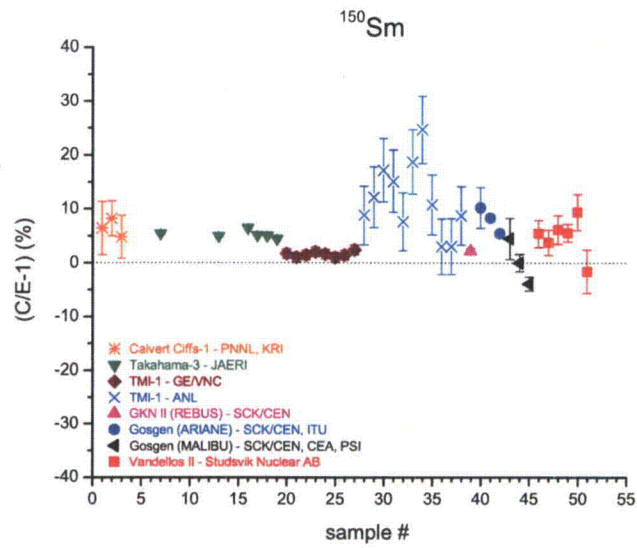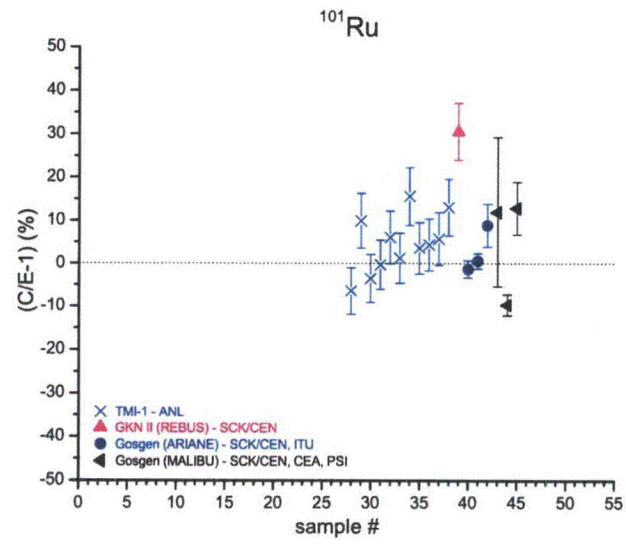
Figure A.38. Comparison of measurements and calculated values for ^{150}Sm.
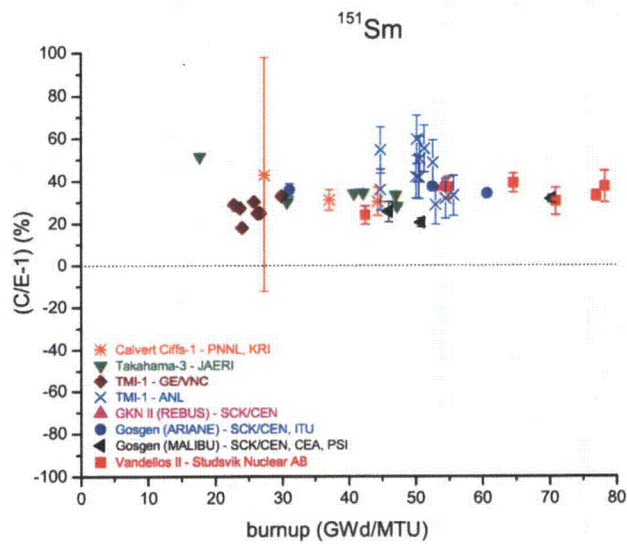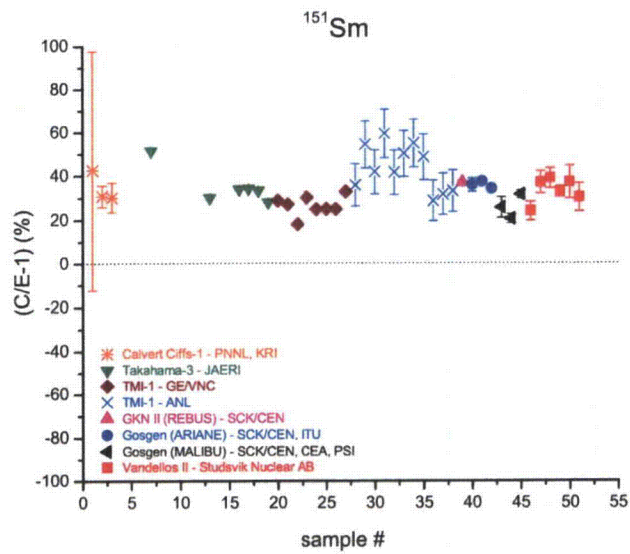
Figure A.39. Comparison of measurements and calculated values for ^{151}Sm.
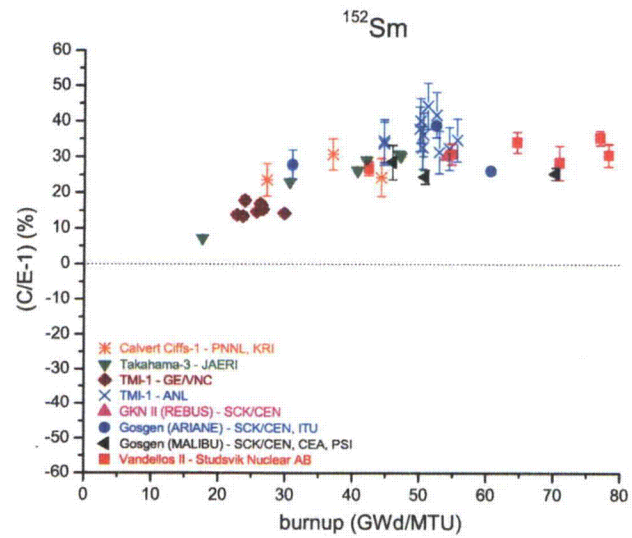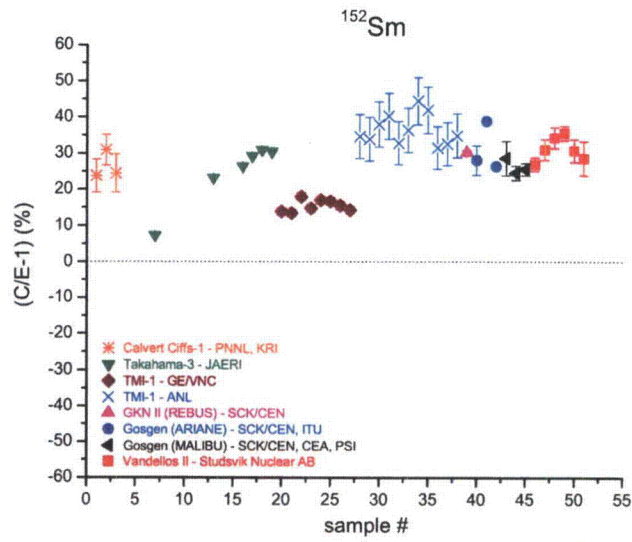
Figure A.40. Comparison of measurements and calculated values for ¹⁵²Sm.
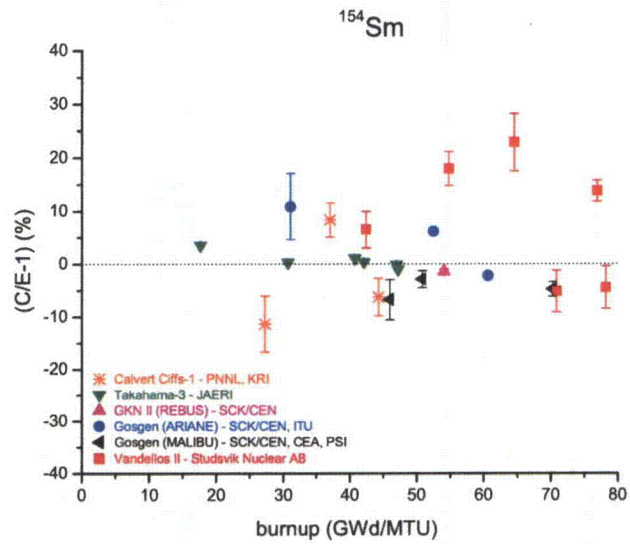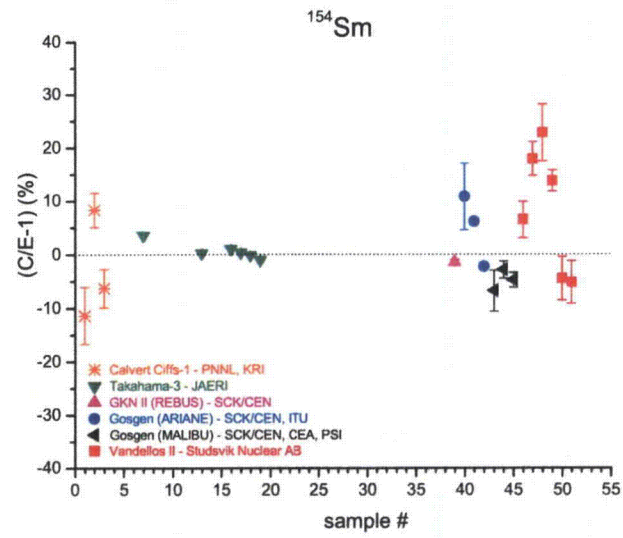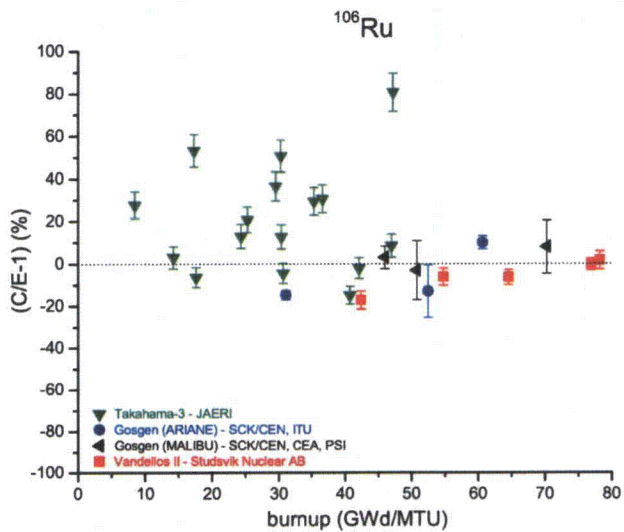
^{154}Sm

^{154}Sm

Figure A.41. Comparison of measurements and calculated values for ^{154}Sm.

A-42
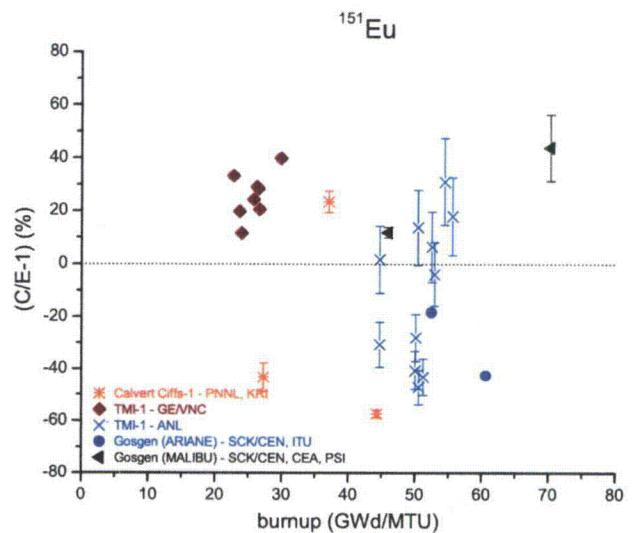
Figure A.42. Comparison of measurements and calculated values for ^{151}**Eu.**

Figure A.43. Comparison of measurements and calculated values for ^{153}Eu.

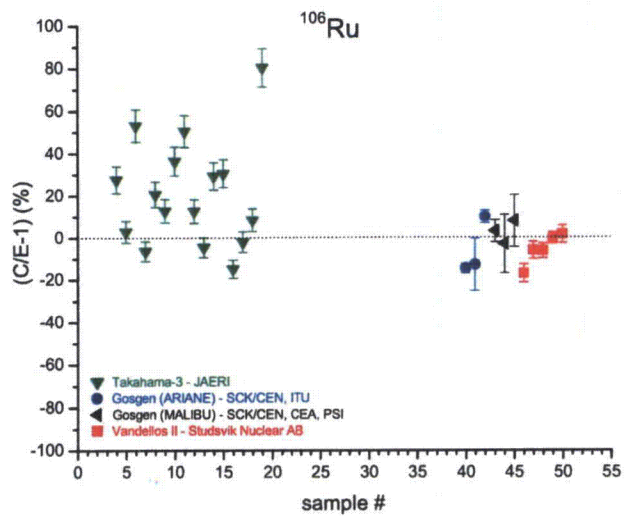**Figure A.44. Comparison of measurements and calculated values for ^{154}Eu.**

Figure A.45. Comparison of measurements and calculated values for ^{155}Eu.

Figure A.46. Comparison of measurements and calculated values for ^{154}Gd.

Figure A.47. Comparison of measurements and calculated values for ^{155}Gd.
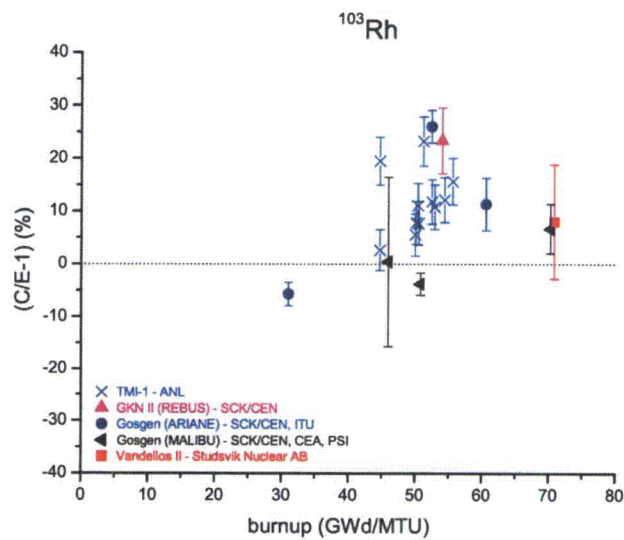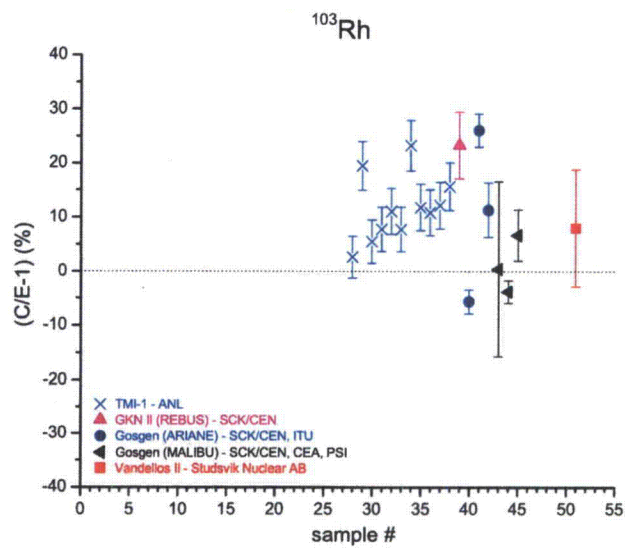
Figure A.48. Comparison of measurements and calculated values for [156]Gd.

Figure A.49. Comparison of measurements and calculated values for ^{158}Gd.

Figure A.50. Comparison of measurements and calculated values for ^{160}Gd.

Figure A.51. Comparison of measurements and calculated values for [90]Sr.

Figure A.52. Comparison of measurements and calculated values for ^{95}Mo.

Figure A.53. Comparison of measurements and calculated values for [99]Tc.

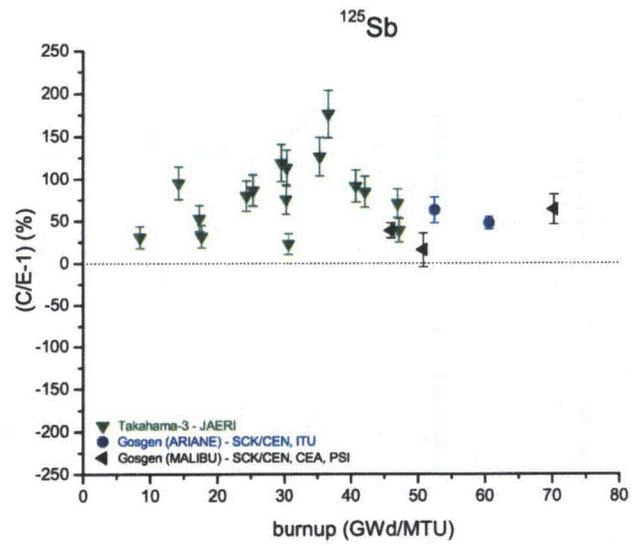Figure A.54. Comparison of measurements and calculated values for ^{101}Ru.

Figure A.55. Comparison of measurements and calculated values for ^{106}Ru.

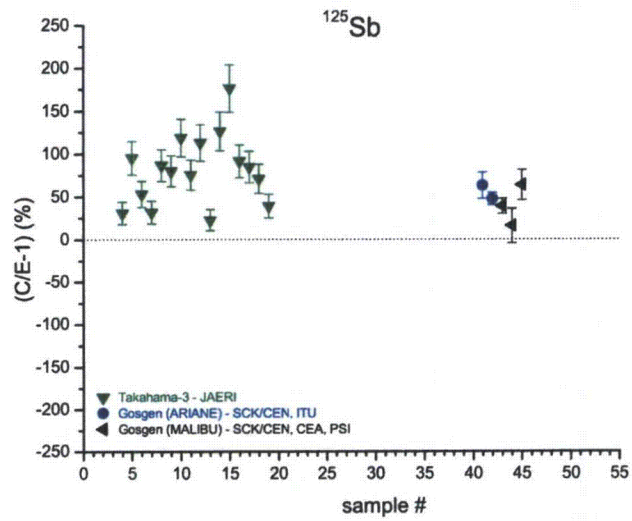Figure A.56. Comparison of measurements and calculated values for ^{103}Rh.

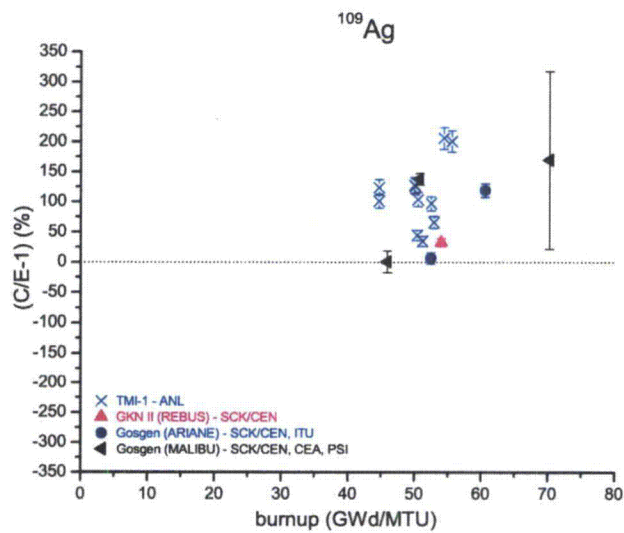Figure A.57. Comparison of measurements and calculated values for ^{125}Sb.

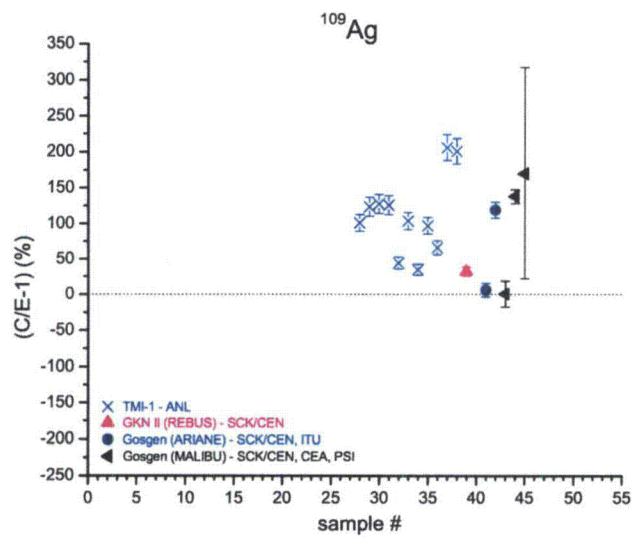Figure A.58. Comparison of measurements and calculated values for ^{109}Ag.

BIBLIOGRAPHIC DATA SHEET

(See instructions on the reverse)

NUREG/CR- 7012
(ORNL/TM-2010/41)

2. TITLE AND SUBTITLE

Uncertainties in Predicted Isotopic Compositions for High Burnup PWR Spent Nuclear Fuel

3. DATE REPORT PUBLISHED	
MONTH	YEAR
January	2011

4. FIN OR GRANT NUMBER
N6540

5. AUTHOR(S)

I. C. Gauld, G. Ilas, and G. Radulescu

6. TYPE OF REPORT

Technical

7. PERIOD COVERED *(Inclusive Dates)*

8. PERFORMING ORGANIZATION - NAME AND ADDRESS *(If NRC, provide Division, Office or Region, U.S. Nuclear Regulatory Commission, and mailing address; if contractor, provide name and mailing address.)*

Oak Ridge National Laboratory
Managed by UT-Battelle, LLC
Oak Ridge, TN 37831-6170

9. SPONSORING ORGANIZATION - NAME AND ADDRESS *(If NRC, type "Same as above"; if contractor, provide NRC Division, Office or Region, U.S. Nuclear Regulatory Commission, and mailing address.)*

Division of Systems Analysis
Office of Nuclear Regulatory Research
U.S. Nuclear Regulatory Commission
Washington, DC 20555-0001

10. SUPPLEMENTARY NOTES

M. Aissa, NRC Project Manager

11. ABSTRACT *(200 words or less)*

Experimental isotopic assay data for 51 spent fuel samples acquired from domestic and international programs have been compiled to provide a database to validate computational predictions of spent fuel isotopic compositions important to criticality safety (burnup credit), reactor physics, spent fuel storage and transportation, and waste management applications. The data were selected on the basis that they include extensive actinide and fission product isotopic assay measurements. The experimental data were acquired for fuels irradiated in six different pressurized water reactors: the Three Mile Island 1 and Calvert Cliffs 1 reactors operated in the United States, the Vandellós II reactor in Spain, the Gösgen reactor in Switzerland, the GKN II reactor in Germany, and the Takahama-3 reactor in Japan. The fuel samples cover enrichments from 2.6 to 4.7 wt % ^{235}U, and a wide burnup range, from 9 to 78 GWd/MTU. In this report, spent fuel isotopic compositions calculated using two-dimensional isotope depletion models and ENDF/B-V–based cross section libraries in the SCALE 5 code system are benchmarked against the experimental isotopic data to validate the code and nuclear data libraries and provide estimates of isotopic bias and uncertainty for nuclides of highest importance to safety and licensing applications. The procedures used to evaluate the experimental data and assess the results are described.

12. KEY WORDS/DESCRIPTORS *(List words or phrases that will assist researchers in locating the report.)*

SCALE, spent nuclear fuel, validation, TRITON, ORIGEN-S, burnup credit, isotopic uncertainties

13. AVAILABILITY STATEMENT

unlimited

14. SECURITY CLASSIFICATION

(This Page)

unclassified

(This Report)

unclassified

15. NUMBER OF PAGES

16. PRICE

**UNITED STATES
NUCLEAR REGULATORY COMMISSION**
WASHINGTON, DC 20555-0001

OFFICIAL BUSINESS